DIMENSIONALITY REDUCTION OF LINEAR OPEN QUANTUM SYSTEMS WITH DELAYED COHERENT FEEDBACK

A DISSERTATION
SUBMITTED TO THE DEPARTMENT OF APPLIED PHYSICS
AND THE COMMITTEE ON GRADUATE STUDIES
OF STANFORD UNIVERSITY
IN PARTIAL FULFILLMENT OF THE REQUIREMENTS
FOR THE DEGREE OF
DOCTOR OF PHILOSOPHY

Gil Tabak
November 2018

This dissertation is online at: http://purl.stanford.edu/mz410nm6680

I certify that I have read this dissertation and that, in my opinion, it is fully adequate in scope and quality as a dissertation for the degree of Doctor of Philosophy.

Hideo Mabuchi, Primary Adviser

I certify that I have read this dissertation and that, in my opinion, it is fully adequate in scope and quality as a dissertation for the degree of Doctor of Philosophy.

Patrick Hayden

I certify that I have read this dissertation and that, in my opinion, it is fully adequate in scope and quality as a dissertation for the degree of Doctor of Philosophy.

Tsachy Weissman

Approved for the Stanford University Committee on Graduate Studies.

Patricia J. Gumport, Vice Provost for Graduate Education

This signature page was generated electronically upon submission of this dissertation in electronic format. An original signed hard copy of the signature page is on file in University Archives.

Preface

Broadly, this work discusses a dimensionality reduction method suitable for linear open quantum systems with coherent time-delayed feedback. The background section provides a succinct introduction to relevant material needed for the other chapters. The remainder of the work is divided into two main chapters. The first chapter deals with the simpler case of passive systems (beamsplitters, phase shifters, time delays, etc.) while the second chapter tackles the more general case of generic linear systems.

The basis of the method is to first describe the input-ouput behavior of a given system using its transfer function, and then write that function as an infinite product of terms of a certain form. Each of these terms should correspond to a physically realizable system (in our case having a single degree of freedom). To obtain an approximate system, a truncation is made to the product. In the case of passive linear systems, it suffices to use the input-output relation of the annihilation fields only. It turns out we can use the Potapov-Blaschke factorization, a matrix-valued function extension of the Blaschke factorization from complex analysis. In the case of active linear systems, a description including both the creation and annihilation fields is required to properly capture the input-output relations. Unfortunately, the Potapov-Blaschke factorization was no longer applicable for this case (in particular, a typical transfer function considered is no longer J-unitary). Despite this, we were able to obtain another analogous factorization theorem for a wide class of active linear systems.

A reduced model resulting from our framework can be represented as a component within the SLH framework, a useful formalism for representing a large class of open quantum systems. This makes our method immediately useful for obtaining effective models of aggregate parts of networks consisting internally of coherent time-delayed feedback loops, which can be used for simulation purposes. In some sense, our factorization captures the 'natural' modes of a given system, so we can capture the important behavior of a given system using few degrees of freedom. This is

important for simulation purposes, especially if the (reduced) linear system is coherently combined with a nonlinear quantum system. In this case, a full quantum simulation of the dynamics is often required, and using more degrees of freedom than necessary can quickly become computationally prohibitive.

Acknowledgments

My PhD was supported by an NDSEG fellowship awarded by the DoD and a Stanford University Graduate Fellowship. This work was also supported by ARO under grant "W911NF-16-1-0086."

I would also like to thank discussions with Tatsuhiro Onodera, Nikolas Tezak, Hendra Nurdin, John E. Gough, Edwin Ng, Daniel B. Soh, Niels Lorch, and Eric Chatterjee. My advisor Hideo Mabuchi suggested the idea of finding 'trapped' modes in the presence of time delays from which this project stemmed, and I am thankful for his guidance throughout. I would also like to especially thank Ryan Hamerly who has made significant contributions to this project.

Finally, I would like to thank my parents for all the opportunities they have provided me with.

Contents

List of Figures

Chapter 1

Introduction

This work will concern quantum input-output networks, which consist of localized quantum components interacting via (directed) bosonic fields. The inputs and outputs of such a network are the bosonic fields traveling along one-way channels. We refer to such networks as open quantum systems.

There are many quantum network modeling scenarios in which it is necessary to capture the impact of time delays in the propagation of signals between components. For example in large-area communication networks there is a obvious need to analyze synchronization issues; in integrated photonic circuits the high natural bandwidth of nanoscale components may create problems of delay-induced feedback instability, and may support the design of devices (such as oscillators) that exploit finite optical propagation delays. Understanding the effects of delays is also important in the context of quantum control, where finite delay propagation can have non-negligible effects in real systems, although most work has focused on the zero delay limit. Recently it has also been shown that coherent delayed feedback can be utilized as a tool to improving enhanced squeezing of coherent states ([30], [39]).

In considering how best to represent and simulate time delays in quantum networks we would like to strike an expedient balance between the need to minimize additional computational overhead and the desire to derive intuitive approximate models. Our main interest in this work is to develop a systematic approach to modeling the leading-order effects of signal propagation time delays in a quantum optical network that can be specified naturally using the so-called SLH formalism of

Gough, James and co-workers [13, 16, 14, 19, 60, 61, 6]. Whereas series and feedback interconnections of open quantum systems in the SLH formalism are generally treated as having vanishing signal propagation time delay, we seek to treat a class of systems having finite delays. Our approach utilizes additional degrees of freedom to capture the behavior of trapped resonant modes created by the system's internal network of feedback pathways and time delays, targeting a specific frequency range that corresponds to the intrinsic bandwidths of components in the network.

The study of time-delay systems has a long history (see [50] for a thorough overview). In the context of quantum systems, a number of approaches different than ours have been suggested. Within the quantum control scenario, incorporating time-delayed coherent feedback has been analyzed recently by Grismo [21]. In that work, a series of cascaded systems is introduced, such that the system is driven by past versions of itself. Later in [58], this work was extended to include the case of multiple delays of different durations. The construction developed by Grismo appears most suitable for use in scenarios with very large feedback time delay, requiring a much higher computational overhead than should be necessary when propagation delays are relatively small.

Recently Pichler and Zoller [46] have described an approach to modeling the dynamics of a finite-delay quantum channel that discretizes the delays as bins and exploits the Matrix Product State formalism for computational efficiency, and demonstrate its use in analyzing quantum feed-forward and feedback dynamics. Simulation and design of quantum networks using such an approach has been further explored in [35] and applied in ([57, 45]). Our work here is distinguished by showing how networks incorporating feedback via many coupled signal channels can be treated efficiently and by focusing on SLH-compatible modeling at the level of quantum stochastic differential equations (QSDEs). The method we present can straightforwardly be incorporated into the Quantum Hardware Description Language (QHDL) framework [56] for automated model construction for complex quantum networks.

Our work provides an extension of some prior papers, and is closely related to others. In [22] and [41], the authors obtain a cascade realization from a given linear quantum stochastic system. Our work here can be considered a natural extension in the case that delayed feedback is included. Isolated loops with time delays are also discussed in the context of linear quantum systems in [17].

Chapter 2

Background

2.1 Quantum states and observables

To represent physical states, a system is identified with a Hilbert space $\mathcal{H}$. Generally it may be infinite-dimensional, but for computational purposes one must often consider a finite-dimensional Hilbert space. A physical state of an isolated system is described using a 'ray' in $\mathcal{H}$, i.e. by a set of nonzero vectors $\psi \in \mathcal{H}$ that can be obtained from one another by multiplication of a nonzero scalar. In general, states that can be represented using rays on a Hilbert space are known as 'pure states'. Throughout, unless otherwise declared, when we pick a representative for a state ψ it will be assumed to have norm 1 (and will sometimes just be referred to as the 'state'). Common notation we will sometimes use is the 'bra-ket' notation: $|\psi\rangle$ for 'column' vectors and $\langle\psi|$ for 'row' vectors (to be multiplied as matrices).

An observable A is self-adjoint operator (Hermitian in the finite-dimensional case) on $\mathcal{H}$. Its expectation value is determined by $\langle A\rangle = \langle\psi| A |\psi\rangle$. In the standard theory, it is assumed that when an observable is measured, the state settles into one of its eigenvectors of the observable, and the measurement yields the eigenvalue of the observable as the observed value. Suppose we expand the state prior to measurement in terms of the observable's eigenvectors: $|\psi\rangle = \sum_i c_i |\psi_i\rangle$. Then the probability of the state settling to eigenvector i and the measurement resulting in eigenvalue i is the norm of the ith component, $|c_i|^2$.

When there are multiple interacting systems, the composite system is described by the tensor product of the individual systems. For example, the composite system of two individual systems

1 and 2 with respective Hilbert spaces $\mathcal{H}_1$ and $\mathcal{H}_2$ is described using $\mathcal{H}_1 \otimes \mathcal{H}_2$. If system 2 is inaccessible to measurements, we may wish to describe the state of system 1 only. In this case, it is necessary to use the mixed states formalism to describe the state of system 1.

In the mixed state formalism, we represent the state of a system using an operator on the Hilbert space $\mathcal{H}$ of the system $\rho = \sum_i c_i |\psi_i\rangle \langle\psi_i| \in L(\mathcal{H})$. Here ψ_i are pure states in $\mathcal{H}$ and c_i are their probabilities (which must be non-negative and sum up to 1). From this definition, the expectation value of an observable can be found:

$$\langle A \rangle = \sum_i c_i \langle\psi_i| A |\psi_i\rangle = \mathrm{tr}\left(\rho A\right). \tag{2.1}$$

The result of the measurement process is also analogous to the pure-state case. Remembering A is self-adjoint, we can decompose it as $A = \sum_i c_i \Pi_i$, where c_i are the eigenvalues of A and Π_i are the orthogonal projectors corresponding to each eigenvalue. The probability of observing c_i is $\mathrm{tr}(\rho\Pi_i)$, resulting in the new density matrix $\Pi_i \rho \Pi_i / \mathrm{tr}(\rho\Pi_i)$.

To obtain the mixed state of system 1 from the composite system 1 and 2, we an first construct the mixed state of the composite system: $\rho_{12} = |\psi_{12}\rangle \langle\psi_{12}|$, where ψ_{12} is the pure state of the composite system. Then, we take the partial trace with respect to system 2 to obtain the mixed state $\rho_1 = \mathrm{tr}_2(\rho_{12})$. The partial trace tr_2 is the unique linear operator from $L(\mathcal{H}_1 \otimes \mathcal{H}_2)$ to $L(\mathcal{H}_1)$ that satisfies $\mathrm{tr}_2(\rho_1 \otimes \rho_2) = \rho_1 \mathrm{tr}(\rho_2)$. The choice of the partial trace can be physically motivated by consistency conditions of measurements made on system 1 alone versus measurements on the composite system 1 and 2 [51]. In the finite-dimensional case, the partial trace can be computed efficiently using e.g. [38]. In general, the partial trace results in mixed states that may not be representable as pure states, even when the composite system was representable as a pure state.

2.2 Dynamics

We set $\hbar = 1$ throughout. For an isolated quantum system, the dynamics evolve in time according to the Schrödinger equation:

$$\frac{d\,|\psi(t)\rangle}{dt} = -iH(t)\,|\psi(t)\rangle\,. \tag{2.2}$$

Here $H(t)$ is the Hamiltonian of the system. The mixed state analogously evolves according to

$$\frac{d\rho(t)}{dt} = -i[H(t), \rho(t)]. \tag{2.3}$$

Here, $[A, B] = AB - BA$ is the commutator between two operators A and B. These two equations preserve the norm of $|\psi(t)\rangle$ and the trace of $\rho(t)$. For a isolated system, we can also find the time evolution operator $U(t)$ satisfying

$$\frac{dU(t)}{dt} = -iH(t)U(t), \qquad U(0) = I. \tag{2.4}$$

The time evolution operator can then be used to find $|\psi(t)\rangle = U(t)\,|\psi(0)\rangle$, or any operator in the Heisenberg picture: $A(t) = U(t)^\dagger A_0 U(t)$.

2.2.1 Quantum Stochastic Differential Equations

We will be interested in the dynamics of open quantum systems. One typical starting point used to derive open system dynamics is a system with Hamiltonian H_S interacting with a bath with Hamiltonian H_B via an interaction Hamiltonian H_I. The dynamics of the 'universe' (system and bath together) are then considered to be an isolated system with Hamiltonian $H = H_S + H_B + H_I$. It will be understood in this notation that H_S is an operator acting only on the system (i.e. we actually mean an operator $H_S \otimes I$), and similarly for H_B. The bath is often represented an infinite set of harmonic oscillator modes:

$$H_B = \int_{-\infty}^{\infty} \frac{1}{2\pi} d\omega \omega b^\dagger(\omega) b(\omega), \tag{2.5}$$

We assume the interaction term has form

$$H_I = i \int_{-\infty}^{\infty} \frac{1}{2\pi} d\omega (L^\dagger b(\omega) - L b^\dagger(\omega)), \tag{2.6}$$

where the L is a system operator. Here the bath modes $b(\omega)$ satisfy the commutation relations $[b(\omega), b^\dagger(\omega')] = 2\pi\delta(\omega - \omega')$. Meanwhile, the system Hamiltonian remains arbitrary in this model.

This interaction term (Eq. 2.6) can be obtained from a common interaction type of the form $i\int_{-\infty}^{\infty} \frac{1}{2\pi} d\omega \kappa(\omega)(b(\omega) + b^\dagger(\omega))(c - c^\dagger)$ for a system operator c under certain assumptions, most importantly that the interaction strength $\kappa(\omega)$ varies slowly in ω (effectively causing the bath to be

Markovian) and the rotating wave approximation (dropping interaction terms that oscillate quickly after a change of frame). See [6].

Going to the rotating wave frame by making the substitution $b(\omega) \mapsto b(\omega)e^{-i\omega t}$ results in the H_B term dropping out, and switching to the time domain via $b(t) = \int_{-\infty}^{\infty} \frac{1}{2\pi} d\omega b(\omega)$, we obtain

$$H = H_S + i(L^\dagger b(t) - L b^\dagger(t)). \tag{2.7}$$

In this picture each bath mode (in the time domain) interacts with the system at a different time. We can think of the bath as a channel passing through the system. This picture will be important later because we will want to concatenate multiple systems via interaction channels. We also assume that each bath mode is initially in the vacuum state. When modeling components with nonzero vacuum inputs, we could insert a component modifying the state of the bath modes before they pass through subsequence components.

The time evolution operator can be found by integrating its dynamical equation in time:

$$U(t) = \exp\left\{\int_0^t -iH(s)ds\right\}, \qquad U(0) = I. \tag{2.8}$$

To avoid dealing with the singular commutation relations $[b(t), b^\dagger(t')] = \delta(t - t')$, it is convenient to introduce the time-integrated quantities:

$$dB(t) = \int_t^{t+dt} b(s)ds, \qquad dB^\dagger(t) = \int_t^{t+dt} b^\dagger(s)ds. \tag{2.9}$$

The expectation values of these terms with respect to the vacuum state satisfy

$$\left\langle dB(t)dB^\dagger(s)\right\rangle = \begin{cases} dt \text{ if t=s,} \\ 0 \text{ otherwise.} \end{cases} \tag{2.10}$$

$$\left\langle dB(t)dB(s)\right\rangle = \left\langle dB(t)^\dagger dB(s)\right\rangle = \left\langle dB^\dagger(t)dB^\dagger(s)\right\rangle = 0. \tag{2.11}$$

The $dB(t)$ 'noise' terms are analogous to the Brownian increments in classical stochastic calculus. Usually we take the expectation with respect to the vacuum, allowing us to replace each of the terms above by their expectation. Also, we can integrate along these increments, just as in the classical case. We can choose to use Stratonovich or Ito integrals, defined in the same way as in the

classical case: for a function $f(t)$, it's Ito integral is given by

$$\int_0^t f(s)dB(s) \equiv \lim_{n\to\infty} \sum_{i=0}^{n-1} f(t_i)[B(t_{i+1}) - B(t_i)]. \tag{2.12}$$

The Stratonovich integral uses the midpoints at each increment instead:

$$\int_0^t f(s)dB(s) \equiv \lim_{n\to\infty} \sum_{i=0}^{n-1} f\left(\frac{1}{2}(t_i + t_{i+1})\right)[B(t_{i+1}) - B(t_i)]. \tag{2.13}$$

Our choice of Ito versus Stratonovich is important, and will result in different terms. In practice it is often more useful to use the Ito formalism. In this case we have to be careful because of the modified chain rule (which arises analogously to the classical case):

$$d(X(t)Y(t)) = dX(t)Y(t) + X(t)dY(t) + dX(t)dY(t). \tag{2.14}$$

To recast the singular bath modes $b(t)$ in (Eq. 2.7) in terms of the increments $dB(t)$ in (Eq. 2.11), we can formally replace $b(s)ds \mapsto dB(s)$, but specifically in the Stratonovich interpretation. The reason is that the substitution has to be accurate to second order in each increment due to the stochastic terms, and the midpoint approximation used in the Stratonovich formulation satisfies this condition. Fortunately it is not difficult to translate between the two formalisms. Another nice way to determine the correct form is to remember $U(t)$ must remain unitary throughout its evolution and apply the Ito rule (Eq. 2.14) as in[24, 42]. Either way, we find there is a term $-\frac{1}{2}L^\dagger L$ that must be added for the case of our Hamiltonian in (Eq. 2.7). Finally, this tells us that the propagator of $U(t)$ in the Ito formulation is given by

$$dU(t) = \left[-(iH_S + \frac{1}{2}L^\dagger L) + LdB^\dagger(t) - L^\dagger dB(t)\right]U(t), \qquad U(0) = I. \tag{2.15}$$

From this type of equation, we will be able to derive the Lindblad master equation, which controls the dynamics of the state $\rho(t)$ assuming no knowledge of measurements, as well as quantum filtering equations, which describe the evolution of $\rho(t)$ given a measurement record. Before we do that, let's generalize (Eq. 2.15) in two ways. First, there will be N channels connecting the system to N separate heat baths having operators $b_n(\omega)$, via operators L_n for $n = 1, ..., N$. Second, there will be additional linear interactions between the bath modes facilitated by the system, which can be encapsulated by an additional Hamiltonian term of the form $\sum_{n,m=1}^{N} b_n^\dagger(t)M_{nm}b_m(t)$. In the time domain picture, this interaction occurs only at time t, when the modes $b_n(t)$ are 'passing' through the system. Because the new Hamiltonian term is quadratic in the bath modes, we will need to

introduce a new operator $\Lambda(t)$, known as the gauge process, in order to write the propagator using time-integrator quantities. The increments of $\Lambda(t)$ are given by

$$d\Lambda_{nm}(t) = \int_t^{t+dt} b_n^\dagger(s) b_m(s) ds. \tag{2.16}$$

Similarly to the $dB(t)$ and $dB^\dagger(t)$ noise terms, it is possible to multiply some combinations of increments $d\Lambda(t)$, $dB(t)$, and $dB^\dagger(t)$ resulting in increments of non-negligible order (as before, under vacuum expectations):

$$\langle dB_i d\Lambda_{kl} \rangle = \delta_{ik} dB_l, \qquad \left\langle dB_i dB_k^\dagger \right\rangle = \delta_{ik} dt, \tag{2.17}$$

$$\langle d\Lambda_{ij} d\Lambda_{kl} \rangle = \delta_{jk} d\Lambda_{il}, \qquad \left\langle d\Lambda_{ij} dB_k^\dagger \right\rangle = \delta_{jk} dB_i^\dagger. \tag{2.18}$$

In this more general setting we can find an equation generalizing (Eq. 2.15) as done in [23]. The correct form can be obtained as done in [24] by requiring the Ito form of the chain rule (Eq. 2.14) and the preservation of the unitarity of the operator $U(t)$ given the Ito rules (Eq. 2.17-2.18). The result has form

$$dU(t) = \Big[-(iH_S + \sum_{n=1}^{N} \frac{1}{2} L_n^\dagger L_n) + \sum_{n=1}^{N} L_n dB_n^\dagger(t) - \sum_{n,m=1}^{N} L_n^\dagger S_{nm} dB_m(t) \tag{2.19}$$

$$+ \sum_{n,m=1}^{N} (S_{nm} - I_{nm}) d\Lambda_{nm} \Big] U(t), \qquad U(0) = I. \tag{2.20}$$

The L_n operators in (Eq. 2.19) are modified from the ones appearing in the Hamiltonian and the Hamiltonian H_S becomes renormalized due to the newly added gauge process increments. Here each S_{nm} is an operator with the unitarity constraints $S_{nl} S_{ml}^\dagger = \delta_{nm} I$, $S_{ln}^\dagger S_{lm} = \delta_{nm} I$. We can check that when the scattering matrix is the identify, i.e. $S_{mn} = \delta_{mn} I$, the propagator (Eq. 2.19) with a single channel reduces to the previous case (Eq. 2.15).

At this point it is useful to collect the L_n terms to form a vector $\mathbf{L} = [L_1, ..., L_N]$, the dB_n terms to form a vector $d\mathbf{B} = [dB_1, ..., dB_N]$, the S_{nm} operators to similarly form an $N \times N$ matrix $\mathbf{S}$, and the gauge processes $d\Lambda_{nm}$ to form an $N \times N$ matrix $d\mathbf{\Lambda}$. This allows us to conveniently write

$$dU(t) = \Big[-(iH_S + \frac{1}{2} \mathbf{L}^\dagger \mathbf{L}) + d\mathbf{B}^\dagger(t) \mathbf{L} - \mathbf{L}^\dagger \mathbf{S} d\mathbf{B} + \mathrm{tr}\left[(\mathbf{S} - I) d\mathbf{\Lambda}^T \right] \Big] U(t), \qquad U(0) = I. \tag{2.21}$$

From this equation we can find the evolution of each operator $A(t)$ in which we are interested,

known as the Heisenberg-Langevin equations. This is done by evaluating

$$A(t) = U^\dagger(t)(A_0 \otimes I)U(t), \tag{2.22}$$

where A_0 is understood to be defined on the system alone. Remembering to keep second order terms as indicated by the Ito chain rule (Eq. 2.14) and using the Ito rules (Eq. 2.17-2.18), we can obtain the evolution of a generic operator $A(t)$:

$$dA(t) = \mathcal{L}(H_S, \mathbf{L}, A(t))dt + [\mathbf{L}^\dagger, A(t)]\mathbf{S}d\mathbf{B} + d\mathbf{B}^\dagger\mathbf{S}^\dagger[A(t), \mathbf{L}] + \mathrm{tr}[(\mathbf{S}^\dagger\mathbf{I}_{A(t)}\mathbf{S} - \mathbf{I}_{A(t)})d\mathbf{\Lambda}^T], \tag{2.23}$$

where

$$\mathcal{L}(H_S, \mathbf{L}, A(t)) = -i[A(t), H_S] + \sum_{n=1}^{N}\left(L_n^\dagger A(t)L_n - \frac{1}{2}\left(L_n^\dagger L_n A(t) + A(t)L_n^\dagger L_n\right)\right), \tag{2.24}$$

and $\mathbf{I}_{A(t)}$ is an $N \times N$ matrix with A on the diagonal and zero otherwise.

The $(\mathbf{S}, \mathbf{L}, H)$ triplet captures the dynamics of the system and has particularly useful modular properties (see Section 2.2.4). This description is known in the literature as the SLH formalism.

2.2.2 Lindblad Master Equation

We can also obtain the Lindblad master equation, which controls the dynamics of the state $\rho(t)$. One way to do so (as in [26]) is by taking the expectation value of an arbitrary observable:

$$\langle A(t)\rangle = \mathrm{tr}(\rho(t)A(0)) = \mathrm{tr}(\rho(0)A(t)). \tag{2.25}$$

Taking the time derivative and dropping the noise terms due to the expectation value,

$$\frac{d}{dt}\langle A(t)\rangle = \mathrm{tr}\left(\frac{d}{dt}\rho(t)A(0)\right) = \mathrm{tr}\left(\rho(0)\mathcal{L}(H_S, \mathbf{L}, A(t))\right\rangle = \langle\rho(t)\mathcal{L}(H_S, \mathbf{L}, A(0))) \tag{2.26}$$

$$= \mathrm{tr}\left(\left\{-i[H_S, \rho(t)] + \sum_{n=1}^{N}\left[L_n\rho(t)L_n^\dagger - \frac{1}{2}\left(\rho(t)L_n^\dagger L_n + L_n^\dagger L_n\rho(t)\right)\right]\right\}A(0)\right). \tag{2.27}$$

In the last step above we rearranged the terms using the cyclic trace property. Since the operator $A(0)$ was an arbitrary observable, we can recover

$$\frac{d}{dt}\rho(t) = -i[H_S, \rho(t)] + \sum_{n=1}^{N}\left[L_n\rho(t)L_n^\dagger - \frac{1}{2}\left(\rho(t)L_n^\dagger L_n + L_n^\dagger L_n\rho(t)\right)\right]. \tag{2.28}$$

The master equation (Eq. 2.28) describing the evolution of $\rho(t)$ corresponds to the partial trace of the system and bath state with respect to the bath. It is the most general form of a generator for the 'smooth' time evolution $\rho(t)$ which is time-homogeneous, Markovian, and preserves the desired properties of density matrices (trace-preserving, completely positive, and Hermiticity-preserving) (see [51, 34, 4, 59])

2.2.3 Input-output relationship

Notice the master equation describes only the internal evolution of the system, and does not depend on $\mathbf{S}$. We can also obtain the output of the system by considering the transformed fields:

$$\mathbf{B}_{\text{out}}(t) = U^\dagger(t)\mathbf{B}(t)U(t), \qquad \mathbf{\Lambda}_{\text{out}}(t) = U^\dagger(t)\mathbf{\Lambda}(t)U(t). \tag{2.29}$$

Expanding the increments between times t and $t + dt$, one can find

$$d\mathbf{B}_{\text{out}}(t) = \mathbf{S}(t)d\mathbf{B}(t) + \mathbf{L}(t)dt, \tag{2.30}$$

$$\begin{aligned} d\mathbf{\Lambda}_{\text{out}}(t) = {} & \mathbf{L}^*(t)\mathbf{L}^T(t)dt + \mathbf{S}^*(t)d\mathbf{\Lambda}(t)\mathbf{S}^T(t) \\ & + \mathbf{S}^*(t)d\mathbf{B}^*(t)\mathbf{L}^T(t) + \mathbf{L}^*(t)d\mathbf{B}^*(t)\mathbf{S}^T(t). \end{aligned} \tag{2.31}$$

Input-output relationship for linear systems

For linear systems in particular, it is possible to describe the input-output relationship using the state-space formalism (i.e. via matrices A, B, C, D, which can be related to the SLH parameters). This is especially useful as we can take the Laplace transform and describe the input-output relationships via the transfer function formalism. In particular, the internal degrees of a system are described by an annihilation and creation mode, $a_i(t)$ and $a_i^\dagger(t)$, satisfying the canonical bosonic commutation relations $[a_i(t), a_j(s)^\dagger] = \delta(t-s)\delta_{i,j}$.

The L_n operators and the Hamiltonian H in the SLH formalism are linear and quadratic, respectively, in the $a_i(t)$ and $a_i(t)^\dagger$ degrees of freedom. In general, it is necessary to include in the dynamics

of both the creation and annihilation operators to be able to capture the effects of squeezing, but for passive linear systems there is no squeezing and considering only the annihilation modes suffices. For this reason, when considering non-passive linear systems, it is convenient to use the notation $\breve{\mathbf{a}} = (\mathbf{a}, \mathbf{a}^\dagger)^T$.

Supposing $L_n = \sum_{m=1}^N \phi_{nm}^- a_m + \phi_{nm}^+ a_m^\dagger$ and $H = \sum_{n,m}^N a_n^\dagger \omega_{nm}^- a_m + a_n^\dagger \omega_{nm}^+ a_m^\dagger + a_n \omega_{nm}^{+*} a_m$, we can construct the matrices $\Phi^\pm$ and $\Omega^\pm$ consisting of the constant components $\phi_{ij}^\pm$ and $\omega_{ij}^\pm$, respectively. the state-space matrices can be obtained using (see [6, 19]):

$$\tilde{\Phi} = \begin{pmatrix} \Phi_- & \Phi_+ \\ \Phi_+^* & \Phi_-^* \end{pmatrix} \qquad \tilde{\Omega} = \begin{pmatrix} \Omega_- & \Omega_+ \\ -\Omega_+^* & -\Omega_-^* \end{pmatrix}$$

$$\tilde{A} = -\frac{1}{2}\tilde{\Phi}^\flat \tilde{\Phi} - i\tilde{\Omega}, \qquad \tilde{B} = -\tilde{\Phi}^\flat \tilde{D},$$
$$\tilde{C} = \tilde{\Phi}, \qquad \tilde{D} = \begin{pmatrix} S & 0 \\ 0 & S^* \end{pmatrix}.$$

Here we use the notation $M^\flat \equiv JM^\dagger J$ for $J = \mathrm{diag}(I_n, -I_n)$.

Explicitly, the dynamics are given by the dynamical system of equations

$$\frac{d}{dt}\breve{\mathbf{a}}(\mathbf{t}) = \breve{A}\breve{\mathbf{a}}(\mathbf{t}) + \breve{B}\breve{\mathbf{b}}(\mathbf{t}) \tag{2.32}$$
$$\breve{\mathbf{b}}_{\mathrm{out}}(\mathbf{t}) = \breve{C}\breve{\mathbf{a}}(\mathbf{t}) + \breve{D}\breve{\mathbf{b}}(\mathbf{t}). \tag{2.33}$$

Conversely, given state-space matrices A, B, C, D, specific conditions can be given in order to ensure that a system is physically realizable [18].

Taking the Laplace transform, we can obtain the transfer function

$$T(z) = \breve{D} - \breve{C}(Iz - \breve{A})^{-1}\breve{B}. \tag{2.34}$$

In the case of passive linear systems, $\Phi^+ = 0$ and $\Omega^+ = 0$, and we get two sets of equivalent equations for $\mathbf{a}$ and $\mathbf{a}^\dagger$. Thus it suffices to write down dynamical equations for only the annihilation

fields:

$$\frac{d}{dt}\mathbf{a}(\mathbf{t}) = A\mathbf{a}(\mathbf{t}) + B\mathbf{b}(\mathbf{t}) \tag{2.35}$$

$$\mathbf{b}_{\text{out}}(\mathbf{t}) = C\mathbf{a}(\mathbf{t}) + D\mathbf{b}(\mathbf{t}). \tag{2.36}$$

Simplifying with $\Phi = \Phi^-$, The state-space matrices in this case are given by

$$A = -\frac{1}{2}\Phi^\dagger\Phi - i\Omega, \qquad B = -\Phi^\dagger D, \tag{2.37}$$

$$C = \Phi, \qquad \tilde{D} = S. \tag{2.38}$$

2.2.4 SLH Composition Rules

Several systems in the SLH framework can be combined using a set of rules found in [16, 15]. We will denote $\mathcal{G}_i = (\mathbf{S}_i, \mathbf{L}_i, H_i)$ for $i = 1, 2$ There are three main types of rules:

Concatenation product: This denotes two systems places in parallel (not directly interacting). The two systems can have different number of channels (say N_1 and N_2). The resulting system has $N_1 + N_2$ channels.

$$\mathcal{G}_1 \boxplus \mathcal{G}_2 = \left(\begin{pmatrix} \mathbf{S}_1 & 0 \\ 0 & \mathbf{S}_2 \end{pmatrix}, \begin{pmatrix} \mathbf{L}_1 \\ \mathbf{L}_2 \end{pmatrix}, H_1 + H_2 \right). \tag{2.39}$$

Series product: This denotes two systems placed in series. They must have the same number of channels (here all channels from system 1 feed into system 2).

$$\mathcal{G}_2 \triangleleft \mathcal{G}_1 = \left(\mathbf{S}_2\mathbf{S}_1, \mathbf{L}_2 + \mathbf{S}_2\mathbf{L}_1, H_1 + H_2 + \Im(\mathbf{L}_2^\dagger \mathbf{S}_2 \mathbf{L}_1) \right). \tag{2.40}$$

Here the 'imaginary' part of an operator A is denoted by $\Im A = \frac{1}{2i}(A - A^\dagger)$.

Feedback Operation: For a system $\mathcal{G} = (\mathbf{S}, \mathbf{L}, H)$, suppose there is a total of $N = N_1 + N_2$ channels. We will consider the first N_1 to be the 'internal' channels and the last N_2 to be the 'external' channels. By this, we mean that in applying the feedback operation, the outputs of the internal channels are directed immediately to the inputs of the same channels. Meanwhile, the inputs and outputs of the 'external' channels remain inputs and outputs after the feedback operation is applied.

We split the $\mathbf{S}$ and $\mathbf{L}$ matrices to blocks:

$$\mathbf{S} = \begin{pmatrix} \mathbf{S}_{ii} & \mathbf{S}_{ie} \\ \mathbf{S}_{ei} & \mathbf{S}_{ee} \end{pmatrix}, \qquad \mathbf{L} = \begin{pmatrix} \mathbf{L}_i \\ \mathbf{L}_e \end{pmatrix}. \tag{2.41}$$

The indices i or e represent with which channels each block of the $\mathbf{S}$ and $\mathbf{L}$ is interacting (i for internal and e for external). For the $\mathbf{S}$ blocks, the first index corresponds to the input and the second index the output channels along which the interaction mediated by each block occurs as the bath modes interact with the system. The SLH of the resulting system once the feedback operation is performed is given by

$$\mathbf{S}_{\text{feedback}} = \mathbf{S}_{ee} + \mathbf{S}_{ei}(I - \mathbf{S}_{ii})^{-1}\mathbf{S}_{ie}, \tag{2.42}$$

$$\mathbf{L}_{\text{feedback}} = \mathbf{L}_e + \mathbf{S}_{ei}(1 - \mathbf{S}_{ii})^{-1}\mathbf{L}_i, \tag{2.43}$$

$$H_{\text{feedback}} = H + \Im\left(\sum_{j=i,e} \mathbf{L}_j^\dagger \mathbf{S}_{ji}(1 - \mathbf{S}_{ii})^{-1}\mathbf{L}_i\right). \tag{2.44}$$

2.2.5 Open quantum systems with measurement – quantum filtering

Up to now, we have described the dynamics of open quantum systems without measurement feedback. Measurement feedback results when an output channel is being measured, affecting the state of the system. We will consider three types of measurements most common in quantum optics involving the continuous monitoring of the outputs: photon counting, homodyne measurement, and heterodyne measurement. Experimentally, measurements have a certain efficiency, but here we will only consider perfect measurements (i.e. perfect efficiency). It turns out if the system starts in a pure state and its outputs are being continuously monitored with one of these three measurement methods (having perfect efficiency), the system remains in a pure state. This is because performing a measurement on the outputs can be thought of as tracing out any parts outside of the system that could have become entangled with it. Thus it is sufficient for us to consider the evolution of pure states. We will write the equations of motion in each case. Because of the measurement process, there is a probabilistic component in each equation. In the photon counting case this manifests as a jump process (whenever a photon is detected, the knowledge of the state is updated). In the case of homodyne or heterodyne detection, an output signal is being continuously measured. This results in stochastic terms in the equation of motion.

For each type of measurement setup, although the trajectories can be quite different, they can be averaged in a certain sense to recover the master equation. Specifically, averaging the quantity

$|\psi(t)\rangle\langle\psi(t)|$ over many trajectories will recover $\rho(t)$ given by the master equation (which is independent of any measurement process). Trajectories of pure states with this property are called 'unravellings' of the master equation. Interestingly, quantum state diffusion, the stochastic differential equation corresponding to continuous heterodyne detection, can be recovered in certain limits from quantum jumps [47]. Simulating the master equation can sometimes be done more easily than running multiple probabilistic trajectories, since it just involves a linear ODE. However, the dimensionality of the master equation is quadratic with the dimensionality of the Hilbert space, making it impractical for larger systems. In addition, quantum jumps can often reveal behavior that is not immediately clear from the master equation, like bistable behavior.

Quantum filtering has been explored mathematically in detail in [3]. For our purposes we will simply cite the equations of motion of the different unravellings.

Quantum Jumps (see [11, 5, 27]):

The state evolution is given by a modified Schrödinger equation with non-Hermitian Hamiltonian given by

$$H = H_S - \frac{i}{2}\sum_{n=i}^{N} L_n^\dagger L_n, \tag{2.45}$$

and is interrupted by jumps. A jump corresponds to a photon measurement in the output of channel n. The probability of each such jump in a short time δt is given by

$$\delta p = \delta t \langle\psi(t)| L_n^\dagger L_n |\psi(t)\rangle . \tag{2.46}$$

When a jump occurs in channel n, the state is transferred to

$$|\psi(t)\rangle \mapsto \frac{L_n|\psi(t)\rangle}{\langle\psi(t)| L_n^\dagger L_n |\psi(t)\rangle^{1/2}}. \tag{2.47}$$

Note: A standard implementation is given in QuTiP ([18]).

Homodyne Detection [23, 29]

We will consider a single channel here for simplicity. In this type of measurement, the output field is projected onto one of its quadratures (say $X \propto L + L^\dagger$). It produces a measurement process

$dM_X(t) = \langle L(t) + L^\dagger(t) \rangle dt + dW_t$, where dW_t is an increment of a Wiener process satisfying $dW_t^2 = dt$. The state evolves conditionally on the measurement process according to

$$d|\psi\rangle = \left(-(iH_S + \frac{1}{2}L^\dagger L dt) + L dM_X(t) \right) |\psi\rangle . \tag{2.48}$$

This equation is often called the stochastic Schrödinger equation. Above in (Eq. 2.48) one can also include normalization terms, but in practice it is convenient to simulation the unnormalized equation and then directly normalize the state.

Heterodyne Detection [23]

In this case both quadrants are being measured, with noise terms being induced equally on both. This can be thought of as projecting the system onto a coherent state. This results in the measurement process $dM(t) = \langle L(t) \rangle dt + d\xi_t$, where $d\xi_t = \frac{dW_t^{(1)} + i dW_t^{(2)}}{\sqrt{2}}$ and each $dW_t^{(i)}$ is an independent increment of a Wiener process (ξ_t is known as a complex Wiener process). The state evolves conditionally on the measurement according to

$$d|\psi\rangle = \left(-(iH_S + \frac{1}{2}L^\dagger L dt) + L dM^*(t) \right) |\psi\rangle . \tag{2.49}$$

As before it is possible to include normalization terms. This equation is often called quantum state diffusion.

Remark: The above equations can be extended naturally to the case when a system has multiple channels, and each channel is being measured by a detector.

Chapter 3

Passive linear systems with coherent feedback

Abstract

Networks of open quantum systems with feedback have become an active area of research for applications such as quantum control, quantum communication and coherent information processing. A canonical formalism for the interconnection of open quantum systems using quantum stochastic differential equations (QSDEs) has been developed by Gough, James and co-workers and has been used to develop practical modeling approaches for complex quantum optical, microwave and optomechanical circuits/networks. In this chapter we fill a significant gap in existing methodology by showing how trapped modes resulting from feedback via coupled channels with finite propagation delays can be identified systematically in a given network. Our method is based on the Blaschke-Potapov multiplicative factorization theorem for inner matrix-valued functions, which has been applied in the past to analog electronic networks. Our results provide a basis for extending the Quantum Hardware Description Language (QHDL) framework for automated quantum network model construction [56] to efficiently treat scenarios in which each interconnection of components has an associated signal propagation time delay.

This chapter was published as an article in [55], and was slightly adapted for the purposes of the dissertation.

3.1 Preliminaries

In the spirit of SLH/QHDL we assume that we are given a network of open quantum systems whose input and output ports are connected by passive linear channels. We additionally assume that an end-to-end propagation time delay is specified for each channel. If feedback loops are created by the network topology, trapped modes will be created that may need to be modeled dynamically in order to accurately simulate the overall behavior of the network.

The basic problem lies in choosing a procedure for embedding new stateful dynamics into the "space between components" in an SLH network. Prior work such as [46] has addressed the question of how to model an individual channel with finite time delay efficiently, however, our philosophy here will be to work at the level of more complex sub-networks that mediate interconnections among multiple-input/multiple-output components. Our method is restricted to sub-networks that are linear and passive, and thus may include components such as beam-splitters and phase shifters but not, *e.g.*, gain elements or nonlinear traveling-wave interactions. We nevertheless gain a significant advantage by considering linear passive sub-networks in that we are able to recognize the creation of trapped modes by feedback with finite time delays, and can provide a systematic procedure for adding the stateful dynamics required to simulate the behavior of such modes within a frequency band of interest.

We treat channels as passive linear quantum stochastic systems [36, 37, 43, 44] whose input-output behavior can be characterized by the relationship of the input and output annihilation fields only. The input-output relationship for a linear system must satisfy certain physical realizability conditions. Our systematic method preserves the physical realizability condition while allowing us to simulate the system with only a small number of degrees of freedom.

Essentially our approach introduces an approximation with finitely many state-space variables to a given system (we will refer to such a system as a finite-dimensional system). For a system with N input and output ports and M oscillator modes $a_1, ..., a_M$ satisfying the canonical commutation relations

$$[a_i, a_j^*] = \delta_{ij}, \qquad [a_i, a_j] = 0, \qquad [a_i^*, a_j^*] = 0, \tag{3.1}$$

a passive linear model can be described by the input-output relations Eq. (2.35). The A, B, C, D are complex-valued matrices of appropriate size. We will refer to this formulation as the state-space representation, or the $ABCD$ formulation, of the system. It is related to the SLH formalism by Eq. (2.37).

Our approach seeks to approximate the transfer function within a given frequency range by selecting only a finite subset of the original modes and generating a state-space representation using the information close to the zeros or poles of the modes. The resulting approximation is a passive linear system satisfying the physical realizability condition. We discuss a sufficient condition for our approximation to converge to the true transfer function for a large class of possible transfer functions.

There are other approaches that could be used to obtain a different set of modes that may approximate the system of interest. For example, one approach may involve approximating each delay term in the system using a symmetric Padé approximation, which would result in a physically realizable component (see Appendix A.4). Although this approach can be simple to use, the Padé approximation will not always introduce the zeros and poles of the transfer function at the correct locations, and may introduce spurious zeros and poles to the approximated transfer function. On the other hand, the zero-pole interpolation by construction adds zeros and poles to the approximated transfer function only when they are present in the original transfer function. This feature of our approach may be important in many physical applications because the locations of the zeros and poles have physically meaningful consequences, including the resonant frequencies and linewidths of the effective trapped cavity modes resulting in the network due to feedback. Nevertheless, as discussed in Section 3.7, there are passive linear systems for which the zero-pole interpolation is insufficient – in this case, a finite-dimensional state-space representation will necessarily have spurious zeros and poles.

3.2 Problem Characterization

Throughout we work in the frequency domain. Unless otherwise noted, we will be working specifically in the s-domain. This representation of a linear system is obtained from the time-domain representation of the state-space by applying the Laplace transform. Below $F(z)$ is the Laplace transform of $f(t)$:

$$F(z) = \int_{-\infty}^{\infty} e^{-zt} f(t) dt. \tag{3.2}$$

Here, $z = \sigma + i\omega$ for $\sigma, \omega \in \mathbb{R}$. When $\sigma = 0$, $z = i\omega \in i\mathbb{R}$ represents a real frequency. We consider a linear system with N input and N output ports. We will primarily be interested in a system which is linear, passive, and has a transfer function $T(z)$ that is unitary for all $z \in i\mathbb{R}$. The last condition guarantees that the system conserves energy. We remark that more generally the loss of energy can

be considered for example by adding additional ports. We assume throughout the transfer function is a meromorphic matrix-valued function. For simplicity, we assume that each pole has multiplicity one.

We will be particularly interested in a system consisting of time delays and beamsplitters. A delay of length T has transfer function of the form e^{-zT}. In general, any system of delays and beamsplitters can be written as

$$\begin{pmatrix} H \\ H_{\text{out}} \end{pmatrix} = \begin{pmatrix} M_1 & M_2 \\ M_3 & M_4 \end{pmatrix} \begin{pmatrix} E(z)H \\ H_{\text{in}} \end{pmatrix}. \tag{3.3}$$

Here H_{out} and H_{in} are respectively the N-dimensional input and output signals, and H are internal signals of the system. The values of H are taken on each edge with a delay before the signal passes through the delay. The M_i are constant matrices of the appropriate size determined by the specific details of the system. $E(z)$ is a diagonal matrix whose diagonal elements are the transfer functions of the various delays in the system, $e^{-zT_1}, e^{-zT_2}, ..., e^{-zT_N}$. The system is illustrated abstractly in Figure 3.1.

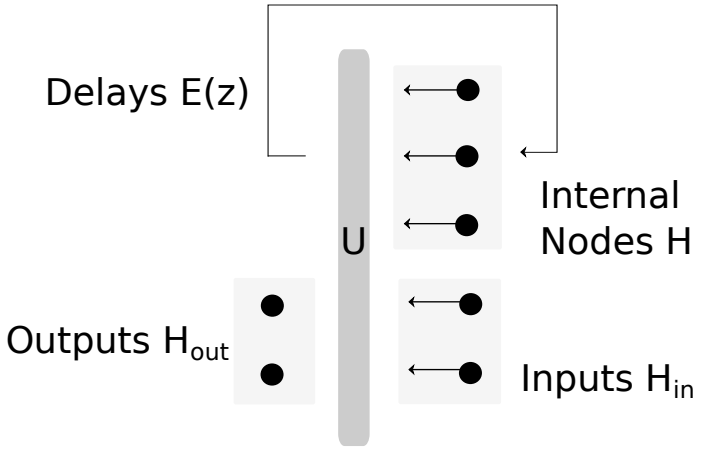

Figure 3.1: An illustration demonstrating the set-up used to characterize the problem. This network is described by eq. 3.4. The U in the figure represents a unitary component.

The transfer function of the given system can be formally solved as

$$H_{\text{out}} = T(z)H_{\text{in}} = [M_3E(z)(I - M_1E(z))^{-1}M_2 + M_4]H_{\text{in}} = [M_3(E(-z) - M_1)^{-1}M_2 + M_4]H_{\text{in}}. \tag{3.4}$$

Notice that this transfer function will have poles when

$$\det(I - M_1 E(z)) = 0. \tag{3.5}$$

We can define the zeros of this transfer function as z satisfying $\det(T(z)) = 0$.

Throughout, we will also assume that the system is asymptotically stable. In terms of the network transfer function, all the eigenvalues of M_1 have norm less than 1, with the consequence that $T(z)$ is bounded for $\Re(z) \geq 0$.

This transfer function has the important feature of being unitary whenever z is purely imaginary. That is, $T(i\omega)T^\dagger(i\omega) = T^\dagger(i\omega)T(i\omega) = I$ whenever $\omega \in \mathbb{R}$. This is exactly the physical realizability condition for a passive linear system. We will refer to this constraint throughout the chapter as the *unitarity constraint*. One consequence of this condition that can be obtained by analytic continuation is that $T(z)T^\dagger(-\overline{z}) = I$ except when a pole is encountered.

Some observations. We see that the poles and zeros occur in pairs $z, -\overline{z}$. In this chapter we will refer to such a pair as a *zero-pole pair*. In general, we observe that there may be infinitely many solutions to eq. (3.5). If we take M_1 to be a real matrix, z is a pole whenever $\overline{z}$ is also a pole. Furthermore, applying the maximum modulus principle shows the system is stable (see Appendix A.2). This implies that the poles appear in the left half-plane.

The solution to eq. (3.5) can be found numerically within a bounded subset of $\mathbb{C}$. There are dedicated algorithms that use contour integration to guarantee finding all the roots within a contour, which we briefly discuss in Section 3.5.1. In the special case when the time delays are commensurate, we can re-write the equation for the poles as a polynomial equation of the variable $w = e^{-zT_0}$ for some T_0. Doing this will make the root fiding procedure much more simple.

If the system has passive linear components other than delays and beamsplitters, the transfer function shown above may be modified. It will still have the same important features that the poles appear on the left half-plane (except when the system is marginally stable) and the function restricted to the imaginary axis is unitary.

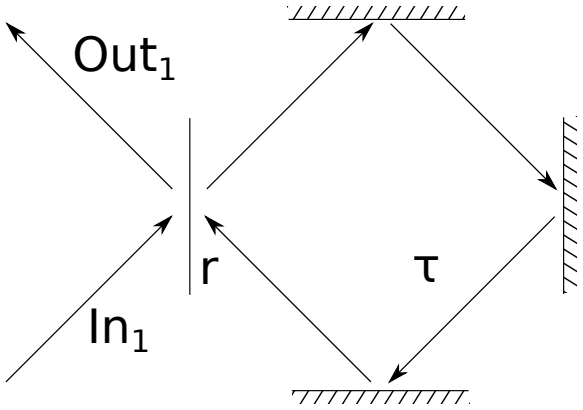

Figure 3.2: An illustration a single time delay τ and a single beamsplitter with reflectiveness r.

3.3 Specific Example and Approximation Procedure: One time delay and one beamsplitter

We will consider the example illustrated in Figure 3.2, where a single beamsplitter and time delay are combined to form a single-input and single-output (SISO). The example here is analogous to the one considered in Section VII B of [19].

In this particular example, with the convention that the beamsplitter has the transfer function

$$T_{BS} = \begin{pmatrix} t & -r \\ r & t \end{pmatrix}$$

where $r^2 + t^2 = 1$. and the time delay of length τ has transfer function

$$T_\tau(z) = e^{-\tau z}.$$

One will find the resulting transfer function of the combined system drawn above is

$$T(z) = \frac{e^{-\tau z} - r}{1 - re^{-\tau z}}. \tag{3.6}$$

The poles p_n for $n \in \mathbb{Z}$ are found to be

$$p_n = \frac{1}{\tau}\left(\ln(r) + 2\pi i n\right). \tag{3.7}$$

Notice that the real part is negative, as it should be for a stable system. Each of the poles in the

system here corresponds to a cavity mode. The imaginary part corresponds to the mode frequency and the real part determines the linewidth properties. With this interpretation, we can readily relate the free spectral range to the delay length. In an attempt to approximate the system, we can consider a product of the following form of terms having the same (simple) poles as $T(z)$, satisfying the unitarity condition, and agreeing in value with $T(z)$ at $z = 0$.

$$\tilde{T}(z) = -\prod_{n\in\mathbb{Z}} \left(\frac{z + \overline{p_n}}{z - p_n} \right). \tag{3.8}$$

For more general infinite products we might need to introduce additional phase factors c_n in each product term to ensure the convergence of the product. However, this is not necessary in the example discussed here.

One interpretation of each term in the product is the frequency-domain representation of a cavity mode. We can obtain an approximation for $T(z)$ by truncating the product with a finite number of poles. The resulting rational function can then be interpreted as the transfer function of a finite-dimensional system.

Notice that the procedure used to obtain $\tilde{T}(z)$ does not guarantee that $\tilde{T}(z) = T(z)$, although this is indeed the case for the example above. In general the procedure above may not capture some of the properties of the system. For example, if we added another delay with no feedback in sequence, we would obtain an additional phase factor dependent on z, while still satisfying the desired properties. For a SISO system satisfying the unitarity constraint with the same root-pole pairs, a phase dependence $T(z) = \tilde{T}(z)e^{-\alpha z}$ ($\alpha \geq 0$) is actually the most general modification we might need. For a system satisfying the same conditions but having N input and output ports, the $e^{-\alpha z}$ term will be replaced by a similar singular function which we will refer to throughout as the *singular* term (see Section 3.4.1 for a discussion). An illustration of $T(z)$ and the transfer function resulting when an additional delay is augmented to the system is illustrated in Figure 3.3.

Notice how the augmented delay substantially changes some of the properties of the transfer function in the complex plane. For instance, when $\Re(z) \to -\infty$, the transfer function in Figure 3.3a approaches a constant, while that in Figure 3.3b diverges. In Section 3.7 we will be able to utilize the difference in behavior of transfer functions to determine whether they incorporate a nontrivial everywhere analytic term, like the exponential resulting from a time delay.

We can check to see if such a factor is needed in the factorization above. Assuming that $\lim_{\Re(z)\to-\infty} \tilde{T}(z) = C \neq 0$, (see Appendix A.5), we can take $\lim_{\Re(z)\to-\infty} T(z)$ to check if the additional phase factor is present in $T(z)$. We see $\lim_{\Re(z)\to-\infty} T(z) = -1/r$, which shows in our example that no such

additional term is needed, and therefore $\tilde{T}(z) = T(z)$. It can be confirmed numerically that the values of $T(z)$ and $\tilde{T}(z)$ agree.

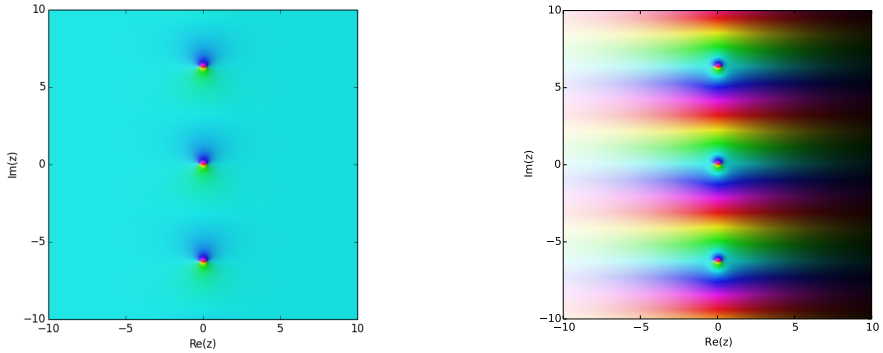

(a) $T(z) = \frac{e^{-z}-r}{1-re^{-z}}$.

(b) $T(z) = \frac{e^{-z}-r}{1-re^{-z}}e^{-z}$.

Figure 3.3: The plots here compare two transfer functions as seen in the complex plane. The hue and the brightness correspond to the phase and magnitude, respectively. The transfer function plotted in Figure 3.3a corresponds to a cavity with $r = 0.8$ and $\tau = 1$ while that in Figure 3.3b in addition augments a delay of length τ in sequence with the original system.

In the rest of the chapter, we will show how a similar procedure can be applied more generally to multiple-input and multiple-output (MIMO) systems.

3.4 Factorization theorem and implications for passive linear systems

Certain kinds of matrix valued functions can be factored using the Potapov factorization thoerem. The more general factorization theorem is discussed in Appendix A.3.2. Here we discuss the special case for a passive linear system satisfying the unitarity condition.

3.4.1 Special case of the factorization theorem for passive systems

To apply the factorization, we need the transfer function to be contractive (That is, $I - T(z)T(z)^\dagger \geq 0$). See Appendix A.2 for the justification of this condition. After some simplifications discussed in

A.3.2, we find that the factorization has the following form.

$$T(z) = UB(z)S(z), \tag{3.9}$$

where

$$B(z) = \prod_{k=1}^{\infty} B_k(z), \qquad S(z) = \overset{\curvearrowright}{\int_0^\ell} e^{-zH(t)dt}. \tag{3.10}$$

In the product, each of the terms B_k has the form

$$B_k(z) = V_k \begin{pmatrix} e^{i\phi_k}\frac{z-\lambda_k}{z+\overline{\lambda_k}} I_{p'_k} & 0 \\ 0 & I \end{pmatrix} V_k^{-1} = I - P_k + A_k(z)P_k. \tag{3.11}$$

The B_k terms are the Blaschke-Potapov factors written in the s-plane (see Appendix A.1), the U is some unitary matrix, and the $S(z)$ is defined in eq. (A.4) in Appendix A.3.1, where we set $J = I$. We use the symbol $\overset{\curvearrowright}{\int}$ to refer to the *multiplicative integral*, or product integral. The P_k is an orthogonal projection, $A_k(z) = \frac{z-\lambda_k}{z+\overline{\lambda_k}} e^{i\phi_k}$, and $\phi_k = \phi_k(\lambda_k)$ is a phase factor to guarantee the convergence of the product. When $B(z)$ is a finite product, the phase factors ϕ_k can be absorbed into U.

We will refer in the future to the terms $B(z)$ and $S(z)$ respectively as the Potapov product and the singular term. Both $B(z)$ and $S(z)$ are inner functions.

3.4.2 Interpretation as cascaded passive linear network

We remark the Blaschke-Potapov factorization for an inner function can be interpreted as a limiting case of a system of beamsplitters, feedforward delays, and cavity modes.

First, we will interpret the Blaschke-Potapov product in the optical setting. Each unitary matrix appearing in the factorization can be interpreted as a generalized beamsplitter. Each Blaschke factor with zero λ_k has the form $B_k(z)$ of eq. (3.11) in Section 3.4.1. We can interpret $A_k(z)$ in eq. (3.11) as the transfer function of a single cavity mode. The location of the zero λ_k in the complex plane determines the detuning and linewidth of the mode. The modes resulting from the Blaschke-Potapov product can be visualized as a sequence of components of the form portrayed in Figure 3.4.

Next, we shall interpret the singular term represented as the multiplicative integral in eq. (A.9)

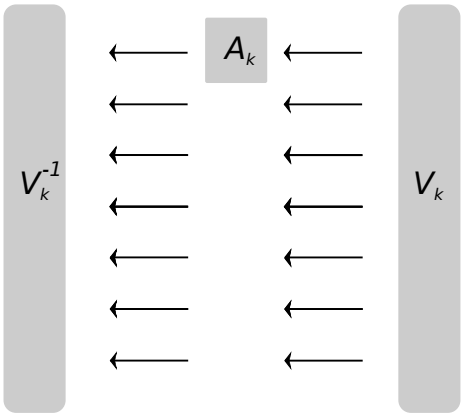

Figure 3.4: A physical interpretation of a single Blaschke-Potapov term for a passive linear system. Here the V_k represents a beamsplitter and the A_k represents a passive SISO system with a single degree of freedom. The zero-pole interpolation generates a series of factors of this form in a cascade.

of Appendix A.3.2. Approximating the multiplicative integral with intervals $\Delta t_k = t_{i+k} - t_k$, we obtain a product of terms of the form

$$e^{-z\Delta H(t_k)} = U_k e^{-zD_k} U_k^\dagger, \tag{3.12}$$

which is interpreted as a component consisting of parallel feedforward delays illustrated in Figure 3.5. Here $\Delta H(t_k) = H_{k+1} - H_k \geq 0$, U_k are some unitary matrices resulting in the diagonalization $\Delta H(t_k) = U_k D_k U_k^\dagger$, and we find $\mathrm{tr}(\Delta H(t_k)) = \Delta t_k$ is the sum of the delays in this component found in the parallel ports. It is possible to further approximate the feedforward delays in the factorization with modes, but for conceptual purposes we do not do this here.

3.5 Approximation Procedure – Zero-Pole Interpolation

In order to reconstruct an approximation for the transfer function $T(z)$ using only a finite number of modes, we will use a two-step procedure. The first step consists of finding the zero-pole pairs in a region of interest. The second step consists of examining the numerical values of the transfer function near the zeros or poles to obtain the correct form of each of the Blaschke-Potapov terms, which are determined up to a constant unitary factor. The product of the resulting terms will equal a truncated version of the Blaschke-Potapov product discussed in Section 3.4.1, and will approximate the transfer function in the region of interest.

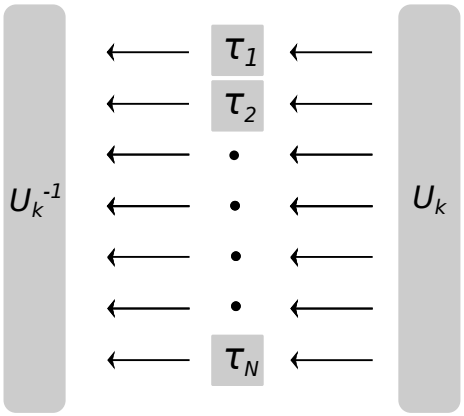

Figure 3.5: An illustration of the physical interpretation of a component resulting in the approximation of the multiplicative integral. Here the U_k represents a beamsplitter and each τ_j $(j = 1, ..., N)$ represents a delay of that duration.

We will take a transfer function T and obtain an M-dimensional approximation by identifying appropriate factors for a Blaschke-Potapov product. It is possible that the transfer function may have a nontrivial singular component (i.e. a nontrivial everywhere analytic term) as discussed in Section 3.4.1, in which case the zero-pole interpolation may not reproduce a converging sequence of approximations to the given transfer function $T(z)$. In this section we assume that the singular term is trivial or otherwise unimportant. In any case we determine U in eq. 3.9 of Section 3.4.1 using $T(0)$.

A trivial example when the above approach might fail is a delay with no feedback at all. In this case, there are no poles to evaluate and the method fails. When a transfer function is entirely singular, or when its singular component cannot be neglected, a different approach will be needed, such as using the Padé approximation. This is discussed in Appendix A.4.

3.5.1 Identifying Mode Location.

We remind the reader that we take our coordinate system in the s-domain. We assume for simplicity that we are interested in the behavior of the system near the origin. However, our procedure can be used to obtain approximations of the given transfer function for arbitrary regions in the s-plane. In order to identify the appropriate modes, we find roots of the transfer function of the full system, $p_1, ..., p_M$. Each root will represent a "trapped" resonant mode. In general, there will be infinitely many such roots in the full system, so it is important to have a criterion for selecting a finite number of roots. Each root will have an imaginary part, which will correspond to the frequency of

the mode, and a real part, which is linked to the linewidth of the mode. One criterion might be to select root whose imaginary part falls in some range $[-\omega_{max}, \omega_{max}]$, so that the approximation is valid for a particular bandwidth. This approximating system may be improved by increasing the maximum frequency, $\omega_{\max}$. As the number of root-pole pairs increases, the quality of the approximation increases, but in addition the approximated system will incur a greater number of degrees of freedom.

Luckily there is a well-known technique that can be used based on contour integration developed in [8]. This algorithm runs in a reasonable time and can essentially guarantee that it does indeed finds all of the desired points. The latter point is an important feature that most typical root-finding algorithms do not have because they do not utilize the properties of analytic functions. For details about a more polished algorithm see [31]. Methods of this kind require a contour in the complex plane as the input in which the roots of the function will be found. This contour may be, for example, a rectangle in the complex plane. In practice we may make use of symmetries in the system and the known regions where poles and zeros are located.

In Figure 3.6 we illustrate the step of our procedure for finding roots or poles. The various contours in dashed lines represent areas where roots and poles will be found. Notice in this plot that the roots and poles lie along a strip close to the imaginary axis. This is a typical feature for systems of this kind. If the maximum possible real part of each root is determined for the system of interest, a computational advantage can be gained since the contour does not need to be extended beyond that value.

3.5.2 Finding the Potapov Projectors

The procedure we use assumes that the given transfer function $T(z)$ has a specific form guaranteed by the factorization theorem (see eq. (3.9) in Section 3.4.1). For the purposes of this section, we neglect the contribution due to the singular term (the $S(z)$ in eq. (3.9)). This procedure is similar to the zero-pole interpolation discussed in [2]. We handle the singular term separately, as we will discuss in 3.7.

We introduce an inductive procedure for this purpose. Each step will involve extracting a single factor of the Blaschke-Potapov product. Suppose the full transfer function being approximated is $T(z)$. write

$$T(z) = \tilde{T}(z)\left(I - P + P\left(\frac{z+\overline{p}}{z-p}\right)\right) \tag{3.13}$$

The P is in general the orthogonal projection matrix onto the subspace where the multiplication by the Blaschke factor takes place. We wish to extract the P given the known location of the pole p, which we assume to be a first-order pole for simplicity. We also assume for simplicity that P is a rank one projection, and so it can be written as the product of a normalized vector

$$P = vv^{\dagger}.$$

The simplifying assumptions above have been sufficient for the systems we inspected, and could be easily removed. Rewriting,

$$T(z)(z-p) = (z-p)\tilde{T}(z)(I-P) + (z+\overline{p})\,\tilde{T}(z)vv^{\dagger}. \tag{3.14}$$

Now take $z \to p$. We assumed that $T(z)$ has a first-order pole at p, so $\tilde{T}(z)$ will be analytic at p. Therefore, the first term on the right hand side goes to zero. Taking $L \equiv \lim_{z\to p} T(z)(z-p)$, we get

$$L = (p+\overline{p})\,\tilde{T}(p)vv^{\dagger}. \tag{3.15}$$

Since we assumed that P is a rank one projector, have obtained an expression where L must also be rank one. In order to find v we can simply find the normalized eigenvector corresponding to the nonzero eigenvalue of L. This task may be done numerically. Finally, we can find the $\tilde{T}(z)$ from eq. (3.13) above.

The procedure outlined above may be repeated for each of the M desired roots of $T(z)$ to obtain a factorization

$$T(z) = T_M(z) \prod_{k=1}^{M} \left(I - P_k + P_k \left(\frac{z+\overline{p}_k}{z-p_k} \right) \right). \tag{3.16}$$

We assume that the $T_M(z)$ is close to a constant in the region of interest. This is exactly true in the case where the transfer function T has only the M roots picked. We can approximate T_M with a unitary factor that can be determined from T and the product in eq. (3.16) evaluated at some point z_0 in the region of interest.

The computer code for this procedure can be obtained by contacting the authors.

3.6 Examples of zero-pole decomposition

In this section, we show two examples. For both examples, we show the network discussed in Figures 3.7 and 3.9. We plot the various components of the transfer functions of these networks along $i\omega$ for $\omega \geq 0$ in Figures 3.8 and 3.10, respectively. Along both examples, we also plot several approximate transfer functions determined by the zero-pole interpolation of Section 3.5. The approximate transfer functions correspond to a Blaschke-Potapov product that has been truncated to a certain order. In both examples we see that as we increase the number of terms, the approximation improves. The first example illustrates the case when the zero-pole interpolation converges to the correct transfer function. In the second example, while the zero-pole interpolation appears to converge, the function to which it converges deviates from the original transfer function. This suggests that the singular term $S(z)$ in Section 3.4.1 makes a contribution for which the zero-pole interpolation does not account. In Section 3.7, we discuss a condition for convergence and show how the effects of the singular term may be separated from the rest of the system. Figure 3.10 also includes the transfer function once the singular term has been removed, demonstrating the zero-pole approximations converge to that function.

3.6.1 Example 1. Zero-pole interpolation converges to given transfer function

The first example we discuss involves two inputs and two outputs. Figure 3.7 shows this network explicitly. In Figure 3.8 we see the zero-pole interpolation appears to converge to the correct transfer function. We can check this by confirming that the M_1 is nonsingular, as we will show in Section 3.7.

The matrices of eq. (3.3) in Section 3.2 are given by

$$M_1 = \begin{bmatrix} 0 & -r_1 & 0 & 0 \\ -r_2 & 0 & t_2 & 0 \\ 0 & 0 & 0 & -r_3 \\ t_2 & 0 & r_2 & 0 \end{bmatrix}, \qquad M_2 = \begin{bmatrix} t_1 & 0 \\ 0 & 0 \\ 0 & t_3 \\ 0 & 0 \end{bmatrix}, \tag{3.17}$$

$$M_3 = \begin{bmatrix} 0 & t_1 & 0 & 0 \\ 0 & 0 & 0 & t_3 \end{bmatrix}, \qquad M_4 = \begin{bmatrix} r_1 & 0 \\ 0 & r_3 \end{bmatrix}. \tag{3.18}$$

Here $\tau_1 = 0.1, \tau_2 = 0.23, \tau_3 = 0.1, \tau_4 = 0.17, r_1 = 0.9, r_2 = 0.4, r_3 = 0.8$.

3.6.2 Example 2. Zero-pole interpolation fails to converge to given transfer function

In the next example, we have two inputs and two outputs, as in the first example of Section 3.6.1. However, the design of the network is significantly different. The network for this example is shown in Figure 3.9. This example combines elements of an interferometer and an optical cavity. In some regimes, such as $\tau_4 << \tau_2$, the zero-pole decomposition yields a good approximation for the transfer function. In general, however, the singular component of the transfer function must be incorporated in some other way.

The matrices of eq. (3.3) in Section 3.2 are given by

$$M_1 = \begin{bmatrix} 0 & 0 & -r & 0 \\ r & 0 & 0 & 0 \\ 0 & r & 0 & t \\ t & 0 & 0 & 0 \end{bmatrix}, \qquad M_2 = \begin{bmatrix} t & 0 \\ 0 & t \\ 0 & 0 \\ 0 & -r \end{bmatrix}, \tag{3.19}$$

$$M_3 = \begin{bmatrix} 0 & 0 & t & 0 \\ 0 & t & 0 & -r \end{bmatrix}, \qquad M_4 = \begin{bmatrix} r & 0 \\ 0 & 0 \end{bmatrix}. \tag{3.20}$$

Here $\tau_1 = 0.1, \tau_2 = 0.039, \tau_3 = 0.11, \tau_4 = 0.08, r = 0.9$.

The important differentiating feature from the previous example of Section 3.6.1 is that the singular term for the transfer function of this network is nontrivial. This can be seen when examining the resulting transfer functions from the zero-pole interpolation, which are shown in Figure 3.10. In Section 3.7 we will show that this condition can be checked by observing that the M_1 in eq. (3.19) is singular.

In Figure 3.10, we see that the zero-pole interpolated transfer functions deviate from the true transfer function in the $(0, 1)$ and $(1, 1)$ phase components. This demonstrates how in general it is important to consider the singular function. On the other hand, for the systems in consideration it is possible to separate the Blaschke-Potapov product from the singular term, which corresponds to feedforward-only components, as discussed in Section 3.7.3. In black we graph the transfer function components resulting once the feedforward-only components have been removed. Up to a unitary factor, this function is equal to the infinite Potapov product. We see that the approximated transfer functions from the zero-pole interpolation converge to this function.

3.7 The Singular Term

In this section, we examine the factorization of the transfer function with $J = I$ given in eq. (3.9) in Section 3.4.1. In the form of the fundamental theorem by Potapov that we obtained, we had an infinite product of Blaschke-Potapov factors and a singular term. Although the zero-pole decomposition allowed us to extract the Blaschke-Potapov factors, they gave us no information regarding the singular term. In some systems, it may be crucial to include the singular term to obtain a good approximation of the system. To learn about this term, we will need a different method.

In this section, we give the condition for the singular term to be trivial. This condition can then be specialized to the network from Section 3.2. Based on this condition, we can develop a method to explicitly separate the network given in eq. (3.4) in Section 3.2 into the Potapov product and the singular term.

3.7.1 Condition for the multiplicative integral term to be trivial

We examine the form of the singular term in the factorization theorem and notice that its determinant becomes large when $\Re(z) \to -\infty$. To avoid mathematical details, we will assume here that the Blaschke-Potapov product $\prod B_k(z)$ is well-behaved in the limit $\Re(z) \to -\infty$ in the sense that the limit of the product converges (to a nonzero constant). Justification for this assumption is discussed further in Appendix A.5. We have the following observations.

Observation. If $\lim_{\Re(z)\to-\infty} T(z)$ is a constant, then the multiplicative integral in eq. (3.9) of Section 3.4.1 is a constant.

This follows from the properties of the multiplicative integral defined in eq. (A.4) of Appendix A.3.1. □

Observation. In particular, for the transfer function $T(z)$ in eq. (3.4) of Section 3.2, $\lim_{\Re(z)\to-\infty} T(z)$ is a constant if and only if M_1 in eq. (3.4) is full-rank. This gives a sufficient condition for when the zero-pole expansion converges exactly.

To obtain this result, it is enough to consider the term $(E(-z) - M_1)^{-1}$ in the limit $\Re(z) \to -\infty$. □

The above observations can be seen in the two examples discussed in Section 3.6. In example 1, the M_1 matrix is full-rank, while in example 2 it is not.

3.7.2 Maximum contribution of singular term

For many applications we anticipate that we may be able to drop the contribution of the singular term altogether. One example is an optical cavity in certain regimes. If the lifetime of the modes in the cavity is long in comparison to the delays in the system, we would expect the delays to be less significant. We would like to be able to provide a justification for when it is acceptable to neglect the singular term.

First, we will obtain the maximum value for ℓ necessary in the multiplicative integral appearing in eq. (3.10) of 3.4.1. This is an important result because it tells us that the lengths of the delays themselves determines the greatest contribution of the singular function.

Remark: To apply the factorization in eq. (3.9) of Section 3.4.1 to the transfer function in eq. (3.4) of Section 3.2, it suffices to take $\ell \leq \sum_k T_k$.

This can be seen by noting the scaling of $\det[(E(-z) - M_1)^{-1}]$ in the limit $\Re(z) \to -\infty$. $\square$

The above bound occurs in the case of several delays feeding forward in sequence.

We can give one condition under which the singular term can be dropped: $|z| << 1/\ell$. Furthermore, crude estimates for the error can now be found using the Taylor expansion of the exponential.

Intuitively, Potapov factors correspond to resonant modes while the singular function corresponds to feedforward-only components. With this interpretation, we see see that the zero-pole interpolation yields a transfer function close to the true transfer function when the feedforward-only term can be neglected. We can interpret ℓ as an upper bound on the duration of time the signal can spend being being fed-forward only. When $1/\ell$ becomes large with respect to the size of the region of interest in the frequency domain, the feedforward-only terms become unimportant.

3.7.3 Separation of the Potapov product and the singular term in an example

In this section, we discuss how for a network of beamsplitters and delays the Blaschke-Potapov product and the singular term of Section 3.4.1 can be separated explicitly. We will give a systematic procedure at least with the simplifying assumption that the delays are commensurate.

To motivate intuitively the procedure we will use, we demonstrate it for the case of the example in Section 3.6.2. In this network, extracting a single feedforward delay is sufficient for obtaining the separation of the two terms we desire. We will assume that $\tau_2 < \tau_4$. The important observation is

that a collection of k parallel delays can be commuted with a given a unitary component U of k ports. This is illustrated in Figure 3.11a.

Next, it becomes apparent in the new network in Figure 3.11a that one of the internal system nodes is unnecessary, since it is followed by a delay of duration zero (call it H_X). For this reason, H_X can be eliminated from the system. In the process, we can combine two of the unitary components preceding and following H_X to form a separate unitary component, illustrated in Figure 3.11b. The network depicted in Figure 3.11b has a feedforward-only component (the identity following In_0 and the delay τ_2 following In_1) followed by a network for which the M_1 matrix is invertible, and therefore has trivial singular part.

3.7.4 Systematic Separation of Potapov product and analytic term for passive delay networks

Suppose we have a system given in the form of eq. (3.4) in Section 3.2. Our observation that in order for the multiplicative integral term to be trivial we need M_1 to be invertible suggests that there may be a way to isolate the Potapov product term from the remaining analytic function. We now present a systematic way of doing this. For simplicity we will assume that all the delays have equal durations, so that $E(z)$ is a multiple of the identity.

The essential idea is to make a change of basis that allows the elimination of a node at the expense of modifying the inputs in such a way that a part of the analytic term can be extracted from the network. We are interested in the case with M_1 not invertible. When this is the case, we can find some change of basis represented by the matrix S such that

$$M_1 = SJS^{-1}, \tag{3.21}$$

where the J is the Jordan decomposition such that the zero eigenvalue block is at the right bottom block of J. We introduce $\bar{H} = S^{-1}H$ and rewrite the equation for H in eq. (3.4) of Section 3.2 as

$$\bar{H} = JS^{-1}E(z)S\bar{H} + S^{-1}M_2H_{\mathrm{in}}. \tag{3.22}$$

Now, $\bar{H}_1 = [S^{-1}M_2H_{\mathrm{in}}]_1$, which depends only on the inputs. We can separate the dependence of the remaining coordinates of $\bar{H}$ on each other and the inputs only. Explicitly, denoting the last column of S by S_1 and the matrix of columns excluding the last $S_{\setminus 1}$, and similarly the vector of components of $\bar{H}$ before the last as $\bar{H}_{\setminus 1}$ and the matrix of rows of J preceding the last as $J_{\setminus 1}$, we

can write

$$\bar{H}_{\setminus 1} = J_{\setminus 1} S^{-1} E(z) \left[S_1 \bar{H}_1 + S_{\setminus 1} \bar{H}_{\setminus 1} \right] + S^{-1} M_2 H_{\text{in}}. \tag{3.23}$$

We can now separate the network into two networks. The first network takes the original inputs H_{in} and yields the outputs

$$\tilde{H}_{\text{in}} = J_{\setminus 1} S^{-1} E(z) S_1 [S^{-1} M_2 H_{\text{in}}] + S^{-1} M_2 H_{\text{in}}. \tag{3.24}$$

Notice the first network is a feedforward network (i.e. no signal feeds back to a node from which it originated). The second network takes the $\tilde{H}_{\text{in}}$ as inputs and yields the outputs

$$\bar{H}_{\setminus 1} = J_{\setminus 1} S^{-1} E(z) S_{\setminus 1} \bar{H}_{\setminus 1} + \tilde{H}_{\text{in}}. \tag{3.25}$$

Using the simplifying assumption that the $E(z) = Ie(z)$ is a multiple of the identity, we obtain

$$\bar{H}_{\setminus 1} = \tilde{J} e(z) \bar{H}_{\setminus 1} + \tilde{H}_{\text{in}}, \tag{3.26}$$

where the $\tilde{J}$ is matrix resulting from dropping the last row and column in J. We see that eq. (3.26) has the same form to the original equation for H in eq. (3.4) in Section 3.2. The difference is that now the $\tilde{J}$ replaces M_1, and has one fewer zero eigenvalue. Conveniently, $\tilde{J}$ is also in its Jordan normal form, so the procedure can be repeated until the matrix ultimately replacing M_1 (call it $\tilde{M}_1$) has no zero eigenvalues left. In this case $\tilde{M}_1$ is an invertible matrix, which is exactly the condition we needed for the transfer function of the network to consist of only the Potapov product and not the multiplicative integral.

A very simple example illustrating the intuition of our procedure is a network where the internal nodes all feed forward in sequence. Explicitly, take

$$M_1 = \begin{pmatrix} 0 & 1 & 0 & 0 \\ 0 & 0 & 1 & 0 \\ 0 & 0 & 0 & 1 \\ 0 & 0 & 0 & 0 \end{pmatrix}. \tag{3.27}$$

Notice that this matrix is already in its Jordan-canonical form, so the analysis becomes transparent. Also notice that all of the eigenvalues of M_1 are zero, which implies that our procedure will extract all the delays and collect them in the singular term.

3.8 Relationship to the ABCD and SLH formalisms

In this section we demonstrate how the approximating system our procedure designs is physically realizable. In particular we show how to extract the ABCD and SLH forms for a single term resulting in the truncated Blaschke-Potapov product designed to approximate the transfer function of the system. Since the transfer function is equal to a product of such terms, we can interpret the approximating system as a sequential cascade of single-term elements of this form.

The state-space representation of the Potapov factor will have the form

$$B(z) = C(Iz - A)^{-1}B + D. \tag{3.28}$$

To obtain the ABCD model for a single Potatpov factor, begin with the following factor.

$$B(z) = I - vv^{\dagger} + vv^{\dagger}\left(\frac{z+\overline{\lambda}}{z-\lambda}\right) = I + vv^{\dagger}\frac{\lambda+\overline{\lambda}}{z-\lambda}. \tag{3.29}$$

In this instance we have also assumed that the orthogonal projector $P = vv^{\dagger}$ has rank one.

There is some freedom in how the B and C matrices may be chosen. In particular, one choice is also consistent with the form used for passive components in the SLH formalism. The ABCD formalism is related to the SLH formalism in the following way for a passive linear system.

$$A = -\frac{1}{2}C^{\dagger}C - i\Omega, \qquad B = -C^{\dagger}S, \qquad D = S. \tag{3.30}$$

In order to satisfy the above equations, we choose

$$B = -\sqrt{-(\lambda+\overline{\lambda})}v^{\dagger}, \qquad C = \sqrt{-(\lambda+\overline{\lambda})}v. \tag{3.31}$$

Finally, we can solve for the Ω.

$$\Omega = [i(A - \frac{1}{2}(\lambda+\overline{\lambda}))] = -[\Im(A)]. \tag{3.32}$$

For the last equality, we use that $\frac{1}{2}(\lambda+\overline{\lambda})$ is exactly the real part of the eigenvalue, and so cancels exactly with the real part of A. The only remaining component is the imaginary part of A, which is multiplied by i. Notice the Ω satisfies the condition of being Hermitian.

3.9 Simulations in Time Domain

We translate our model into the ABCD state-space formalism, as discussed in Section 3.8. Doing this allows us to run a simulation in the time domain. Notice that for linear systems this approach suffices for finding the dynamics in the time domain. We can apply an input field at some frequency and record the output. The relationship between the inputs and outputs at the steady-state will correspond to the value of the transfer function at the appropriate frequency.

As a simple example, we consider the input-output relationship of a Fabry-Pérot cavity with a constant input (i.e. $\omega = 0$) at one of the ports (port 0) and zero input in the other port (port 1). In the steady-state, the signal will be transmitted from the input port 0 to the output port 1. However, if the initial state of the system is different than the steady-state, we will observe some transient behavior in the system. This transient behavior is captured by our simulation and is demonstrated in Figure 3.12. Here, we show the outputs of the two ports based on different numbers of modes selected to approximate the cavity formed due to the delay. As the number of modes is increased, we see the signal from the output ports as a function of time approaches a step function, and we better reproduce the time-domain dynamics of the network with feedback loops. The jumps we see in the time-domain correspond physically to times when a propagating signal arrives at one of the ports. This physical interpretation is further explained in Figure 3.13.

3.10 A method to add non-linear interactions

Since our factorization methodology does not automatically incorporate nonlinear components, one may wish to compute an additional Hamiltonian term representing the interaction between the bosonic field and a chosen One strategy is to follow the conventional approach of expanding the electromagnetic field in terms of a chosen basis for a given Hamiltonian. This can be done if there is a physical interpretation of the spatial profile of each mode generated by our factorization, which we give below.

A typical treatment of modes in quantum electrodynamics assumes the interesting behavior (e.g. interaction between coherent light and an atom) occurs inside of a high-finesse device, resulting in near-orthogonal modes. In our formalism we have not taken this limit, instead considering the complex-valued frequencies corresponding to both a mode frequency and decay. To find the spatial profile of our modes, we will identify them with the quasi-modes of the network, which have both a real and imaginary component, representing the frequency and decay of each mode (see [9],

[1]).

The quasi-modes can be defined as solutions $f(\mathbf{r}, \omega)$ of the equation

$$\nabla \times \nabla \times f(\mathbf{r}, \omega) - \frac{\omega^2}{c^2} \chi(\mathbf{r}) f(\mathbf{r}, \omega) = 0. \tag{3.33}$$

The relation (Eq. 3.33) results from solutions of the electromagnetic field $E(\mathbf{r})$ for Maxwell's equations without sources, $\nabla \times E(\mathbf{r}) = i\omega\mu_0 H(\mathbf{r})$ and $\nabla \times H(\mathbf{r}) = -i\omega\epsilon(\mathbf{r})E(\mathbf{r})$. Here $\epsilon(\mathbf{r}, \omega)$ is the permittivity (for now we will consider the vacuum permittivity ϵ_0 for simplicity), ω is the frequency, $\chi(\mathbf{r}) = \epsilon(\mathbf{r})/\epsilon_0$ is the relative permittivity, μ_0 is the permeability of vacuum (since it tends to be close to a constant we will assume vacuum permeability throughout) and c is the speed of light. The parameter ω is the frequency of the quasimode $(\mathbf{r}, \omega)$, which we will allow to be a complex valued parameter. The domain and boundary conditions are also important – we will define the domain as the internal network edges, and take the boundary conditions to be determined by each component (e.g. beamsplitter) either internally in the network, or combining internal channels with input/output channels. If we only consider planar solutions by fixing the condition $\nabla \cdot (\epsilon(\mathbf{r}) f(\mathbf{r}, \omega)) = 0$ and fix the polarization, and assume there are no free charges, the above equation can be written more simply as

$$\left[\partial^2 - \frac{\omega^2}{c^2}\epsilon_0\right] f(\mathbf{r}, \omega) = 0. \tag{3.34}$$

This is the wave equation, which translates planar solutions (with appropriate initial conditions) along edges of the network in time. From this we see that the time-domain equations (with zero inputs) are equivalent to the Helmholtz equation (one our chosen domain).

We determined the resonance frequencies (and thus the quasi-modes frequencies) by finding the poles of the transfer function, which are solutions of

$$\det\left[I - M_1 E(z)\right] = 0. \tag{3.35}$$

We remind the reader that M_1 was the matrix carrying the transmission information among all internal nodes of the network, while $E(z) = \mathrm{diag}(e^{-zT_1}, e^{-zT_2}, ...e^{-zT_N})$ was the time delay matrix consisting of N non-dimensionalized time delays.

Finally, we can determine the spatial profile of each mode by considering the equation that reproduces the modes at each eigen-frequency,

$$M_1 E(z) x = x. \tag{3.36}$$

Here x is a vector representing the field at each node of the network (i.e. the 'start' of an edge immediately after a boundary condition).

The resulting modes are not orthogonal, and thus interact. This interaction is captured by our factorization method. However, it is not unique, as the order of terms in the factorization can be changed, resulting in a different interactions (but still producing the same input-output relation). This reflects the freedom in how the modes can be chosen (there is no standard way to orthogonalize them). In the limit of high-finesse (i.e. all input-output beamsplitters have reflectivity approaching 1), the modes become increasingly orthogonal. In many applications this limit is sufficient. In many respects using this method to incorporate non-linearities is similar to the so-called 'black-box quantization' method from the superconducting community [40].

This method should be sufficient in many cases, as long as the electromagnetic field can still be well-represented by the chosen basis. If the non-linearity is too strong, the number of required modes may become large.

3.11 Conclusion

In this chapter we have utilized the Blaschke-Potapov factorization for contractive matrix-valued functions to devise a procedure for obtaining an approximation for the transfer function of physically realizable passive linear systems consisting of a network of passive components and time delays. The factorization in our case of interest consists of two inner functions – the Blaschke-Potapov product, a function of a particular form having the same zeros and poles as the original transfer function, and an inner function having no roots or poles (a singular function). The factors in the Potapov product correspond physically to resonant modes formed in the system due to feedback, while the singular term corresponds physically to a feedforward-only component. We also demonstrate how these two components may be separated for the type of system considered.

The transfer function resulting from our approximation can be used to obtain a finite-dimensional state-space representation approximating the original system for a particular range of frequencies. The approximated transfer function can also be used to obtain a physically realizable component

in the SLH framework used in quantum optics. Our approach has the advantage that the zero-pole pairs corresponding to resonant modes are identified explicitly. In contrast, obtaining a similar approximation for a feedforward-only component requires introducing spurious zeros and poles. Our approach has the advantages that we may retain the numerical values of the zero-pole pairs of the original transfer function in our approximated transfer function and that we can conceptually separate these zero-pole pairs from spurious zeros and poles. These advantages may be important in applications and extensions of this work.

In the next chapter we will show how our factorization method can be extended to a more general class of linear systems. We also hope to introduce nonlinear degrees of freedom in a similar way to atoms in the Jaynes-Cummings model and quantum optomechanical devices in the presence of modes formed due to optical cavities.

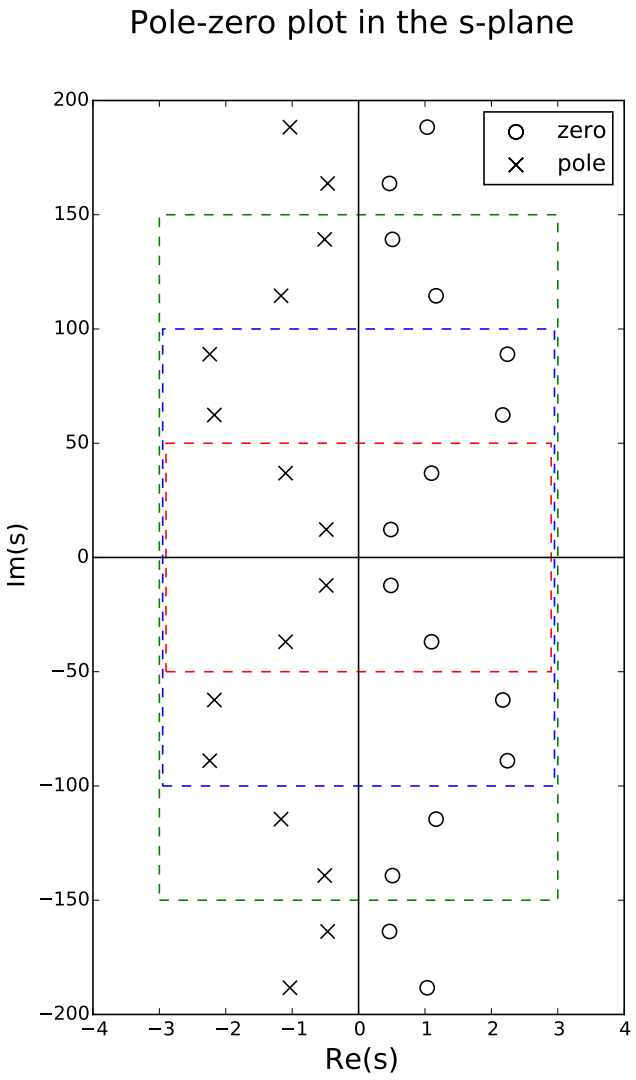

Figure 3.6: This plot illustrates the locations where root-pole pairs may be found. As the contours grow and includes more root-pole pairs, the quality of the approximation improves.

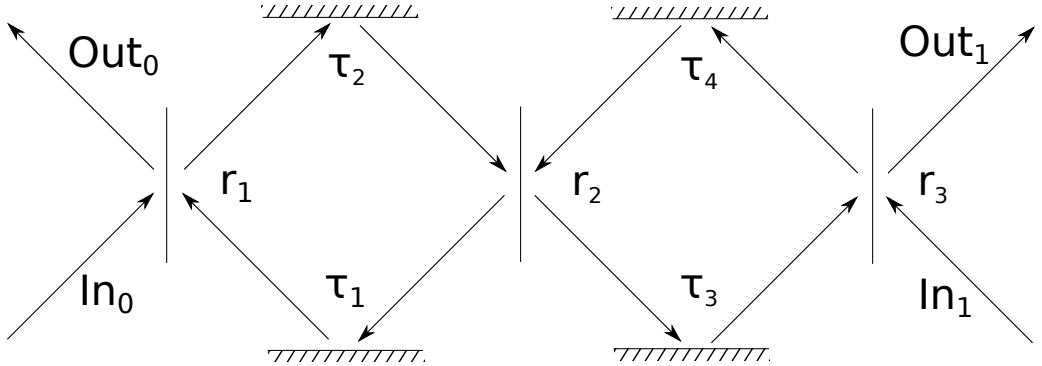

Figure 3.7: An example of a network for which the zero-pole interpolation is accurate due to the absence of the singular term.

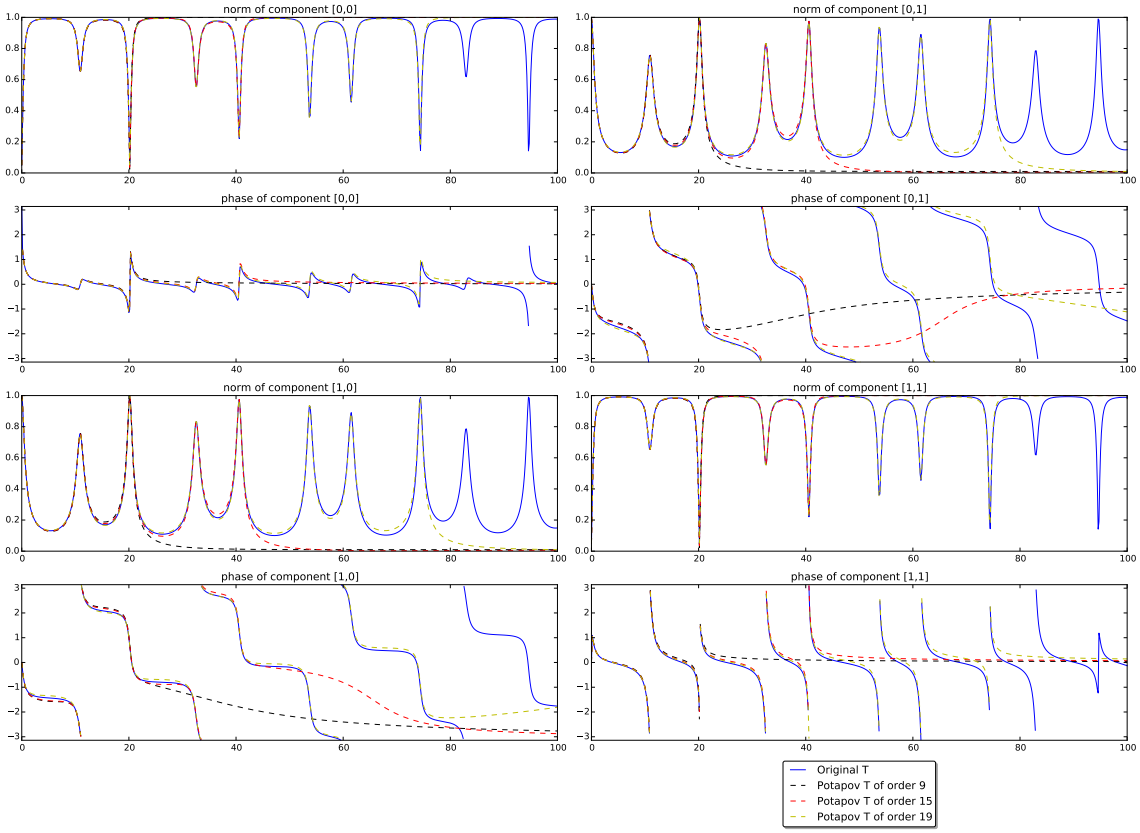

Figure 3.8: Here, we take T to be the transfer function for Example 1 of Section 3.6.1. This is a plot of the various components of $T(i\omega)$ for $\omega \geq 0$ and various approximated transfer functions. We only include nonnegative ω because of the symmetry of both T and its approximations. The zero-pole interpolation appears to converge to the correct transfer function as we add more terms.

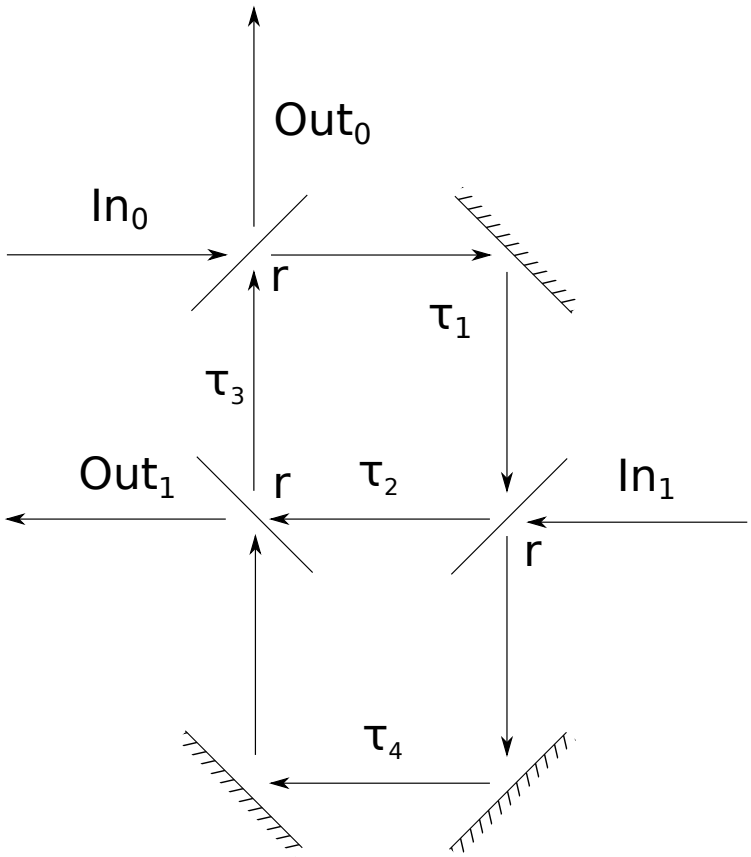

Figure 3.9: An example when the Potapov method would not be wholly applicable.

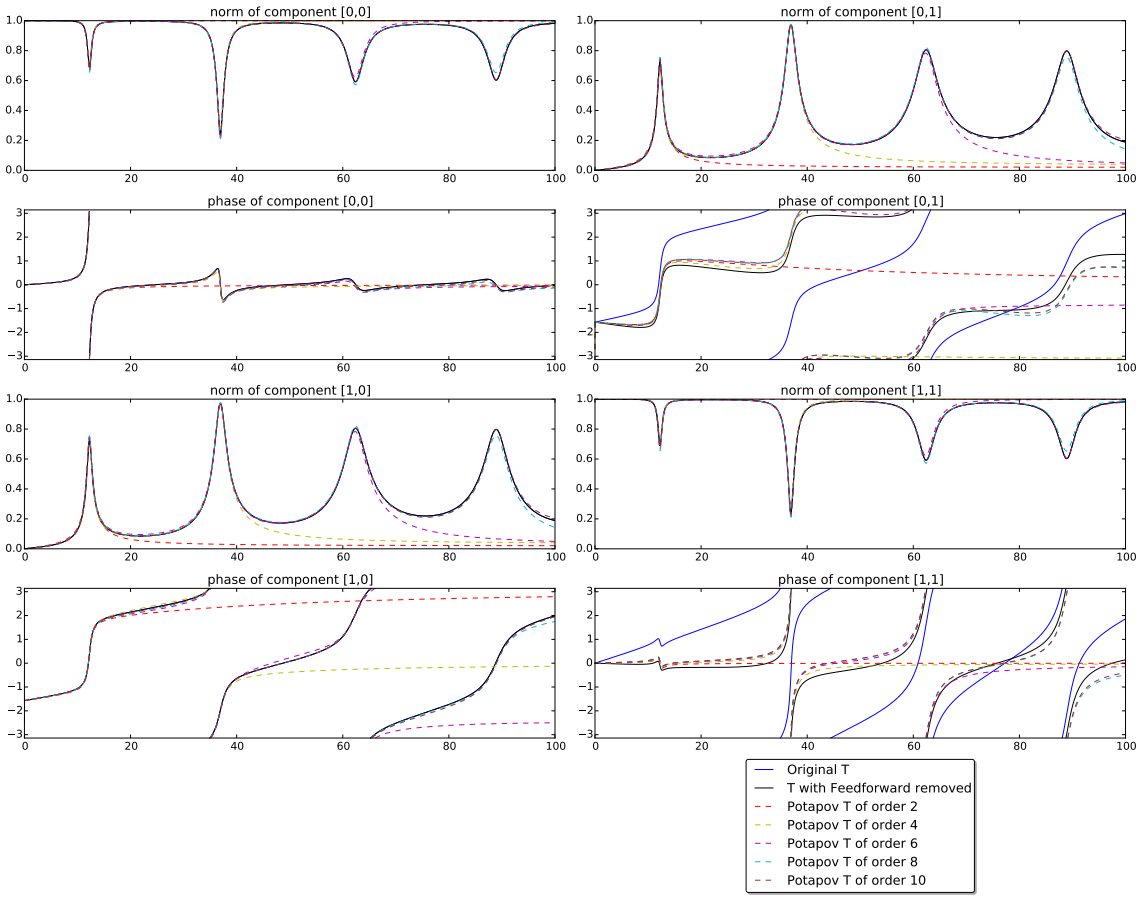

Figure 3.10: Here, we take T to be the transfer function for Example 2 of Section 3.6.2. This is a plot of the various components of $T(i\omega)$ for $\omega \geq 0$ and various approximated transfer functions. We only include nonnegative ω because of the symmetry of both T and its approximations. See Section 3.6.2 for further details.

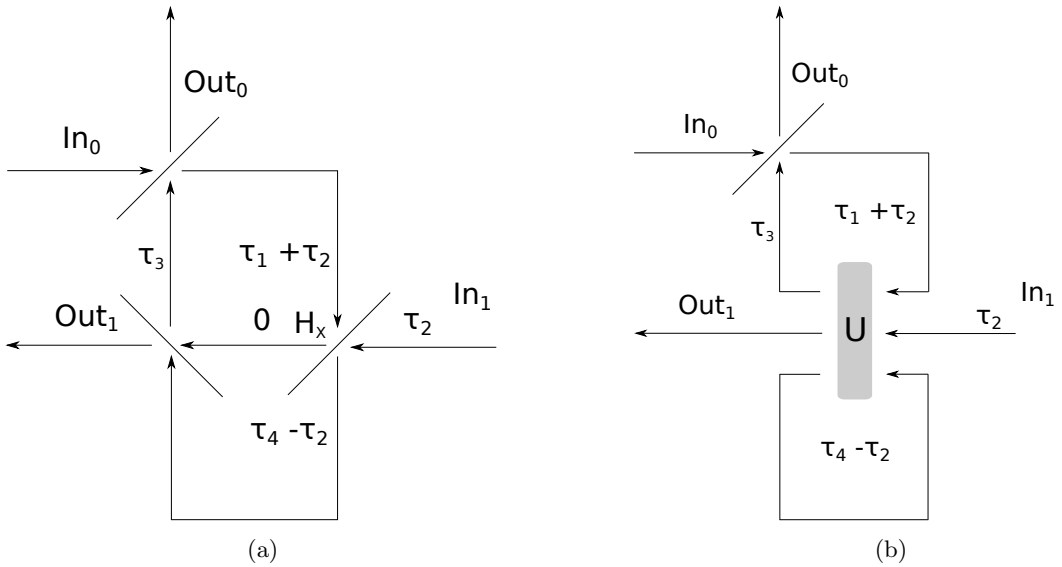

Figure 3.11: This illustration demonstrates one way in which the Potapov product and the singular function can be separated for the particular example from 3.6.2. We notice that some of the parallel delays can be commuted with a beamsplitter, forming the network in Figure 3.11a. The node labeled H_X can then be eliminated, forming the network in 3.11b which has a 3-input 3-output unitary component denoted by U.

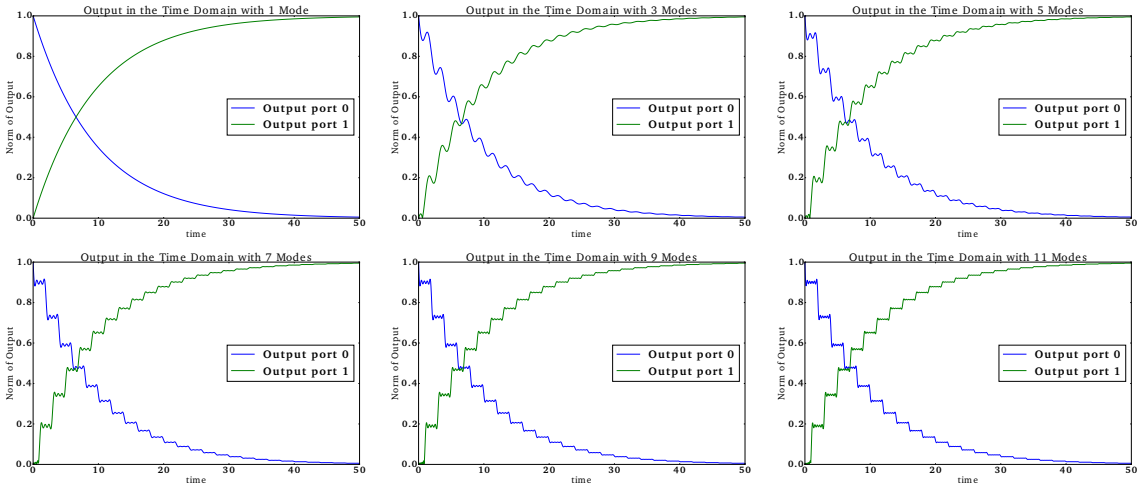

Figure 3.12: The output from a Fabry-Pérot cavity, with initial state zero. The mirror has reflectivity $r = 0.9$ and the duration of the delay is 1. The two output ports represent the signal reflected and the signal transmitted through the cavity. The signal enters the system from port 0 and exists from both ports 0 and 1 (see Figure 3.13). In steady-state, the norm of output 0 converges to zero, an the norm of output 1 converges to 1. The stated number of modes in each diagram is the number of modes used in the delay. We see that adding more modes eventually converges to a piecewise step function. The steps result from the round-trip of the signal inside the cavity.

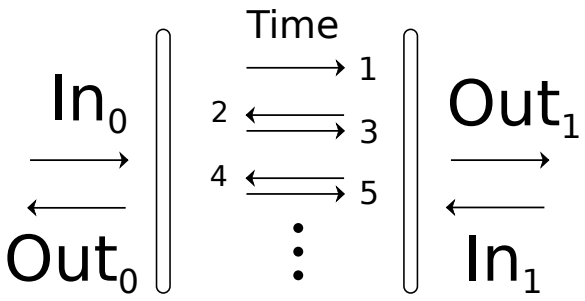

Figure 3.13: Here we interpret the dynamics of the system in the Fabry-Pérot cavity considered. Before the system achieves steady-state, we can learn about the output by tracing the possible paths the signal may follow. The arrows in the diagram between the two mirrors represent the possible paths the signal may follow before leaving through an output port. We use the vertical direction to represent time. For each arrow in each output direction, some of the signal leaves through one of the mirrors. We will therefore see a step in the output as a function of time. This gives a physical interpretation of the steps seen in Figure 3.12.

Appendix A

Appendix for Passive Systems

A.1 The Cayley Transform

Throughout this chapter, we work in the frequency domain common in the engineering literature. In some of the literature, the unit circle $\mathbb{D}$ is used instead of the right half-plane $\mathbb{C}^+$ as the domain on which the properties of the transfer function are studied. These are sometimes known as the z-domain and the s-domain, respectively. These two domains are related by a conformal transformation known as the Cayley transform. We will recall this transformation here.

From the right half-plane to the unit circle:

$$f(z) = \frac{z-1}{z+1}.$$

From the unit circle to the right half-plane:

$$f^{-1}(z) = \frac{1+z}{1-z}.$$

Sometimes in the literature the upper half-plane is used instead of the right half-plane, which slightly changes the transformation.

In our notation, a zero z_k of the Blaschke factor in the disc $\frac{z_k - z}{1-\overline{z_k}z}\frac{|z_k|}{z_k}$ is transformed to a zero in the plane $\lambda_k = \frac{z_k+1}{z_k-1}$ of the factor $c_k \frac{z+\lambda_k}{z-\overline{\lambda_k}}$, for the factor $c_k = \frac{|1-\lambda_k^2|}{1-\lambda_k^2}$. Notice $|c_k| = 1$, and therefore the factor c_k contributes only to the overall phase.

A.2 Unitarity implies a function is inner

(based on [10], lemma 3 on page 223).

This Section will prove the assertion that

$$T(z)T^\dagger(z) = I \text{ for } z \in i\mathbb{R} \implies T(z)T^\dagger(z) \leq I \text{ for } z \in \mathbb{C}^+, \tag{A.1}$$

assuming $T(z)$ is an $N \times N$ matrix-valued analytic (except possibly at infinity) function bounded in $\mathbb{C}^+$.

For any appropriately sized unit vectors u, v, we have from the Cauchy-Schwartz inequality and the maximum modulus principle that

$$|\langle u, T(z)v\rangle|^2 \leq \|u\|\|T(z)v\| \leq 1. \tag{A.2}$$

Since the u, v were arbitrary, the assertion follows.

A.3 Potapov factorization theorem and non-passive linear systems

In this section we cite the Potapov factorization theorem for J-contractive matrices. This factorization, when applicable, consists of several terms which each have a different property. For this chapter we will only need a special case for the theorem, but we cite the full version because it may be conductive to extensions of the work in this chapter. Originally, we were hoping an extension could be found for active linear system, which can be described using a set of 'doubled-up' inputs and outputs for the annihilation and creation fields. In particular, a frequency-domain condition of physical realizability is discussed in [43] and [53], which seems closely related to the J-unitarity condition. However, upon further inspection it was found to be difficult to directly relate the Potapov factorization with generic active linear systems, since one of the hypothesis of the Potapov theorem (the function being J-inner, see Section A.3.1) is not generally satisfied for the transfer function in this formalism. However, there might be a way to modify the transfer function in some way to make it amenable to factorization by the Potapov factorization. Notice in the passive linear system case we were almost automatically able to get the inner condition (see Section A.2), but this is not the case of active linear systems in the doubled-up formalism.

A.3.1 Definitions

First, we introduce some terminology common in the literature. Let $D = \mathbb{D}$ or $\mathbb{C}_+$ (the unit disc or right half-plane, respectively). Further let J be the signature matrix

$$J = \begin{pmatrix} I_m & 0 \\ 0 & -I_r \end{pmatrix}, \tag{A.3}$$

for some m, r. A matrix-valued function $M(z)$ is called:

1. J-contractive, when $M(z)JM(z)^\dagger \leq J'$ for z in D,
2. J-unitary when $M(z)JM(z)^\dagger = J'$ for z on ∂D,
3. J-inner (or J-lossless) when $M(z)$ is J-unitary and J-contractive.

When $J = I$, we drop the J in the definition.

Definition: Stieltjes multiplicative integral (from [48]):

Let $H(t)$ (with $a \leq t \leq b$) be a monotonically increasing family of J-Hermitian matrices with $t = \mathrm{tr}[H(t)J]$ and $f(t)$ $(a \leq t \leq b)$ be a continuous scalar function. Then the following limit exists

$$\lim_{\max \Delta t_j \to 0} e^{f(\theta_0)\Delta H(t_0)} e^{f(\theta_1)\Delta H(t_1)} ... e^{f(\theta_{n-1})\Delta H(t_{n-1})} \tag{A.4}$$

where we take $a = t_0 \leq \theta_0 \leq t_1 \leq ... \leq t_n = b$. The limit is denoted

$$\overset{\curvearrowright}{\int_a^b} e^{f(t)dH(t)}$$

and is called the multiplicative integral.

A.3.2 Potapov Factorization

In much of the mathematical literature the domain of the transfer function is transformed via the Cayley transform (see Appendix A.1). This changes how some of the terms in the factorization are written, but not the fundamental features of the factorization.

Next we will cite some of the theorems by Potapov. In the case $J = I$ the function ω satisfies

the unitarity condition $\omega(z)\omega^\dagger(z) = I$ on the boundary of the disc or half-plane (depending on the domain taken).

The fundamental factorization theorem by Potapov characterizes the class of J-contractive matrices.

Theorem. (from [48]):

Let $\omega(z)$ be an analytic single-valued J-contractive matrix function in the unit circle $|z| < 1$, and suppose that $\det(\omega(z))$ does not vanish identically; then we can write

$$\omega(z) = B_\infty(z) B_0(z) \overset{\curvearrowright}{\int_0^\ell} \exp\left(\frac{z + e^{i\theta(t)}}{z - e^{i\theta(t)}} dE(t)\right). \tag{A.5}$$

Here

$$B_\infty(z) = \prod_k U_k \begin{pmatrix} I & 0 \\ 0 & \frac{1-\overline{\mu}_k z}{\mu_k - z} \frac{\mu_k}{|\mu_k|} I_{q'_k} \end{pmatrix} U_k^{-1} \tag{A.6}$$

is a product of elementary factors associated with the poles μ_k of the matrix function $\omega(z)$ inside the unit circle, $q'_k \leq q$, and U_k is a J-unitary matrix;

$$B_0(z) = \prod_k V_k \begin{pmatrix} \frac{\lambda_k - z}{1-\overline{\lambda}_k z} \frac{|\lambda_k|}{\lambda_k} I_{p'_k} & 0 \\ 0 & I \end{pmatrix} V_k^{-1} \tag{A.7}$$

is a product of elementary factors associated with the zeros in $|z| < 1$ of the determinant of the matrix function $\omega_\infty(z) = B_\infty^{-1}(z)\omega(z)$, which is holomorphic in $|z| < 1$, $p'_j \leq p$, V_j is a J-unitary matrix; the last term is the Stieltjes integral, where $E(t)J$ is a monotone increasing family of Hermitian matrices such that $t = \mathrm{tr}[E(t)J] = t$. $\square$

The integral in the above expression is known as the Riesz-Herglotz integral. It captures the effects of the zeros and poles that occur on the boundary as well as effects not due to zeros or poles. In our case, we will assume there are no zeros or poles on the boundary, and therefore we will be able to obtain a special form for the decomposition, discussed below.

The poles in this factorization may occur inside the unit circle (right half-plane), on the boundary (imaginary axis), or outside the unit circle (left half-plane). In the case of passive, stable systems, we will find the zeros in the interior of the unit circle and the poles on the exterior. We will have no poles or zeros on the boundary. This allows us to ignore the component $B_\infty(z)$ in the above theorem. Further, the next theorem will allow us to express the multiplicative integral in a special

way.

Theorem. (from [48]): An singular matrix function $\omega(z)$, J-contractive in the right half-plane and J-unitary on the real axis, can be represented in the form

$$\omega(z) = \omega(0) \overset{\curvearrowright}{\int_0^\ell} e^{-zH(t)dt} \tag{A.8}$$

where $H(t)$ is a summable non-negative definite J-Hermitian matrix, satisfying the condition $\mathrm{tr}[H(t)J] = t$. $\square$

If the zeros of $\omega(z)$ in eq. (A.5) occur only in the interior of the disc, the B_∞ is trivial. We can detach the Potapov factors $B_0(z)$ from the left, resulting in an singular function $\omega_0(z)$. After applying the Cayley transformation, the factorization eq. (A.8) above can be invoked. Thus we conclude that a matrix function $\omega(z)$, J-contractive on the right half-plane, J-unitary on the imaginary axis, and with zeros only in the right half-plane has the form

$$\omega(z) = B_0(z)\omega_0(0) \overset{\curvearrowright}{\int_0^\ell} e^{-zH(t)dt}. \tag{A.9}$$

Here the $B_0(z)$ is the Blaschke-Potapov product from the factorization theorem written in the coordinates of the half-plane representation. The $\omega_0(0)$ makes a contribution to the overall phase (i.e. a constant unitary factor).

A.4 Using the Padé approximation for a delay

For a system involving only feedforward (i.e. no signal ever feeds back), no poles or zeros will be found in the transfer function. For this reason, the zero-pole interpolation cannot naturally reproduce a transfer function to approximate the system. Instead, a different approach is needed to obtain an approximation for the state-space representation for systems of this kind. Still, any finite-dimensional state-space representation will have poles and zeros in its transfer function. If we use such a system as an approximation of a delay, these zeros and poles will be spurious but unavoidable.

The Padé approximation is often used to approximate delays in classical control theory [33]. When

using the $[n, n]$ diagonal version of the Padé approximation to obtain a rational function approximating an exponential, we obtain

$$e^{-Tz} \approx \exp_{[n,n]}(-Tz) = \frac{Q_n(zT)}{Q_n(-zT)}. \tag{A.10}$$

The $Q_n(z)$ is a polynomial of degree n with real coefficients. Because of this, its roots come in conjugate pairs. As a result, we can write the Padé approximation as a product of Blachke factors:

$$\exp_{[n,n]}(-Tz) = \prod_n -\frac{z + \overline{p_n}}{z + p_n}. \tag{A.11}$$

In particular, note that the approximation preserves the unitarity condition, and is therefore physically realizable. For this reason, it is possible to approximate time delays with this approximation.

Although this approach may be useful for the case of feedforward-only delays, in the case of delays with feedback this may produce undesirable results. To illustrate this, we introduce an example where the Padé approximation is used in order to produce an approximated transfer function for the network discussed in Section 3.6.1. For this approximation, the order used for the approximation of each delay is chosen to be roughly proportional to the duration of the delay. Figure A.1 illustrates the approximated transfer function. Please compare this result to Figure 3.8, where we have used the zero-pole interpolation.

We see in Figure A.1 that the peaks in the approximating functions often do not occur in same locations as the peaks of the original transfer function. This may be problematic when attempting to simulate many physical systems for which the locations of the peaks correspond to particular resonance frequencies that have physical relevance. For instance, if one chooses to introduce other components to the system, such as atoms, the resonance frequencies due to the trapped modes of the network must be described accurately or else the resulting dynamics of the approximating system may not correspond to the true dynamics of the physical system. For this reason, using the Padé approximation may not always be the best choice.

A.5 Blaschke-Potapov Product in the limit $\Re(z) \to -\infty$

In Section 3.7, we proposed a criterion for checking when the multiplicative integral component in Section 3.4.1 was not necessary. We assumed that the Blaschke-Potapov product converged to a

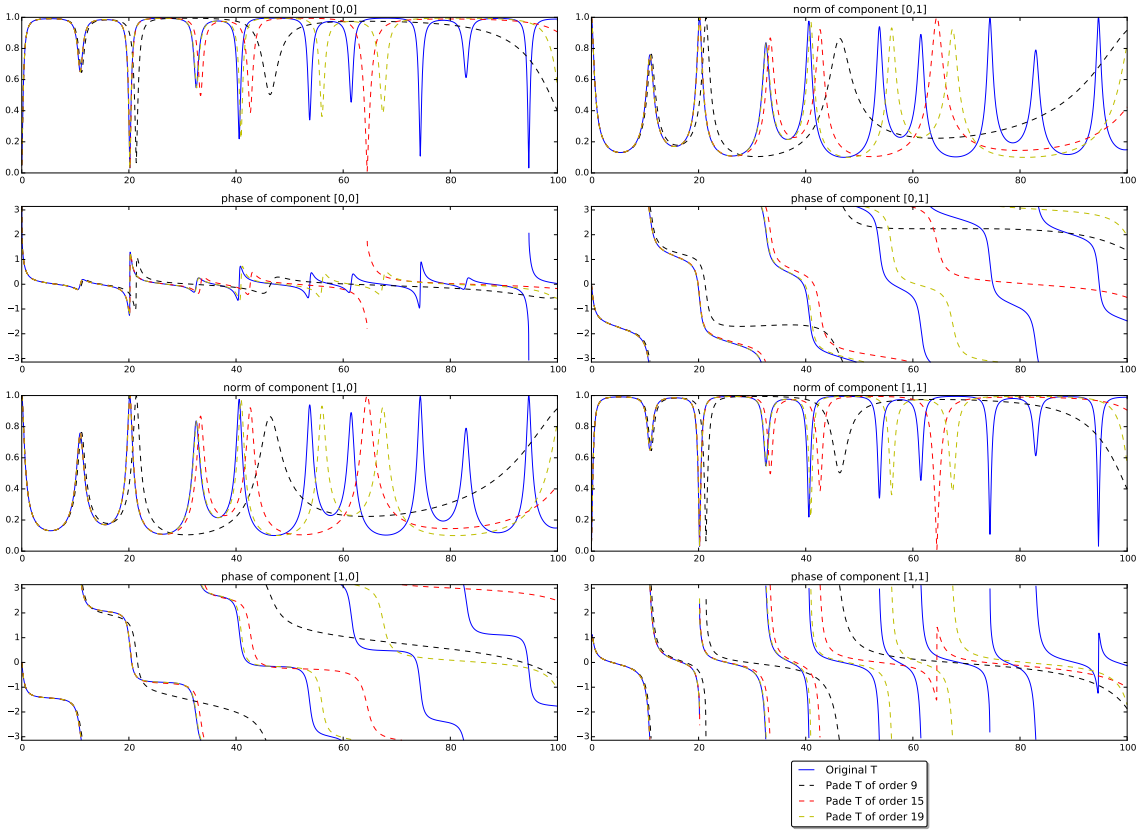

Figure A.1: This figure illustrates approximated transfer functions resulting from applying the Padé approximation on individual delays in the network. Although we see that this approximation converges, the peaks often do not occur at the correct locations, as opposed to the approximations resulting from the zero-pole interpolation (compare to Figure 3.8).

nonzero constant in the limit $\Re(z) \to -\infty$. In this section, for demonstrative purposes we show this is the case for the example of a single trapped cavity discussed in Section 3.3.

In order to examine the convergence of the product in eq. (3.8) of Section 3.3, we write it in the following way. We observe by taking the logarithm with an appropriate branch cut that

$$\prod_n (1 + a_n(z)) \tag{A.12}$$

converges if and only if the infinite sum

$$\sum_n a_n(z) \tag{A.13}$$

converges, assuming $\sum_n |a_n(z)|^2$ converges. We take

$$a_n(z) = 1 - \frac{z + p_n}{z - \overline{p_n}} = \frac{2\Re(p_n)}{z - p_n}. \tag{A.14}$$

Using the relation

$$\cot(z) = \sum_{n\in\mathbb{Z}} \frac{1}{z - n\pi}, \tag{A.15}$$

we get that

$$\lim_{\Re(z)\to-\infty} \sum_n a_n(z) = -\ln(r). \tag{A.16}$$

Actually, higher-order terms of the logarithm expansion of eq. (A.12) go to zero in this limit, so we get that

$$\lim_{\Re(z)\to-\infty} \tilde{T}(z) = \lim_{\Re(z)\to-\infty} -\prod_{n\in\mathbb{Z}} \left(\frac{z + \overline{p_n}}{z - p_n}\right) = \lim_{\Re(z)\to-\infty} -\prod_n (1 + a_n(z)) = -1/r. \tag{A.17}$$

This shows the desired result that the infinite product in this limit goes to a nonzero constant. Also interestingly, we have been able to compute this value and remark that it is indeed equal to $\lim_{\Re(z)\to-\infty} T(z)$.

The above example with a single trapped cavity formed is illustrative of typical behavior for more complicated systems formed by networks of beamsplitters and time delays. The zero-pole pairs of the system occur in a region of bounded positive real part, and roughly uniformly along the imaginary axis. This suggests that the Blaschke-Potapov product resulting from the zero-pole interpolation will converge to a nonzero constant in the $\Re(z) \to -\infty$ limit under quite general circumstances.

Chapter 4

Generic linear systems with coherent feedback

Abstract

We consider the transfer functions describing the input-output relation for a class of linear open quantum systems involving feedback with nonzero time delays. We show how such transfer functions can be factorized into a product of terms which are transfer functions of canonical physically realizable components. We prove under certain conditions that this product converges, and can be approximated on compact sets. Thus our factorization can be interpreted as a (possibly infinite) cascade. Our result extends past work where linear open quantum systems with a state-space realization have been shown to have a pure cascade realization [Nurdin, H. I., Grivopoulos, S., & Petersen, I. R. (2016). The transfer function of generic linear quantum stochastic systems has a pure cascade realization. Automatica, 69, 324-333.]. The functions we consider are inherently non-Markovian, which is why in our case the resulting product may have infinitely many terms.

This chapter will be submitted to publication with authorship by Gil Tabak, Ryan Hamerly, and Hideo Mabuchi. Ryan has made significant contributions, especially in Sections 4.7.1 and 4.7.2, and edits in other sections.

4.1 Overview

We will be concerned here with a class of non-Markovian linear open quantum systems, which we will construct by incorporating coherent time-delayed feedback to a (Markovian) finite-dimensional open quantum system (which can be represented using the SLH formalism). By finite dimension, we mean that the system has a finite number of internal degrees of freedom. The transfer function of such a system is a rational function, having specific physical realizability constraints. After the procedure of incorporating delayed feedback, the transfer function may no longer correspond to a rational function. Our main result is that under certain conditions the input-output relationship of such systems can be realized as a (possibly infinite) cascade of physically realizable canonical components with a single degree of freedom. To obtain this result, we will factorize the transfer function into an infinite product of canonical terms, where each term corresponds to a physically realizable component. Each such term will be identified using a pair of poles and zeros. The delayed-feedback system can then be approximated using a finite truncation of the infinite product.

In the case of rational transfer functions, properties of the the state-space representation matrices can be used to determine if a system is physically realizable. It has been shown in [53] that under some non-degeneracy assumptions these conditions are equivalent to certain properties of the transfer function in the frequency domain. Essentially, as long as the state-space realization matrices are in 'doubled-up' form and certain non-degeneracy conditions hold, the physical realizability of the system is equivalent to the transfer function having the J-unitary property (and a property preventing static squeezing). Once delayed feedback is incorporated, although the system remains linear, it loses its Markovian property and no longer has a corresponding state-space representation. We introduce an extension of the frequency domain constraints for physical realizability and utilize it to obtain our factorization under certain assumptions, stated in Section 4.4.1 and in the non-degeneracy conditions in the hypothesis of Theorems 4.7.1 and 4.7.2. Some of the assumptions follow from our construction starting with a finite-dimensional physically realizable system (Assumptions 1 and 2), and others are introduced for simplicity (Assumptions 4, 5, and 6). Assumption 3 ensures the network does not have effectively time-delayed feed-forward terms. An analysis similar to the one in ([55], i.e. Chapter 3) can be used to isolate such terms.

In Section 4.2, we introduce the various definitions and notation we use throughout. In Section 4.3 we introduce (finite-dimensional) linear quantum stochastic systems and discuss the physical realizability conditions of transfer functions. In Section 4.4 we construct a delayed-feedback network and state assumptions we make throughout. In Section 4.5 we provide some properties of our delayed-feedback network. In Section 4.6 we provide theorems that relate the transfer function of

the delayed-feedback network with a simpler transfer function resulting from replacing the internal components of the network with static components. These theorems will be useful in providing convergence results. In Section 4.7 we introduce physically realizable canonical transfer functions having only two poles and two zeros. Finally, in Section 4.8, we provide our factorization result.

We anticipate our work will have applications in modeling and simulating open quantum systems, as well as conceptually help understanding linear open quantum systems with delayed feedback. There is interest in how feedback can be used for control, although the effect of delays has not been thoroughly explored. For example, in [7], a network of OPOs was interpreted in terms of a quantum plant and a quantum controller. In that work, coherent feedback was shown to be capable of shifting the frequency of maximum squeezing and broadening the spectrum over a wider frequency band. The effects of a time delay in coherent feedback networks on optical squeezing have been studied in [30] and [39]. In these works, it was demonstrated that the enhanced squeezing of quantum feedback networks may be improved by incorporating a time delay in the feedback loop. Depending on the implementation, the time delay can increase squeezing either on or off resonance.

4.2 Definitions

The definitions below are frequently used in the literature (e.g. [19],[20],[53]).

definition 4.2.1 *The signature matrix J of dimension $2n$ is a diagonal matrix with alternating $(+1,-1)$ on its diagonal.*

definition 4.2.2 *For a matrix M we use the notation $M^\flat = JM^\#J$.*

definition 4.2.3 *A doubled-up matrix has the form*

$$\breve{M} = \Delta(M_-, M_+) \equiv \begin{pmatrix} M_- & M_+ \\ M_+^\# & M_-^\# \end{pmatrix}. \tag{4.1}$$

A doubled-up column vector has the form

$$\breve{v} = \begin{pmatrix} v \\ v^\# \end{pmatrix}. \tag{4.2}$$

Here $M^\#, v^\#$ denote the elementwise conjugates of M, v.

definition 4.2.4 *A matrix M is J-unitary iff*

$$MJM^\dagger = M^\dagger JM = J. \tag{4.3}$$

definition 4.2.5 *A matrix-valued function $M(z)$ is J-unitary iff*

$$M(z)JM(z)^\dagger = M(z)^\dagger JM(z) = J, \tag{4.4}$$

for z on the imaginary axis.

It a transfer function is J-unitary and meromorphic on the plane, then satisfies $M(z)JM(-\overline{z})^\dagger = J$ on its domain.

It will be convenient to permute the annihilation and creation operators using the symmetric permutation matrix P, exchanging the first N indices, $1, 2, ..., N$ with the odd indices up to $2N$, and exchanging the last N indices $N+1, ..., 2N$ with the even indices up to $2N$. When this is the case (Section 4.4 and beyond) it will be understood that doubled-up matrices will have the form $\tilde{M} = PMP^T$ instead. For example, the matrix

$$M = \Delta(M_-, M_+) = \begin{pmatrix} M_{-,11} & M_{-,12} & M_{+,11} & M_{+,12} \\ M_{-,21} & M_{-,22} & M_{+,21} & M_{+,22} \\ M^\#_{+,11} & M^\#_{+,12} & M^\#_{-,11} & M^\#_{-,12} \\ M^\#_{+,21} & M^\#_{+,22} & M^\#_{-,21} & M^\#_{-,22} \end{pmatrix} \tag{4.5}$$

would be re-arranged as

$$PMP^T = \begin{pmatrix} M_{-,11} & M_{+,11} & M_{-,12} & M_{+,12} \\ M^\#_{+,11} & M^\#_{-,11} & M^\#_{+,12} & M^\#_{-,12} \\ M_{-,21} & M_{+,21} & M_{-,22} & M_{+,22} \\ M^\#_{+,21} & M^\#_{-,21} & M^\#_{+,22} & M^\#_{-,22} \end{pmatrix}. \tag{4.6}$$

definition 4.2.6 *We will say a rational transfer function is in 'doubled-up' form when it has a realization given by matrices A, B, C, D, (i.e. $T(z) = D + C(zI - A)^{-1}B$), where each is in doubled-up form.*

definition 4.2.7 *Given a dimension b, let*

$$\Sigma_b = \begin{pmatrix} 0 & I_b \\ I_b & 0 \end{pmatrix} \tag{4.7}$$

The subscript b will be dropped when the dimension is clear from context.

It will be understood that when the annihilation and creation ports are permuted as discussed above, we will use $\tilde{\Sigma} = P\Sigma P^T$ instead.

remark 4.2.1 *A matrix M is doubled-up if and only if it satisfies*

$$M\Sigma = \Sigma M^{\#}, \tag{4.8}$$

4.2.1 Zeros and poles

In the literature, there are different definitions for zeros and poles of a matrix-valued function. We will describe two kinds of definitions, which we will denote respectively by (I) and (II):

definition 4.2.8 *A complex number z is called a pole(I) of $A(z)$ if it is a pole of one of the entries of $A(z)$, and z is called a zero(I) of $A(z)$ if it is a pole(I) of $A(z)^{-1}$. This is the definition used in Ref. [49].*

definition 4.2.9 *A complex number z is called a pole(II) of $A(z)$ if it is a pole of* $\det A(z)$*, and z is called a zero(II) of $A(z)$ if it is a zero of* $\det A(z)$*. This is the definition used in Ref. [55]. Note that definition 4.2.9 implies 4.2.8, but not the converse.*

remark 4.2.2 *The definitions (I) could have a pole and a zero in the same location. Instead, for definitions (II) this cannot occur. If zeros (I) and poles (I) do not occur in the same location, then the definitions (I) and (II) coincide. For simplicity, we will assume that is the case (Assumption 5).*

definition 4.2.10 *(eigenvectors at zeros and poles, adapted from Ref. [49]) Suppose z_0 is a zero(I) of matrix valued function $A(z)$. A nonzero column vector x_1 is called an eigenvector of $A(z)$ at z_0 if there exist column vectors $(x_2, x_3, \ldots)$ such that $f(z) = A(z)\sum_{j=0}^{\infty} x_{j+1}(z - z_0)^j$ is analytic at z_0 and has a zero at z_0. We will say the order of the zero of $A(z)$ with eigenvector x_1 at z_0 is the order of $f(z)$ at z_0.*

Similarly, if z_0 is a pole of $A(z)$, then y_1 is a pole vector of $A(z)$ at z_0 (we will sometimes say an eigenvector at the pole) if there exist vectors $(y_2, y_3, \ldots)$ such that $g(z) = \sum_{j=0}^{\infty} y_{j+1}(z - z_0)^j A(z)^{-1}$

is analytic at z_0 and has a zero at z_0. We will say the order of the pole of $A(z)$ with eigenvector y_1 at z_0 is the order of $g(z)$ at z_0.

remark 4.2.3 *Definition 4.2.10 is most intuitive in the case where zeros and poles do not overlap and have order and multiplicity one. In this case, the auxiliary vectors $(x_2, x_3, \ldots)$ and $(y_2, y_3, \ldots)$ are unnecessary, and an eigenvector x_1 for zero(I) z_0 occurs when $f(z) = A(z)x_1$ is zero-valued at z_0, and a pole vector y_1 for pole(I) z_0 occurs when $g(z) = y_1 A(z)^{-1}$ is zero-valued at z_0.*

4.3 Finite-Dimensional Linear Quantum Stochastic Systems (LQSS)

We provide a brief introduction here for (finite-dimensional) LQSS. Consider a system with a finite-dimensional state $x(t)$ driven by a bosonic input field $b_{\text{in}}(t)$ and generating a bosonic output field $b_{\text{out}}(t)$. The most general form of a linear system preserving the commutation relations in the input-output relationship has the form

$$\frac{\mathrm{d}}{\mathrm{d}t}x = (A_- x + A_+ x^{\#}) + (B_- b_{\text{in}} + B_+ b_{\text{in}}^{\#}) \tag{4.9}$$

$$b_{\text{out}} = (C_- x + C_+ x^{\#}) + (D_- b_{\text{in}} + D_+ b_{\text{in}}^{\#}). \tag{4.10}$$

Using the notation $\breve{M} = \Delta(M_-, M_+)$ for matrices and $\breve{v} = (v, v^{\#})^T$ for vectors (e.g. as used in [20]), this can be written as

$$\frac{\mathrm{d}}{\mathrm{d}t}\breve{x} = \breve{A}\breve{x} + \breve{B}\breve{b}_{\text{in}} \tag{4.11}$$

$$\breve{b}_{\text{out}} = \breve{C}\breve{x} + \breve{D}\breve{b}_{\text{in}}. \tag{4.12}$$

The matrices $\breve{A}, \breve{B}, \breve{C}, \breve{D}$ must satisfy special physical realizability constraints (e.g. Ref. [53]).

The input-output relationship may be characterized by the transfer function of the system. This function is obtained by taking the Laplace transform of the equations of motion, defined by $Y(z) = \int_0^\infty e^{-zt} y(t) dt$. Letting $X(z), B_{\text{in}}(z)$, and $B_{\text{out}}(z)$ be the Laplace transforms of $x(t), b_{\text{in}}(t)$, and $b_{\text{out}}(t)$, respectively, and eliminating $X(z)$ from the resulting equations, one obtains $B_{\text{out}}(z) = T(z)B_{\text{in}}(z)$, where $T(z) = \breve{D} + \breve{C}(zI - \breve{A})^{-1}\breve{B}$. In Section 4.4 we will build upon finite-dimensional LQSS, introducing time-delayed feedback. We will do so by considering the Laplace transform of the newly constructed network including the time-delayed feedback.

Theorem 4 in Ref. [53] states an equivalent condition for physical realizability in the frequency domain when $\breve{A}, \breve{B}, \breve{C}, \breve{D}$ are doubled up in the sense of Eq. (4.1) and assuming the state space realization is minimal and the eigenvalues of $\breve{A}$ satisfy $\lambda_i(\breve{A}) + \lambda_j(\breve{A}) \neq 0$ (a condition which always holds for stable systems with $A < 0$). With these assumptions the system is physically realizable if and only if

1. The transfer function $T(z)$ is J-unitary.
2. The matrix $\breve{D}$ has form $\breve{D} = \Delta(S, 0)$ for a unitary matrix S.

The first condition ensures the commutation relations are preserved, while the second condition ensures there is no static (infinite-bandwidth) squeezing in the system (this would lead to energy divergences and breaks the Hudson-Parthasarathy quantum stochastic calculus). We will show in the following sections that the state space matrices being doubled-up and the first condition above can be generalized for the cases when there is no finite-dimensional state-space. However, the second condition has no clear analogue (see in particular the discussion in Section 4.8.4).

4.4 Linear Quantum Stochastic Systems with Delayed Feedback

We begin with an LQSS as described in Section 4.3 having $2(N+M)$ inputs and $2(N+M)$ outputs. $N+M$ of the input/output ports correspond to the input/output annihilation field, and the other $N+M$ of the input/output ports correspond to the input/output creation field. For convenience, we permute the input and output ports, so that the odd-labeled ports correspond to the creation fields and the even ports to the creation fields.

We assume this transfer function corresponds to a finite-dimensional (i.e. it is a proper rational function) throughout (see Assumption 1). The transfer function of this system has form

$$T(z) = \begin{pmatrix} T_1(z) & T_2(z) \\ T_3(z) & T_4(z) \end{pmatrix}, \tag{4.13}$$

where the matrix has been partitioned into blocks of size $2N \times 2N$, $2N \times 2M$, $2M \times 2N$, and $2M \times 2M$.

Remark: A complex-valued function on the extended plane is a proper rational function if and only if it is meromorphic on the extended complex plane and analytic at infinity. This applies to the

components of $T(z)$, and will be important throughout.

Next, we add delays with feedback to the system. In the case for linear quantum systems, we use

$$E(z) = \text{diag}(e^{-T_1 z}, e^{-T_1 z}, ..., e^{-T_M z}, e^{-T_M z}). \tag{4.14}$$

$$\tilde{T}(z) = T_1(z) + T_2(z)E(z)(I - T_4(z)E(z))^{-1}T_3(z) \tag{4.15}$$

$$= T_1(z) + T_2(z)(E(-z) - T_4(z))^{-1}T_3(z). \tag{4.16}$$

Each time delay occurs in two terms of $E(z)$, once for annihilation and once for the creation field. Notice that $E(-z) = E(z)^{-1}$ because of its special form. This notation will be used throughout. Figure 4.1 shows conceptually how the blocks $T_i(z)$ for $i = 1, 2, 3, 4$ are used to construct the new transfer function $\tilde{T}(z)$. It can be shown $E(z)$ is J-unitary. This is a similar setup to [19]. This term can be derived from the Fourier transform on an linear quantum system with delayed input ports.

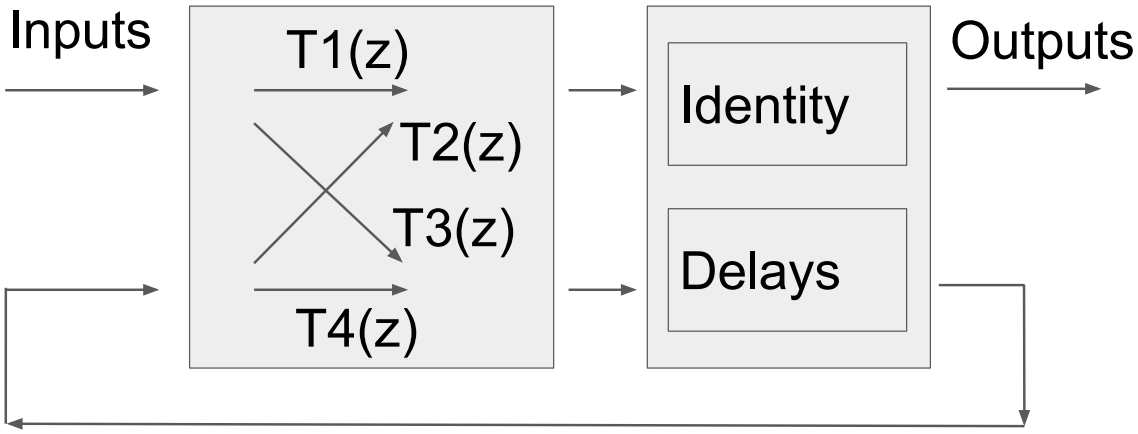

Figure 4.1: The setup of the network with delayed feedback constructed in Eq. (4.14). The arrows in the left box indicate how the blocks $T_i(z)$ for $i = 1, 2, 3, 4$ relate the inputs and outputs of $T(z)$ to the inputs and outputs of $\tilde{T}(z)$ with respect to the time delays.

4.4.1 Assumptions

These are assumptions we will make throughout.

1. The transfer function $T(z)$ is a proper rational function. This means that each of its components can be expressed as a ratio of polynomials, and that the degree of the numerator is never greater than the denominator. Notice in particular this implies $T(z)$ is analytic at infinity.

2. The transfer function $T(z)$ is doubled-up and J-unitary.

3. There is some C so that for $\{z : |z| > C\}$, $T_2(z), T_3(z), T_4(z)$ are invertible, and their singular values are bounded away from zero by some positive constant. This generalizes the condition in section 8.1 of reference ([55], i.e. Chapter 3) where the network components were static and passive. Here, $T_4(z)$ replaces the static matrix M_1. This condition on $T_4(z)$ excludes a series product with delay $B \triangleleft A$. For systems that do not satisfy this assumption, an approach similar to that used in ([55], i.e. Chapter 3) may be used in order to separate out terms corresponding to feedforward time delays. The condition on $T_2(z)$ and $T_3(z)$ allows us to prove Lemma 4.6.1.

4. periods $T_1, ..., T_N$ are commensurate. This suffices for practical purposes, and simplifies some of the proofs.

5. Zeros(I) and poles(I) from Definition 4.2.8 do not occur in the same location.

6. For simplicity, suppose that whenever we find a zero or pole of a transfer function of interest, there is up to a scalar only one eigenvector at the zero/pole (i.e. the multiplicity of each zero/pole is one). Also, each zero/pole has order one in the sense of Definition 4.2.10.

There are additional specific non-degeneracy assumptions discussed in Section 4.7.2.

4.5 Properties of transfer functions

Claim 4.5.1

- *If two transfer functions are J-unitary, then so is their product.*
- *If two transfer functions can be written in doubled-up notation, then so can their product.*
- *The inverse of a J-unitary function is J-unitary.*

proofs: Direct computation.

Claim 4.5.2 *If a rational transfer function is doubled-up, then so is its inverse.*

proof: This follows using a realization of the inverse of a transfer function, which is valid when D is invertible (see e.g. reference [32]):

Denoting a transfer function by $G(z) = D + C(zI - A)^{-1}B$ by $\left(\begin{array}{c|c} A & B \\ \hline C & D \end{array}\right)(z)$, its inverse is

$$\left(\begin{array}{c|c} A & B \\ \hline C & D \end{array}\right)^{-1}(z) = \left(\begin{array}{c|c} A - BD^{-1}C & -BD^{-1} \\ \hline D^{-1}C & D^{-1} \end{array}\right)(z). \tag{4.17}$$

From this one sees that the matrices for the state space representation of the inverse are also doubled up. ■

Claim 4.5.3 *J-unitarity is preserved under concatenation, series, and feedback products.*

proof: The case for the concatenation product is trivial:

$$\begin{bmatrix} T_1(z) & 0 \\ 0 & T_2(z) \end{bmatrix} J \begin{bmatrix} T_1(z) & 0 \\ 0 & T_2(z) \end{bmatrix}^\dagger = \begin{bmatrix} T_1(z)J_1T_1(z)^\dagger & 0 \\ 0 & T_2(z)J_2T_2(z)^\dagger \end{bmatrix} = \begin{bmatrix} J_1 & 0 \\ 0 & J_2 \end{bmatrix} = J \tag{4.18}$$

The series product follows from associativity:

$$\big(T_1(z)T_2(z)\big)J\big(T_1(z)T_2(z)\big)^\dagger = T_1(z)\big(T_2(z)JT_2(z)^\dagger\big)T_1(z)^\dagger = T_1(z)JT_1(z)^\dagger = J \tag{4.19}$$

The only nontrivial case is the feedback product. Here we start with a transfer function

$$T(z) = \begin{bmatrix} T_1(z) & T_2(z) \\ T_3(z) & T_4(z) \end{bmatrix} \tag{4.20}$$

J-unitarity implies:

$$\begin{aligned} T_1JT_1^\dagger + T_2JT_2^\dagger &= J \\ T_1JT_3^\dagger + T_2JT_4^\dagger &= 0 \\ T_3JT_1^\dagger + T_4JT_2^\dagger &= 0 \\ T_3JT_3^\dagger + T_4JT_4^\dagger &= J \end{aligned} \tag{4.21}$$

Expanding $TJT^\dagger$ using $T = T_1 + T_2(1 - T_4)^{-1}T_3$, and using the rules (4.21) to trade T_1, T_3 for

T_2, T_4, we find:

$$T(z)JT(z)^\dagger = J + T_2(1-T_4)^{-1}\Big[-(1-T_4)J(1-T_4^\dagger) - T_4J(1-T_4^\dagger) \\ - (1-T_4)JT_4^\dagger - T_4JT_4^\dagger + J\Big](1-T_4^\dagger)^{-1}T_2^\dagger \tag{4.22}$$

The terms inside the square brackets vanish, leaving J, so $T(z)$ is J-unitary. ■

Claim 4.5.4 *If $T(z)$ is unitary (J-unitary), then so is $\tilde{T}(z)$ defined above.*

proof: $\tilde{T}(z)$ is be obtained from $T(z)$ and $E(z)$ using concatenation, series and feedback operations. Since these preserve J-unitarity, $\tilde{T}(z)$ must be J-unitary as well. ■

4.5.1 Properties of the Roots and Poles of $\tilde{T}(z)$.

Claim 4.5.5 *If a transfer function $T(z)$ is J-unitary, its (complex) poles and zeros come in pairs of the form $z_0, -\overline{z}_0$. Furthermore, suppose x is an eigenvector of the zero z_0 of $T(z)$ in the sense of [49]. Then $x^\dagger J$ is an eigenvector of the pole $-\overline{z}_0$ at $T(z)$ in the sense of [49].*

proof: This follows from $T(z)JT(-\overline{z})^\dagger = J$. In particular, we can re-arrange to get

$$T^{-1}(z) = JT^\dagger(-\overline{z})J. \tag{4.23}$$

Since z_0 is an eigenvalue of $T(z)$ with eigenvector x, there are some vectors $x_2, x_3, ...$ such that $T(z)[x + x_2(z-z_0) + ...]$ is analytic with a zero at z_0. Multiplying on the left of Eq. (4.23) by $x^\dagger J + x_2^\dagger J(z + \overline{z_0}) + ...$, we find the expression is analytic with a zero at $-\overline{z}_0$. ■

Claim 4.5.6 *If a rational transfer function $T(z)$ is doubled-up, then it satisfies*

$$T(z) = \Sigma T(\overline{z})^\# \Sigma. \tag{4.24}$$

proof: $T(z)$ is doubled-up if and only if for each matrix R among A, B, C, D, $\Sigma R \Sigma = R^\#$. The rest is straightforward algebra. ■

The property $T(z) = \Sigma T(\overline{z})^\# \Sigma$ generalizes the notion of a doubled-up transfer function for a finite dimensional system to more general functions (i.e. $T(z)$ is no longer required to be rational).

Claim 4.5.7 *Given a transfer function $T(z)$ satisfying the property $T(z) = \Sigma T(\overline{z})^{\#}\Sigma$, if z_0 is a zero of $T(z)$, then so is $\overline{z_0}$. If x is an eigenvector of $T(z)$ at z_0, then $\Sigma x^{\#}$ is an eigenvector of $T(z)$ at $\overline{z_0}$.*

Similarly, if z_0 is a pole of $T(z)$, then so is $\overline{z_0}$. If x is an the eigenvector of $T(z)$ at z_0, then $\Sigma x^{\#}$ is an eigenvector of $T(z)$ at $\overline{z_0}$.

proof: Since z_0 is a zero of $T(z)$, there are some vectors $x_2, x_3, ...$ such that $T(z)[x + x_2(z - z_0) + ...]$ is analytic with a zero at z_0. Applying the property $T(z) = \Sigma T(\overline{z})^{\#}\Sigma$, and using the fact that $f(z)$ is analytic if and only if $\overline{f(\overline{z})}$ is analytic, we obtain the desired result.

The proof for the poles follows similarly. ■

Corollary 4.5.1 *If the zero z_0 with eigenvector x is real, then $y = \Sigma x^{\#}$ is also an eigenvector at z_0.*

Claim 4.5.8 *Suppose $T(z)$ is a rational transfer function that can be written in doubled-up form. If z is a pole of $\tilde{T}(z)$, then so is $\overline{z}$.*

proof: This follows from the fact that $\Sigma\tilde{T}(\overline{z})^{\#}\Sigma = \tilde{T}(z)$, proved using the identities $\Sigma E(z)\Sigma = E(\overline{z})^{\#}$ and $\Sigma A\Sigma = A^{\#}$, etc., below:

$$\begin{aligned}\Sigma\tilde{T}(\overline{z})^{\#}\Sigma &= \Sigma\left[D^{\#} + C^{\#}(zE(-\overline{z})^{\#} - A^{\#})^{-1}B^{\#}\right]\Sigma \\ &= D + C(zE(-z) - A)^{-1}B = \tilde{T}(z)\end{aligned} \tag{4.25}$$

From here we use Claim 4.5.7 to show that $\bar{z}$ is also a pole of $\tilde{T}(z)$. ■

4.5.2 The poles of $\tilde{T}(z)$ have bounded real part

We begin by showing that if $T_4(z)$ has singular values bounded away from zero for all $z \in \{|z| > C\}$ for some C (Assumption 3), then the poles of $\tilde{T}(z)$ have bounded real part. We will also use that $T_4(z)$ is a rational function (Assumption 1), and therefore its singular values are also bounded from above.

The original transfer function $T(z)$ is rational, so it has a finite number of poles. Therefore for the purposes of showing a bound for the real part of the poles of $\tilde{T}(z)$, we can ignore the poles of $T(z)$. The remaining poles of $\tilde{T}(z)$ can only occur when $(E(-z) - T_4(z))^{-1}$ has a pole. We will obtain our desired bounds using the following lemma:

Lemma 4.5.1 *Given matrices A, B with singular values satisfying $\sigma_{\min}(A) - \sigma_{\max}(B) > \epsilon$, the matrix $A - B$ is invertible, and $\sigma_{\min}(A - B) > \epsilon$.*

proof: The key step employs the triangle inequality:

$$\begin{aligned}\sigma_{\min}(A-B) &= \inf_{\|x\|=1} \|(A-B)x\| \geq \inf_{\|x\|=1} (\|Ax\| - \|Bx\|) \\ &\geq \inf_{\|x\|=1} \|Ax\| - \sup_{\|x\|=1} \|Bx\| = \sigma_{\min}(A) - \sigma_{\max}(B) > \epsilon. \end{aligned} \tag{4.26}$$

The matrix $A - B$ is invertible since all of its singular values are positive. ■

Lemma 4.5.2 *If $T_4(z)$ has singular values bounded away from zero for all $z \in \{|z| > C\}$ for some C, then there is a strip $\mathcal{S} = \{z : C_{low} < \Re(z) < C_{high}\}$ outside of which $\|\tilde{T}(z)\|$ is bounded from above.*

proof: We assumed that for all $z \in \{|z| > C\}$ for some C, the smallest singular value $\sigma_{\min}(T_4(z))$ is bounded away from zero. Notice when $\Re(z) < 0$, the greatest singular value of $E(-z)$ is $\exp(T_{\min}\Re(z))$, where $T_{\min}$ is the shortest delay. Thus when $\Re(z)$ becomes sufficiently negative, the greatest singular value of $E(-z)$ is smaller than the smallest singular value of $T_4(z)$, which is bounded from below. Hence, using Lemma 4.5.1, $E(-z) - T_4(z)$ is invertible for some $\Re(z) < C_{low}$, and its smallest singular value is bounded from below. A bound can be computed explicitly in terms of T_{min} and the lower bound on $\sigma(T_4(z))$.

Similarly, as $\Re(z)$ grows in the positive direction, the smallest singular value of of $E(-z)$ diverges. Using the boundedness of the singular values of $T_4(z)$ for sufficiently large $\Re(z)$ and applying Lemma 4.5.1, we find $E(-z) - T_4(z)$ is invertible for some $\Re(z) > C_{high}$, and that its singular value is bounded from below.

Combining the two results above, we obtain a strip $\mathcal{S} = \{z : C_{low} < \Re(z) < C_{high}\}$ such that all the poles of $\tilde{T}(z)$ occur inside $\mathcal{S}$, and the smallest singular value of $E(-z) - T_4(z)$ is bounded from below outside the strip. Thus we can bound $\|(E(-z) - T_4(z))^{-1}\|$ and therefore $\|\tilde{T}(z)\|$ from above outside $\mathcal{S}$. ■

4.6 Approximation using a static component

We will construct a transfer function $\tilde{S}(z)$, which behaves similarly to $\tilde{T}(z)$ for large $|z|$ by replacing $T(z)$ with a constant S. This corresponds to replacing the internal components of the system with

static counterparts. $\tilde{S}(z)$ is simpler to analyze than $\tilde{T}(z)$, and will be useful for several of the proofs.

4.6.1 Relation Between $\tilde{T}(z)$ and $\tilde{S}(z)$

Since we have assumed that $T(z)$ is finite-dimensional, in the limit $|z| \to \infty$ we have $T(z) \to S$, where S is a constant J-unitary, doubled-up matrix. We partition S in the same way as we did $T(z)$ into four blocks of the same sizes:

$$S = \lim_{|z|\to\infty} T(z) = \begin{pmatrix} S_1 & S_2 \\ S_3 & S_4 \end{pmatrix}. \tag{4.27}$$

Define

$$\tilde{S}(z) = S_1 + S_2 E(z) \left(I - S_4 E(z)\right)^{-1} S_3. \tag{4.28}$$

Finding a convergent factorization for $\tilde{S}(z)$ in terms of canonical factors will be a precursor to a similar factorization for $\tilde{T}(z)$. The relationship between $\tilde{S}$ and $\tilde{T}(z)$ for large $|z|$ is described in Lemma 4.6.3 below.

It will be useful to introduce $f_T(z) = \det(I - T_4(z)E(z))$ and $f_S(z) = \det(I - S_4 E(z))$.

Lemma 4.6.1 *Restricted to sufficiently large $|z|$, the poles of $\tilde{T}(z)$ and $\tilde{S}(z)$, respectively, are the roots of the functions $f_T(z)$ and $f_S(z)$.*

proof: This follows using Assumption 3 and that each $T_i(z)$ is rational ($i = 1, 2, 3, 4$). Specifically, the poles of $T_i(z)$ are bounded, so when $|z|$ is large enough $\tilde{T}(z)$ can only have poles when $f_T(z)$ has zeros (and similarly for $\tilde{S}(z)$). By Assumption 3, when $|z|$ is large enough, $T_2(z)$ and $T_3(z)$ have singular values bounded away from zero, and hence S_2 and S_3 have no zero singular values. Therefore, all of the zeros of $f_T(z)$ and $f_S(z)$ for large enough $|z|$ are also poles of $\tilde{T}(z)$ and $\tilde{S}(z)$, respectively. ■

Lemma 4.6.2 *Rate of convergence.*

(i) The rate of convergence of $T_4(z) \to S_4$ is $O(1/|z|)$.

(ii) When $\Re(z)$ is bounded, the rate of convergence of $f_T(z) \to f_S(z)$ is $O(1/|z|)$.

proof (i): From Assumption 1, $T_4(z)$ is analytic at infinity. Since $T_4(z) \to S_4$ as $|z| \to \infty$, the Laurent series of each of the components of $T_4(z)$ at infinity has the form $\sum_{n=0}^{\infty} \frac{c_n}{z^n}$. This implies

the rate of convergence of $T_4(z) \to S_4$ is $O(1/|z|)$. ■

proof (ii): Expand the determinant as a polynomial function for $f_T(z)$ and $f_S(z)$. Notice for both $f_T(z)$ and $f_S(z)$, the coefficients and the entries of $E(z)$ are the same. The desired estimate follows by subtracting the two expressions, using the triangle inequality, and noting each of the entries of $E(z)$ is bounded when $\Re(z)$ is bounded. ■

Lemma 4.6.3 *When $|z|$ is large, $\tilde{T}(z)$ approaches $\tilde{S}(z)$ in the following sense. For sufficiently large M, there exists $\epsilon_M = O(M^{-1})$ such that the following hold:*

(i) For each zero (pole) w_0 of $\tilde{S}(z)$ satisfying $|w_0| > M$, there is exactly one zero (pole) z_0 of $\tilde{T}(z)$ inside $B_{\epsilon_M}(w_0)$, and w_0 is the only zero (pole) of $\tilde{S}(z)$ in $B_{\epsilon_M}(z_0)$. Similarly, the statement holds if we exchange $\tilde{S}(z)$ and $\tilde{T}(z)$.

(ii) For z_0 and w_0 above, the orthogonal projectors P_T, P_S onto the span of the eigenvectors of $\tilde{T}(z)$ at z_0 and $\tilde{S}(z)$ at w_0, respectively, satisfy $\|P_T - P_S\| = O(\epsilon_M)$.

(iii) Given arbitrary but fixed ϵ, if $|z| > M$ and $z \notin B_\epsilon(w_0), B_\epsilon(z_0)$ for all poles w_0 and z_0 of $\tilde{S}(z)$ and $\tilde{T}(z)$, then we can estimate $\|\tilde{T}(z) - \tilde{S}(z)\| = O(1/M)$.

The proof is given in Appendix B.1.

4.7 Fundamental Factors of Quantum Linear Systems

In this section we will use the notation from Definitions 4.2.2 and 4.2.3.

Our goal will be to show that $\tilde{T}(z)$ can be factorized as $B\prod P_i(z)$ where $P_i(z)$ are elementary transfer functions of physically realizable components and B is a constant J-unitary and doubled-up matrix. For the $P_i(z)$ terms, we will use the transfer function of a generic physically realizable linear system with only two root and pole pairs. Such a system can be described using the SLH framework (see e.g. [6]) by

$$(S, L, H) = \left(I_{2\times 2}, \Lambda\breve{a}, \frac{1}{2}\breve{a}^*\Omega\breve{a} \right). \tag{4.29}$$

Above in Eq. (4.29), $\breve{a} = [a, a^*]^T$, $\Lambda = [\Lambda_-, \Lambda_+]$, and $\Omega = \Delta(\omega, \epsilon)$ is a Hermitian matrix. Specifically, $\breve{a}$ represents the internal field (creation / annihilation operators), Λ is related to the Lindblad terms in the master equation (coupling to environment) and Ω is related to the system Hamiltonian.

Defining $\breve{\Lambda} = \Delta(\Lambda_-, \Lambda_+)$, the state-space realization of this system is given by

$$A = -\frac{1}{2}\breve{\Lambda}^\flat\breve{\Lambda} - i\Omega J, \qquad B = -\breve{\Lambda}^\flat, \tag{4.30}$$

$$C = \breve{\Lambda}, \qquad D = I. \tag{4.31}$$

We can normalize $\breve{\Lambda}$ using $V = \breve{\Lambda}/\sqrt{\kappa}$ with $\kappa = |\Lambda_-|^2 - |\Lambda_+|^2$. This results in the form

$$P(z) = I - VV^\flat + V\frac{z - \frac{1}{2}\kappa + i\Omega J}{z + \frac{1}{2}\kappa + i\Omega J}V^\flat. \tag{4.32}$$

In Eq. (4.32) above, notice V is a doubled-up matrix satisfying $V^\flat V = I$, and $P_v = VV^\flat$ is the projector onto the subspace in which the input-output field interacts with the system.

4.7.1 Canonical form of the fundamental factors

There are two possibilities for the form of the transfer function, depending on whether its roots are complex or purely real. If the roots of the transfer function are complex ($|\omega| > |\epsilon|$), they come in pairs $(z_0, \overline{z_0})$, and the transfer function can be rewritten as:

$$P(z) = I - VV^\flat + V\begin{pmatrix} \frac{z-z_0}{z+\overline{z}_0} & 0 \\ 0 & \frac{z-\overline{z_0}}{z+z_0} \end{pmatrix}V^\flat. \tag{4.33}$$

If the roots (z_1, z_2) are purely real ($|\omega| < |\epsilon|$), the transfer function can be rewritten as:

$$P(z) = I - VV^\flat + \frac{1}{2}V\begin{pmatrix} 1 & i \\ 1 & -i \end{pmatrix}\begin{pmatrix} \frac{z-z_1}{z+z_2} & 0 \\ 0 & \frac{z-z_2}{z+z_1} \end{pmatrix}\begin{pmatrix} 1 & 1 \\ -i & i \end{pmatrix}V^\flat. \tag{4.34}$$

To derive this form, first write the form of the Hermitian matrix $\Omega = \begin{pmatrix} a & b\,e^{i\phi} \\ b\,e^{-i\phi} & a \end{pmatrix}$, where $a, b > 0$ without loss of generality (the $a < 0$ case is straightforward to transform into this form).

In the case when $i\Omega J$ has complex roots, we find $a > b$. Using $\eta = \tanh^{-1}(b/a)$ and $c = \sqrt{a^2 - b^2}$, we can write $\Omega = c\begin{pmatrix} \cosh(\eta) & \sinh(\eta)e^{i\phi} \\ \sinh(\eta)e^{-i\phi} & \cosh(\eta) \end{pmatrix} = c\begin{pmatrix} \cosh(\eta/2) & \sinh(\eta/2)e^{i\phi} \\ \sinh(\eta/2)e^{-i\phi} & \cosh(\eta/2) \end{pmatrix}^2 = cS^2$. Since S is unitary and J-unitary, $i\Omega J = icS^2J = icSJS^{-1}$. Finally, S is also doubled-up, so it can be

absorbed into V in Eq. (4.32). This leads to Eq. (4.33) with $z_0 = -\frac{1}{2}\kappa + ic$.

In the case when $i\Omega J$ has real roots, we find $a < b$. Using $\eta = \tanh^{-1}(a/b)$ and $c = \sqrt{b^2 - a^2}$, we can write $\Omega = c \begin{pmatrix} \sinh(\eta) & \cosh(\eta)e^{i\phi} \\ \cosh(\eta)e^{-i\phi} & \sinh(\eta) \end{pmatrix}$. Ω can then be transformed to its canonical form $\begin{pmatrix} 0 & ic \\ -ic & 0 \end{pmatrix}$ using the Bogoliubov transformation $\Omega \to S\Omega S^\dagger$, with

$$S = \begin{pmatrix} \cosh(\eta/2)e^{i(\pi/4-\phi/2)} & -\sinh(\eta/2)e^{i(\pi/4+\phi/2)} \\ -\sinh(\eta/2)e^{i(-\pi/4-\phi/2)} & \cosh(\eta/2)e^{i(-\pi/4+\phi/2)} \end{pmatrix} \tag{4.35}$$

as the J-unitary and doubled-up transformation matrix. Once we have transformed Ω to its canonical form, we can diagonalize $i\Omega J = \frac{1}{2}S^{-1}\begin{pmatrix} 1 & i \\ 1 & -i \end{pmatrix}\begin{pmatrix} c & 0 \\ 0 & -c \end{pmatrix}\begin{pmatrix} 1 & 1 \\ -i & i \end{pmatrix}S$, from which Eq. (4.32) can be used to derive the form Eq. (4.34) with $z_1 = \frac{1}{2}\kappa - c$, $z_2 = \frac{1}{2}\kappa + c$.

For the real roots case, the new matrices $\begin{pmatrix} 1 & 1 \\ -i & i \end{pmatrix}$ and $\begin{pmatrix} 1 & i \\ 1 & -i \end{pmatrix}$ are inserted explicitly instead of being absorbed into V to preserve the properties of V. It can be checked that both transfer functions Eq. (4.33) and Eq. (4.34) satisfy $P(z)JP^\dagger(-\overline{z}) = J$ and $P(z) = \Sigma P(\overline{z})^\#\Sigma$.

4.7.2 Constructing elementary factors to match a transfer function at a zero or pole

In this section we discuss how to construct transfer functions of the forms in Eq. (4.33) and Eq. (4.34) that match the zeros/poles and eigenvalues of a J-unitary and doubled-up transfer function $F(z)$. We also discuss the conditions under which it is not possible to construct terms of the desired form.

In Section 4.7.4, we will show how a particular term $P(z)$ with matching zeros/poles and eigenvalues can be detached from $F(z)$. In Section 4.8 we will discuss how such terms can be detached sequentially, giving the desired factorization.

For the case of a complex root z_0 and its eigenvector v_0, we use the term in Eq. (4.33) for $P(z)$. In this case another zero $\overline{z_0}$ and its eigenvector $\Sigma v_0^\#$, along with two poles $-\overline{z_0}$ and $-z_0$ and their eigenvectors, $v_0^\dagger J$ and $\Sigma v_0^T J$, respectively, are all determined for both $F(z)$ by Claims 4.5.5 and 4.5.7.

Theorem 4.7.1 *Given a rational J-unitary and doubled-up transfer function $F(z)$ with a conjugate pair of complex roots z_0 and $\overline{z_0}$ with respective eigenvalues v_0 and w_0 with $w_0 = \Sigma v_0^{\#}$ and $v_0^\dagger J v_0 \neq 0$, there exists a term of the form Eq. (4.33) with the same zeros and eigenvalues.*

proof: The proof is constructive:

1. Normalize v_0 so that $v_0^\dagger J v_0 = 1$. Since $w_0 = \Sigma v_0^{\#}$, it follows $w_0^\dagger J v_0 = 0$. From this it follows $w_0^\dagger J w_0 = -1$.

2. Set $V = [v_0, w_0]$ in Eq. (4.33). From the condition $w_0 = \Sigma v_0^{\#}$ it follows V is in doubled-up form. Using the identities in the previous step, one can show v_0 and w_0 are eigenvectors of $T(z)$ in the sense:

$$T(z)v_0 = \frac{z - z_0}{z + \overline{z}_0} v_0, \qquad\qquad T(z)w_0 = \frac{z - \overline{z}_0}{z + z_0} w_0. \tag{4.36}$$

   The eigenvalues are analytic in z and have a zeros at z_0 and $\overline{z}_0$, so v_0 and w_0 are their respective eigenvectors in the sense of Definition 4.2.10.

Since the term Eq. (4.33) is also J-unitary and doubled-up, the term found by Theorem 4.7.1 also has the same poles $-\overline{z_0}$ and $-z_0$ and their eigenvectors (up to a scalar), $v_0^\dagger J$ and $\Sigma v_0^T J$.

Next, we discuss the case of real roots. We will assume that the number of real roots is even, so that they can be paired to form terms of the form Eq. (4.34). Suppose a pair of zeros z_1 and z_2 of $F(z)$ is given, along with their corresponding eigenvectors v_1 and v_2. In this case the poles $-z_1$ and $-z_2$ and their eigenvectors $v_1^\dagger J$ and $v_2^\dagger J$ are determined by Claims 4.5.5.

Theorem 4.7.2 *Given a rational J-unitary doubled-up transfer function $F(z)$ with two real roots z_1 and z_2 and corresponding eigenvectors v_1 and v_2 respectively, such that $v_1^\dagger J v_2 \neq 0$, there exists a term $P(z)$ of the form Eq. (4.34) with the same zeros and eigenvectors.*

proof:

1. Using Corollary 4.5.1 and the assumption that each eigenspace is one dimensional (Assumption 6), the phase of the eigenvectors can be chosen such that $v_1 = \Sigma v_1^{\#}$ and $v_2 = \Sigma v_2^{\#}$. This implies $v_1^\dagger J v_1 = v_2^\dagger J v_2 = 0$.

2. There are two remaining degrees of freedom for how the eigenvectors can be chosen, corresponding to their norms. Notice the value $v_1^\dagger J v_2$ is always imaginary due to the previous step. We make one of the constraints $v_1^\dagger J v_2 = i/2$ (we may have to switch the order to get the right sign). The other constraint, corresponding to the relative norms of the two eigenvectors, can

be chosen arbitrarily.

3. Set V by

$$V = (v_1, v_2) \begin{pmatrix} 1 & 1 \\ -i & i \end{pmatrix}. \tag{4.37}$$

As a result of of $v_i = \Sigma v_i^{\#}$ for $i = 1, 2$, the matrix V is doubled-up in the sense of Eq. (4.1).

$$T(z)v_1 = \frac{z - z_1}{z + z_2} v_1, \qquad T(z)v_2 = \frac{z - z_2}{z + z_1} v_2. \tag{4.38}$$

The eigenvalues are analytic in z and have a zeros at z_1 and z_2, so v_1 and v_2 are their respective eigenvectors in the sense of Definition 4.2.10.

Since the term Eq. (4.34) is also J-unitary and doubled-up, the term found by Theorem 4.7.2 also has he same poles $-z_1$ and $-z_2$ as $F(z)$ as well as the same eigenvalues at those poles.

4.7.3 Another form of the elementary factors

The elementary factors in Section 4.7.1 can be re-written in another form, which can be useful. We will focus here on the terms resulting from a canonical factor with two complex roots, Eq. (4.33). We can write this function as

$$P(z) = I - VV^\flat + VF(z)V^\flat. \tag{4.39}$$

Here $V^\flat V = I$ and $F(z) = \operatorname{diag}(a(z), a(\overline{z})^*) = \operatorname{diag}\left(\frac{z-z_0}{z+\overline{z_0}}, \frac{z-\overline{z_0}}{z+z_0}\right)$. With the substitution $W = VJ$, we obtain

$$P(z) = I - WJW^\dagger J + WJF(z)W^\dagger J = (J - WJW^\dagger - WJF(z)W^\dagger)J. \tag{4.40}$$

Also, W satisfies $W^\dagger JW = J$ since $V^\flat V = I$.

Next, we will complete the column space $\mathcal{W}$ of W, forming a J-unitary matrix M. Care must be taken since we use the indefinite inner product given by $[x, y] \equiv x^\dagger Jy$, as opposed to the standard inner product. In our situation, $\mathcal{W}$ is nondegenerate, meaning that if $x \in \mathcal{W}$ and $[x, y] = 0$ for all $y \in \mathcal{W}$ then $x = 0$. Therefore, we can apply proposition 2.2.2 in [12], which implies the orthogonal companion given by $\mathcal{W}^{[\perp]} = \{x \in \mathbb{C}^n | [x, y] = 0 \text{ for all } y \in \mathcal{W}\}$ is the direct complement of $\mathcal{W}$. This result can be used to construct an orthonormal basis $[x_i, x_j] = \pm\delta_{i,j}$, as discussed in [12]

following proposition 2.2.2. Further, proposition 2.2.3 in [12] implies we can pick our basis so that $[x_i, x_j] = J_{ij}$. Stacking the columns $M = [x_1|...|x_{2n}]$, we find M is a J-unitary matrix.

We can use M to write

$$P(z) = M\text{diag}\left(a(z), -a(\overline{z})^*, 1, -1, ..., 1, -1\right) M^\dagger J. \tag{4.41}$$

This term is analogous to the Blachke-Potapov factors Eq. (13) in reference [17], albeit there are some differences due to the indefinite inner product used in the construction.

4.7.4 Zero and Pole Matching

Suppose we are given a transfer function $A(z)$ satisfying $A(z)JA^\dagger(-\overline{z}) = J$ and $A(z) = \Sigma A(\overline{z})^\#\Sigma$. We wish to factorize it according to its roots and poles. By the claims in Section 4.5, we can relate the eigenvector of the zero z_0 to that of a pole at $-\overline{z}_0$. Further, if the zeros are purely complex, there is another zero-pole pair $\overline{z}_0, -z_0$, and the eigenvectors of all four points can be related.

Lemma 4.7.3 *Given two transfer functions $A(z)$ and $P(z)$ both with a pole (zero) at w_0 of partial multiplicity 1 (for simplicity) with the same eigenvectors, and no other poles or zeros at w_0. Then the function $A(z)P(z)^{-1}$ is analytic at w_0 with no zeros or poles.*

Proof: Let Q be the orthogonal projector onto the span of the eigenvectors, and $W = Q/w_0$. As in the proof of theorem 2.1 of [1], we can factorize a pole from both $A(z)$ and $P(z)$:

$$\begin{aligned} A(z)P(z)^{-1} &= A(z)(I - zW)(I - zW)^{-1}P(z)^{-1} \\ &= A(z)(I - zW)[P(z)(I - zW)]^{-1} = \tilde{A}(z)\tilde{P}(z)^{-1}, \end{aligned} \tag{4.42}$$

where $\tilde{A}(z) = A(z)(I - zW)$ and $\tilde{P}(z) = P(z)(I - zW)$. The partial pole multiplicities of $\tilde{A}(z)$ and $\tilde{P}(z)$ at w_0 are all smaller than those of $A(z)$ and $P(z)$, respectively, by 1. The zero multiplicities of $A(z)$ and $\tilde{A}(z)$ at w_0 are the same (the same for tilde $P(z)$ and $\tilde{P}(z)$). Since we have assumed (for simplicity) that the poles all have partial multiplicity 1, the functions $\tilde{A}(z)$ and $\tilde{P}(z)$ are analytic at w_0, which has no poles or zeros. We conclude that $\tilde{A}(z)\tilde{P}(z)^{-1}$ is analytic at w_0 and has no zeros or poles at w_0.

The proof is similar for the case of a zero instead of a pole. In this case, where Q is the orthogonal

projector onto the span of the zero eigenvectors and $W = Q/w_0$, we factorize:

$$\begin{aligned} A(z)P(z)^{-1} &= A(z)(I - zW)^{-1}(I - zW)P(z)^{-1} \\ &= A(z)(I - zW)^{-1}[P(z)(I - zW)^{-1}]^{-1} = \tilde{A}(z)\tilde{P}(z)^{-1}, \end{aligned} \tag{4.43}$$

where $\tilde{A}(z) = (I - zW)^{-1}$ and $\tilde{P}(z) = P(z)(I - zW)^{-1}$. The rest of the argument is similar to the case where w_0 is a pole. ■

4.8 Factorization for quantum linear systems by physically realizable components

Ultimately, we are interested in the setup given in Section 4.1. We wish to detach from $\tilde{T}(z)$ a (possibly infinite) sequence of transfer functions of physically realizable terms, which have the form of Eq. (4.33) or Eq. (4.34), so that the remaining function has no zeros or poles. Explicitly,

$$\tilde{T}(z) = \prod_n P_n(z)B(z), \tag{4.44}$$

where $B(z)$ has no zeros or poles. In order to obtain the product in Eq. (4.44), the appropriate terms $P_n(z)$ will be detached sequentially. We will also show $B(z)$ is a constant given our assumptions. In order to obtain a factorization of the above form, we will use for $P_n(z)$ terms of the form Eq. (4.33) or Eq. (4.34), depending whether two real roots or two complex roots are chosen. This is discussed in Section 4.7.

Before we discuss systems with feedback, we will first discuss the factorization applied to systems without feedback described by a transfer function $T(z)$ in Section 4.8.1. This case is easier since the product in Eq. (4.44) is finite.

When feedback is present, the product in Eq. (4.44) in general may be infinite. In this case, we must show the product converges for some ordering of the factors $P_n(z)$. To this end, we introduced $\tilde{S}(z)$ discussed in Section 4.6. $\tilde{S}(z)$ behaves similarly to $\tilde{T}(z)$ for large $|z|$, and is easier to study. Physically, this corresponds to replacing the components yielding the function $T(z)$ with static counterparts. We will construct our desired factorization for $\tilde{S}(z)$ in Section 4.8.2. In Section 4.8.3 we will discuss the more general factorization of $\tilde{T}(z)$.

4.8.1 Finite dimensional system with no feedback

In this section, we will discuss the factorization of the finite-dimensional system $T(z)$. We make the same assumptions stated above for $T(z)$.

As discussed above, we can choose terms $P_n(z)$ using terms of the form Eq. (4.33) or Eq. (4.34), depending on whether each root is real or complex, with the caveat that the conditions discussed in Section 4.7.2 must hold at each step of the factorization. This leads to a factorization of the form $T(z) = \prod_{n=1}^{N} P_n(z)B(z)$. Here N is a finite number since there are a finite number of zeros and poles for $T(z)$.

In the limit $|z| \to \infty$, we find each of the $P_n(z)$ and the $T(z)$ converges to a constant matrix. Therefore, $B(z)$ is a constant matrix (call it B). It also satisfies the doubled-up and J-unitary properties. Further, if $T(z)$ is physically realizable, then each of the finite $P_n(z)$ can be inverted showing B is also physically realizable.

Notice the existence of a realization of a finite-dimensional state-space matrices A, B, C, D is automatically implied by the physical realization of a system with the appropriate transfer function.

4.8.2 Static System with Nonzero Time Delays

In the special case $T(z) = S$, we find $\tilde{T}(z) = \tilde{S}(z)$ for $\tilde{S}(z)$ in Eq. (4.28).

We will show the following:

Theorem 4.8.1 *Assume that each term $P_n(z)$ can be constructed sequentially as discussed in Section 4.7.2. Then there is a way to pick terms $P_n(z)$ so that the product $\prod_n P_n(z)$ converges uniformly on compact sets, $\tilde{S}(z) = \prod_n P_n(z)B$, and B is a constant matrix.*

The proof is given in Appendix B.2. After the proof we also discuss the rate of convergence of the factorization. See in particular Theorem B.2.1.

4.8.3 Finite Dimensional System with Nonzero Time Delays

Next, we generalize to the case where $T(z)$ replaces the static component $S = \lim_{z\to\infty} T(z)$, to obtain a factorization for $\tilde{T}(z)$ instead of $\tilde{S}(z)$.

As in the case using a static component in Section 4.8.2, again we only need to consider terms $P_n(z)$ with complex roots for convergence, since the number of terms with real roots is finite. For this reason we will again ignore the real roots.

Theorem 4.8.2 *Suppose that the factorization for $\tilde{S}(z)$ in Theorem 4.8.1 exists and converges uniformly on compact sets. Assume that terms $P_n(z)$ can be detached sequentially from $\tilde{T}(z)$ as discussed in Section 4.7.2. Then there is a factorization $\tilde{T}(z) = \prod_n P_n(z)B$ that converges uniformly on compact sets, where B is a constant matrix.*

The proof is given in Appendix B.3, along with a simplified sketch of the proof. We discuss rate of convergence following the proof as well.

remark 4.8.1 *Notice that B in Theorem 4.8.2 is J-unitary and doubled-up. This follows by noticing the product $\prod_n P_n(z)$ is J-unitary and doubled-up, and inverting it to get $B = \tilde{T}(z)\left(\prod_n P_n(z)\right)^{-1}$ and using Claims 4.5.1 and 4.5.2.*

4.8.4 Limiting behavior of $\tilde{T}(z)$

For finite-dimensional systems, one way to characterize systems with no static squeezing was to examine the matrix D in the state-space realization, and ensure it had the form $D = \Delta(\tilde{D}, 0)$, where $\tilde{D}$ is a Hermitian matrix. Since the transfer function had the form $D + C(zI - A)^{-1}B$, we could take $|z| \to \infty$, and the direction along which the limit was taken did not matter. However, as seen in Eq. (B.23), when delayed feedback is present the direction of the limit is important, and can yield different results.

Notice that obtaining different limit values of $\tilde{T}(z)$ as $|z| \to \infty$ is still consistent with the factorization $\tilde{T}(z) = \prod_n P_n(z)B$ of Theorem 4.8.2, even though each term $P_n(z)$ approaches I as $|z| \to \infty$ (along any direction). This is because the convergence of the product is only uniform on compact sets, and not the whole plane. Thus the limit and the product cannot be exchanged.

4.9 Examples

Below we construct several systems as examples. We show how our methodology can be used to construct a reduced model for each. We also discuss applications of some of the examples and some limitations of our methodology.

For each example, we provide a diagram of the poles of the system, an illustration of the transfer function of the original system versus the reduced system, and the squeezing spectrum of the original system versus the reduced system. Below we discuss these further.

In each of the examples, we will see the poles satisfy Claim 4.5.7: If p is a pole of a physically realizable system, then so is its complex conjugate $\overline{p}$. The zeros (on the right side of the complex plane) are not shown, but satisfy the property that z is a zero of a physically realizable transfer function if and only if p is a pole.

In each diagram illustrating a transfer function, we show the real and imaginary components of specific components along $z = i\omega$ (real frequencies). Our examples focus on cases when there is a single input/output port (carrying a creation and an annihilation bosonic field, labeled by indices 0 and 1 respectively). In this case, the transfer function has four complex-valued components, mapping different input-output combinations between the input annihilation and creation fields and their analogous output fields. In the diagrams we illustrate $T[0,0]$ (input annihilation to output annihilation fields) and $T[1,0]$ (input creation to output annihilation fields). The remaining components $T[1,1]$ and $T[0,1]$ are determined by the first two.

Below, we also refer to the squeezing spectrum (power spectral density), which is the amount of output power from the system along a particular quadrature at each frequency. The squeezing spectrum can be computed from the transfer function, using Eq. (28) in [20] (also Eq. (26) in [7]). Explicitly, the output quadrature along angle θ is defined as

$$q_{\text{out},i}(t,\theta) = e^{i\theta} b_{\text{out},i}(t) + e^{-i\theta} b^{\dagger}_{\text{out},i}(t), \tag{4.45}$$

and we define the power spectrum at frequency ω to be given by

$$P_{ij}(\omega,\theta) = \lim_{T\to\infty} \frac{1}{T} \left\langle \int_0^T e^{i\omega t_1} q_{\text{out},i}(t_1,\theta) dt_1 \int_0^T e^{-i\omega t_2} q_{\text{out},j}(t_2,\theta) dt_2 \right\rangle. \tag{4.46}$$

4.9.1 Example 1

In our first example, we have a squeezing component with a single channel, followed by a feedback loop. The squeezing component can be realized by a non-detuned degenerate OPO. In the SLH formalism, it can be represented by:

$$(S, L, H) = \left(1, \sqrt{\kappa}a, i\epsilon \left(a^{\dagger 2} - a^2\right)\right). \tag{4.47}$$

To construct the feedback loop, we will require a beamsplitter with a reflectivity r and transmissivity $t = \sqrt{1-t^2}$, having two channels. A beamsplitter has trivial L and H components. We will use the scattering matrix S_{BS} for the beamsplitter,

$$S_{BS} = \begin{pmatrix} -\sqrt{1-r^2} & r \\ r & \sqrt{1-r^2} \end{pmatrix} = \begin{pmatrix} -t & r \\ r & t \end{pmatrix}. \tag{4.48}$$

Next, we can use the SLH rules to combine the two components, resulting in a system we will denote G below. We align them so that the squeezing component lies in 'series' on the first channel before the input to the beamsplitter. This is analogous to the setup of Example VI.1 of [6]. Specifically, we obtain the system described by Eq. (122) from [6]. The SLH model for system G is

$$(S_G, L_G, H_G) = \left(\begin{pmatrix} -\sqrt{1-r^2} & r \\ r & \sqrt{1-r^2} \end{pmatrix}, \begin{pmatrix} -\sqrt{1-r^2}\sqrt{\kappa}a \\ r\sqrt{\kappa}a \end{pmatrix}, i\epsilon({a^\dagger}^2 - a^2) \right). \tag{4.49}$$

Finally, to complete the feedback loop for this example, we would like to insert time-delayed coherent feedback from the output of the second channel to the input of the second channel of the concatenated system 4.49. This is illustrated in Figure 4.2. To do this, we follow our procedure discussed in Section 4.4. First we translate from the SLH formalism to the state-space formalism in order to find the transfer function $T(z)$ of the system G above. Then we add the time delay term $E(z) = \mathrm{diag}(e^{-Tz}, e^{-Tz})$ as discussed in Section 4.4. The feedback loop is inserted from the second output to the second input. For our analysis below we set the parameters to be $T = 2.0, r = 0.6, \kappa = 1.0, \epsilon = 0.2$.

The poles of the system are shown in Figure 4.3. There are two non-degenerate poles (at $-\frac{1}{2}\kappa \pm \epsilon = -0.3, -0.7$) resulting from the squeezer, and one degenerate real pole (at about -0.1) along with an infinite set of complex poles resulting from the time delay. The two non-degenerate poles can be thought of as coming from the squeezing component, while the rest are from the feedback loop. The reason the poles of the composite system can be partitioned to those of each component is due to how the composite system is set up. The two components (squeezing element and feedback loop) essentially occur in series in this example, so the transfer function of the composed system can be constructed using a product of two transfer functions, one belonging only to the squeezer and the other to the feedback loop. The reason the poles due to the feedback loop are degenerate is because we used the doubled-up notation, which becomes degenerate in the case of a passive system – the transfer function for the annihilation and creation fields do not influence each other and can be

determined from one another.

The complex poles were degenerate in the sense that their eigenvectors did not satisfy the condition $v^\dagger Jv \neq 0$. Two ways to deal with this special case are (1) try to break the degeneracy by adding a phase shift within the loop and (2) perturb the eigenvector and use a modified factor. When using (1), each complex pole and the degenerate real pole split into two complex poles. To obtain the factorization then, one would use the usual construction of complex poles, using every other pole as ordered in the imaginary direction (since each term also includes the conjugate pole, we do not include both nearly overlapping poles). When using (2), we use a modified factor, built of of two separate terms:

$$P(z) = \left(I - VV^\flat + V \begin{pmatrix} \frac{z-z_0}{z+\overline{z_0}} & 0 \\ 0 & \frac{z-\overline{z_0}}{z+z_0} \end{pmatrix} V^\flat\right)\left(I - VV^\flat + V \begin{pmatrix} \frac{z-\overline{z_0}}{z+z_0} & 0 \\ 0 & \frac{z-z_0}{z+\overline{z_0}} \end{pmatrix} V^\flat\right). \tag{4.50}$$

Each term corresponds to one of the terms resulting from the poles being perturbed. To deal with the degenerate real pole using approach (2), one can find the two-dimensional eigenspace at the pole, and use both vectors to construct V in the usual way for real poles. For our example, we tried both approach (1) with a phase shift $\delta = 10^{-3}$ as well as approach (2) where the first entry of v_1 was increased by $\epsilon = 10^{-3}$. The resulting functions were visually indistinguishable when plotted along $z = i\omega$ for real values of ω. The original transfer function is shown against the approximated transfer function with the real poles and a total of six complex poles (or eight if the degenerate real pole is perturbed into two complex poles) in Figure 4.4. The code for the example is available on Github at [54].

Finally, we computed the squeezing spectrum for this example, for both the original as well as reduced system. Since the feedback loop in this example did not alter the squeezing properties, the reduced model resulting from just the two non-degenerate poles (from the squeezing component) was sufficient for capturing the squeezing effects of the system. The end result was that the reduced model and the complete model led to exactly the same squeezing spectrum (see Figure 4.5).

4.9.2 Example 2

The next example is similar to Example 1, except that the feedback loop now includes it in the squeezing component. The construction is similar, except both the input and output ports have been permuted before the time delayed feedback was introduced (see Figure 4.6). The parameters we used for this example were: $\kappa = 1.0, r = 0.97, \epsilon = 0.1, T = 5.0$. The network in this example is similar to the one introduced in [20] and experimentally implemented in [25]. In this network,

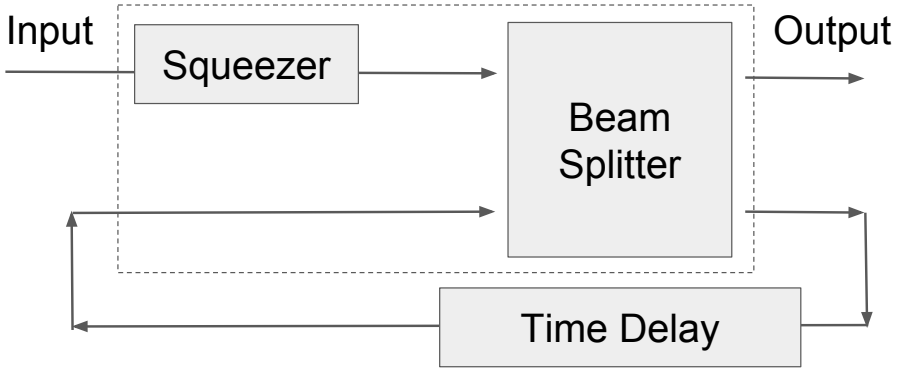

Figure 4.2: An example of a time-delay network. The dashed box shows the system G discussed in the text in Section 4.9.1, generated by concatenating the squeezer with the beamsplitter. Squeezed light enters a feedback loop designed using the beamsplitter and delayed feedback.

placing the squeezer within the feedback loop results in enhanced squeezing. Our modification is the incorporation of a positive time delay in the feedback loop.

The pole diagram (Figure 4.7) is substantially different than that of Example 1. The squeezer is no longer being cascaded in series with the feedback loop, but is now inside of it. As a result, the resulting poles are no longer the collective poles of the component systems. Instead, the effective behavior we see is that of several individual squeezing components, some of which are detuned in frequency. It can be shown that for a squeezing component with $(S, L, H) = (1, a\sqrt{\kappa}, \Delta a^\dagger a + i\epsilon[{a^\dagger}^2 - a^2])$ the location of poles is given by $p = -\kappa \pm \sqrt{\epsilon^2 - \Delta^2}$. Thus when the detuning Δ becomes larger than the squeezing parameter ϵ, the poles become complex-valued. Intuitively, the feedback loop generates a cavity with many modes, each having poles p and $\overline{p}$ with multiplicities 2. When squeezing is introduced, each of the poles splits into two poles. Each resulting pair of conjugate poles corresponds to an effective squeezer. As we examine poles with increasing imaginary part, we see they approach a periodic pattern. This is a consequence of Lemma 4.6.3, where asymptotically the system behaves as if the squeezing component became negligible, and the modes we see approach those of an empty cavity.

We found there were two non-degenerate real poles of multiplicity 1, and each of the complex poles also had multiplicity 1. However, the complex poles were degenerate in the sense that their eigenvectors v had $v^\dagger J v = 0$, thus making them non-normalizable. We resolved this issue by perturbing the first component of each eigenvector. We included two product terms (four complex poles) in this way. Finally, in Figure 4.9 we see good agreement between the squeezing spectrum of the original system versus the reduced system.

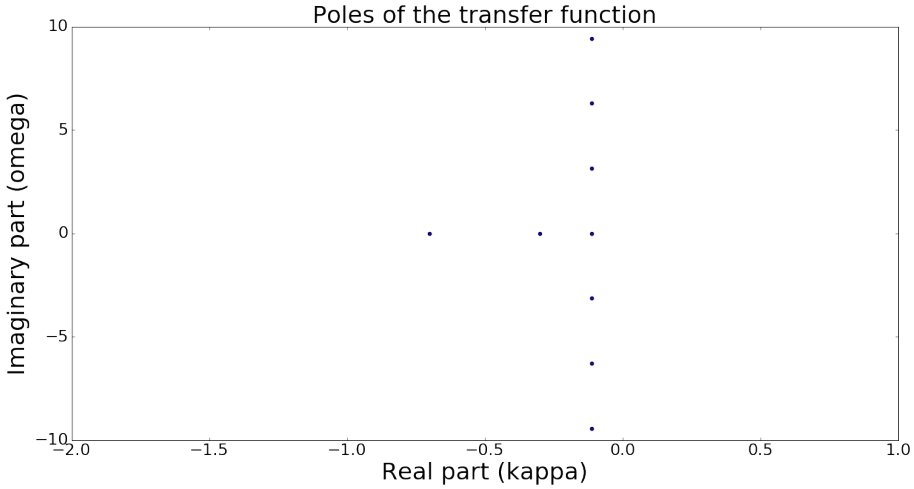

Figure 4.3: The poles of the transfer function of the system in Example 1. The complex poles for this system have multiplicity 2. Two of the real poles result from the squeezing component $(-0.3, -0.7)$, and the rest are degenerate poles due to the feedback loop.

4.9.3 Example 3

This example is based on the system discussed in [39]. Here the squeezing component has two channels, which are used to construct the feedback loop shown in Figure 4.10. Specifically, we started with the SLH model for the squeezer:

$$(S, L, H) = \left(I, \begin{pmatrix} a\sqrt{2\kappa_b} \\ a\sqrt{2\kappa_c} \end{pmatrix}, \frac{i\epsilon}{2}(a^{\dagger 2} - a^2) \right) \tag{4.51}$$

We also allow in our model to have loss, which is modeled using an extra input-output channel along with a beamsplitter. However, for the purposes of the analysis here we made the loss zero (i.e. the beamsplitter has reflectivity $r = 0.0$). Finally, we introduce the delayed feedback as shown in Figure 4.10 (permuting the channels as necessary). For the analysis here we set $\kappa_b = 1.0, \kappa_c = 0.9, \epsilon = 0.2$ and $T = 1.0$.

In Figure 4.11 we demonstrate the poles for the system with out choice of ϵ. In Figure 4.13 we show the poles using several other choices of ϵ. Similar to the previous example, we see the pole splitting as ϵ becomes larger, with degenerate poles when $\epsilon = 0.0$. Qualitatively, the pole behavior is different than Example 2 as the imaginary part becomes large. Instead of the poles converging to a periodic pattern, they instead lie on a transcendental equation (see the caption of Figure 4.13). The reason this is possible is that Assumption 3 is not satisfied. In particular, one can show that $T_4(z)$ has

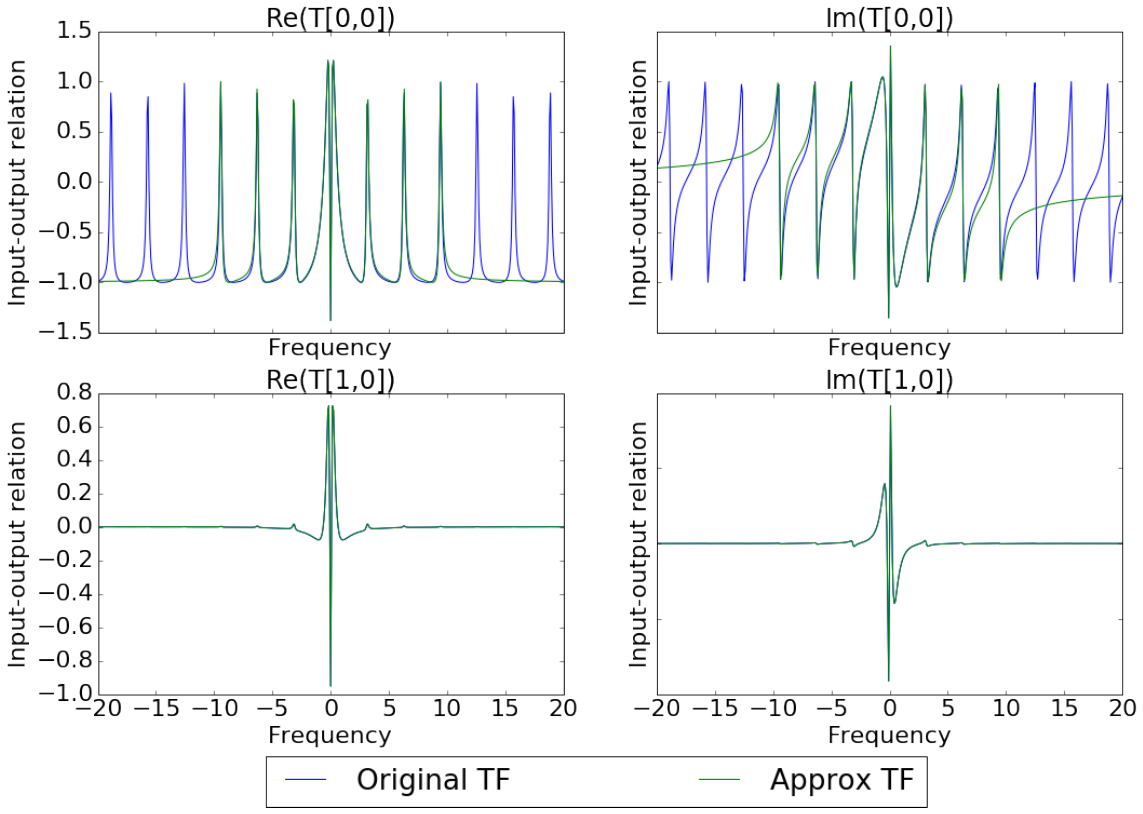

Figure 4.4: The transfer function of the example system, and the transfer function of an approximation generated using the canonical factors. A constant pre-factor was added so that the two functions match at the origin. The real and imaginary parts of two components are shown along $z = i\omega$ for real values of ω.

asymptotically a zero singular value, and thus the transfer function $\tilde{T}(z)$ is not proper. Although this seems concerning since our convergence theorem does not apply, in practice the factorization seems to produce a well-behaved reduced system. Notice if a small change was made to the system (for example by perturbing the scattering matrix S) it is possible to introduce a small positive lower bound to singular values of $T_4(z)$ thus preventing any potential issues.

We remark the most interesting region for this example is where the power spectrum peaks (Figure 4.15. Indeed, this was the original reason the system was studied in [39]. This effect seemed to be the result of the delayed feedback. Our decomposition suggests an interpretation of the system based on the canonical factorization. The poles all move off the real axis after the feedback loop is introduced (so the squeezing moves off resonance), and the resulting poles can be interpreted as effectively detuned squeezers.

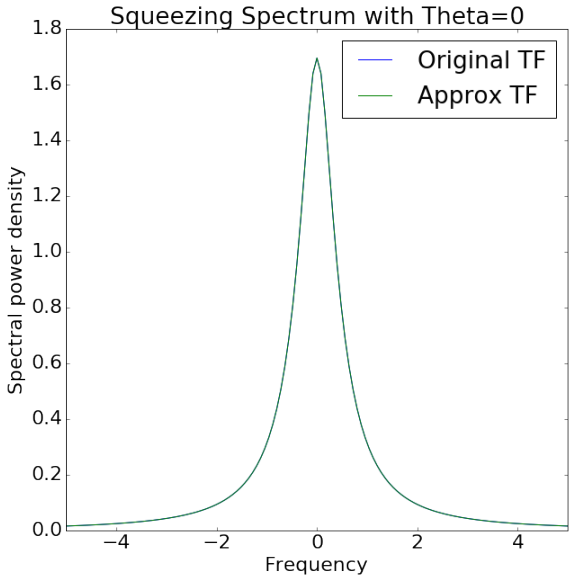

Figure 4.5: The squeezing spectrum of the system in Example 1, along with its reduced counterpart. In this case, the feedback loop has no effect on squeezing, and capturing the effect of the two non-degenerate poles corresponding to the squeezing component is enough to capture the squeezing effect of the system. We also remark in this case the squeezing spectrum was independent of the time delay used.

As in Example 2, we faced a similar degeneracy issue ($v^\dagger Jv = 0$ for complex pole eigenvectors). As before, this was handled by perturbing the first component of each eigenvector. This seemed to work well for the first two pairs of complex poles, but seemed to cause numerical issues for further terms. We anticipate there may be a more stable way to avoid this issue. Nevertheless, the transfer function of the reduced model (Figure 4.14) and the power spectrum (Figure 4.15) seem close to those of the original system. This was especially the case in the regime of interest, where the squeezing peaks.

4.10 Conclusion

We have shown how a factorization theorem can be obtained for a linear quantum network with delayed feedback under some stated assumptions. The conditions are fairly general, and allow for a wide class of quantum linear systems which may be active. The factorization generates a cascade of possibly infinitely many 2×2 quantum linear systems, with transfer functions $P_i(z)$. These canonical terms can also include squeezing. Our theorem states that the factorization has

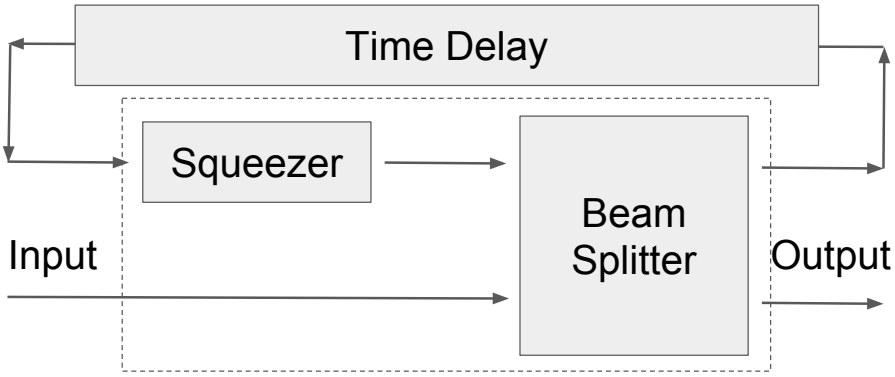

Figure 4.6: An example of a time-delay network (Example 2). The dashed box shows the system G discussed in the text in Section 4.9.1, generated by concatenating the squeezer with the beamsplitter. In this example the squeezer is inside the feedback loop, given significantly different behavior than the system in Example 1.

form $\tilde{T}(z) = B\prod_i P_i(z)$, where B is a constant matrix. We show that this product converges on compact sets. The B matrix must be J-unitary and doubled-up as well.

One of our assumptions excludes cases with essentially feedforward delays, and other assumptions are made for simplicity. To get each individual factor, we also require non-degeneracy conditions to be met. However, as we showed in the examples in Section 4.9, it is possible to find good approximations even when the non-degeneracy conditions are not met by perturbing the system.

We have shown how our methodology can be applied in a number of examples. These have applications in enhancing squeezing and controlling its range, which has wider applicability in quantum technology. Our procedure results in an effective system that has similar behavior in the desired range, and hence can be easier to handle in the case of simulations, especially when the system is integrated into a larger network. For isolated linear systems, simulation is not an issue since the state-space formalism can be used in place of a full quantum simulation. However, if an encompassing network has nonlinear components then a full quantum simulation may be required. In this case, other methods of capturing time delays may become prohibitive. However, using a reduced system captured by our procedure, we utilize the minimal number of degrees of freedom to capture the effective behavior of a particular linear coherent feedback network.

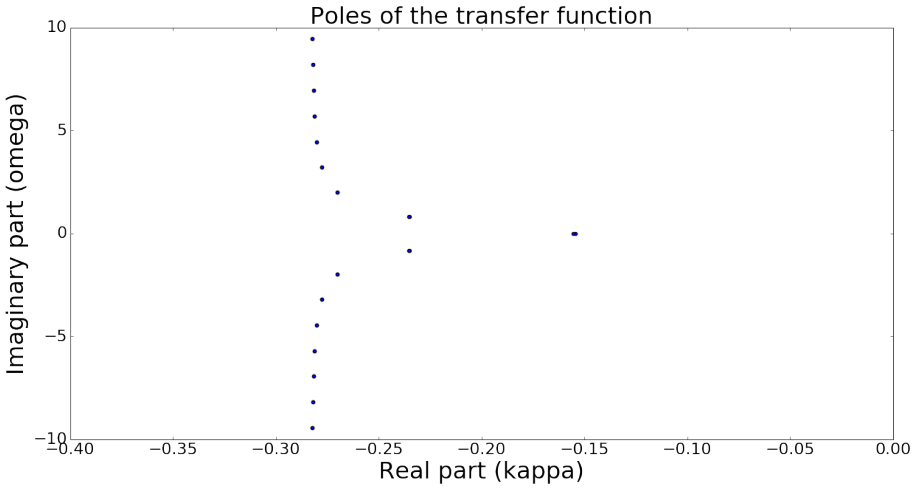

(a)

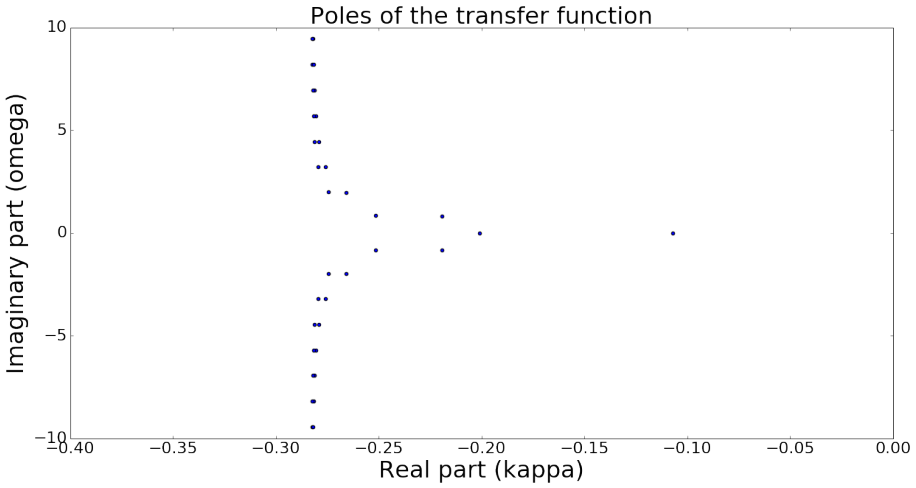

(b)

Figure 4.7: The poles of the transfer function of the system in Example 2, for different parameters. The complex poles are have multiplicity 1, but become asymptotically close to each other as the imaginary component increases. This is because the effect of the squeezer become weaker and thus the pole splitting due to the squeezer have a smaller effect. In the top diagram (Figure 4.7a) we choose $\epsilon = 0.001$ to illustrate the pole splitting when squeezing is introduced. In the bottom diagram (Figure 4.7b) we show the pole diagram for $\epsilon = 0.1$, the parameter we use for the remaining analysis.

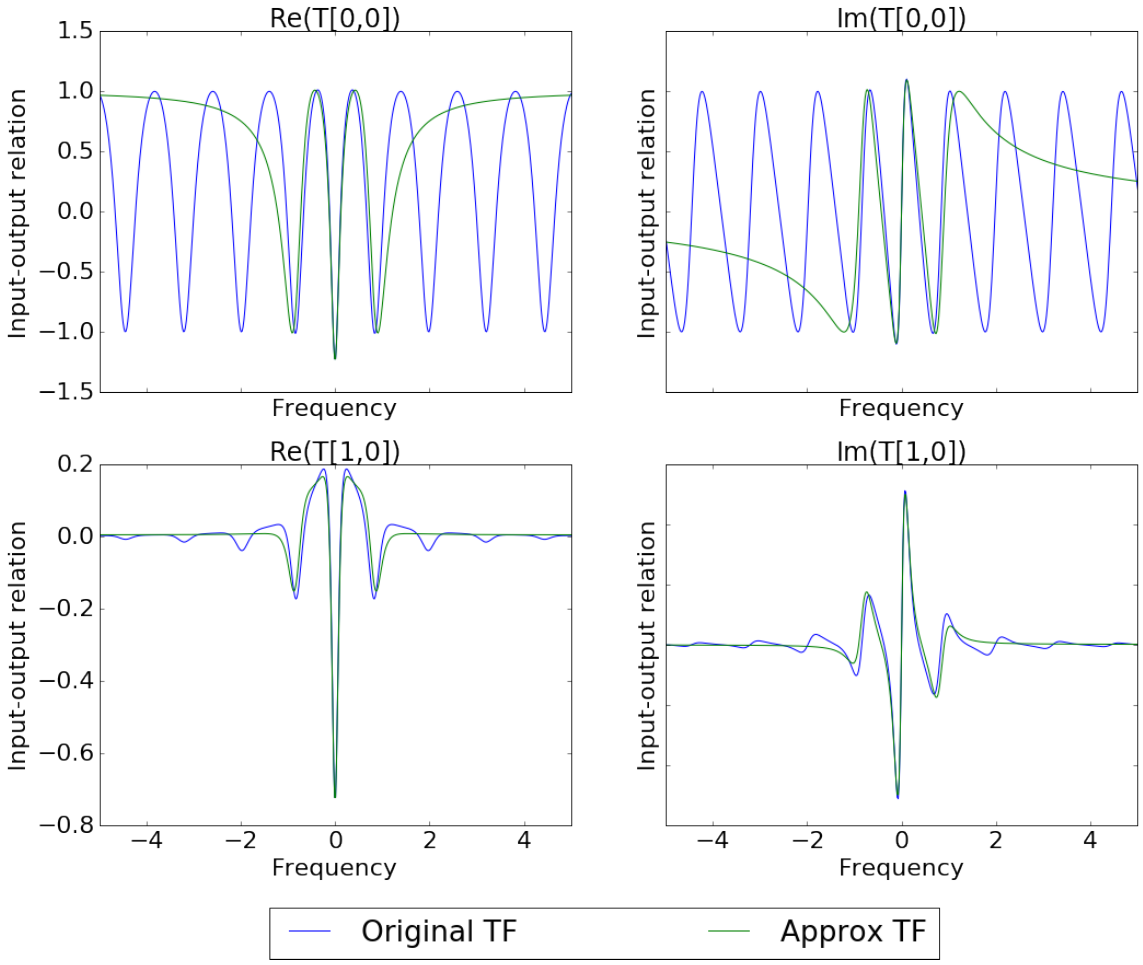

Figure 4.8: The transfer function of Example 2, and the transfer function of an approximation generated using the canonical factors. A constant pre-factor was added so that the two functions match at the origin. The real and imaginary parts of two components are shown along $z = i\omega$ for real values of ω.

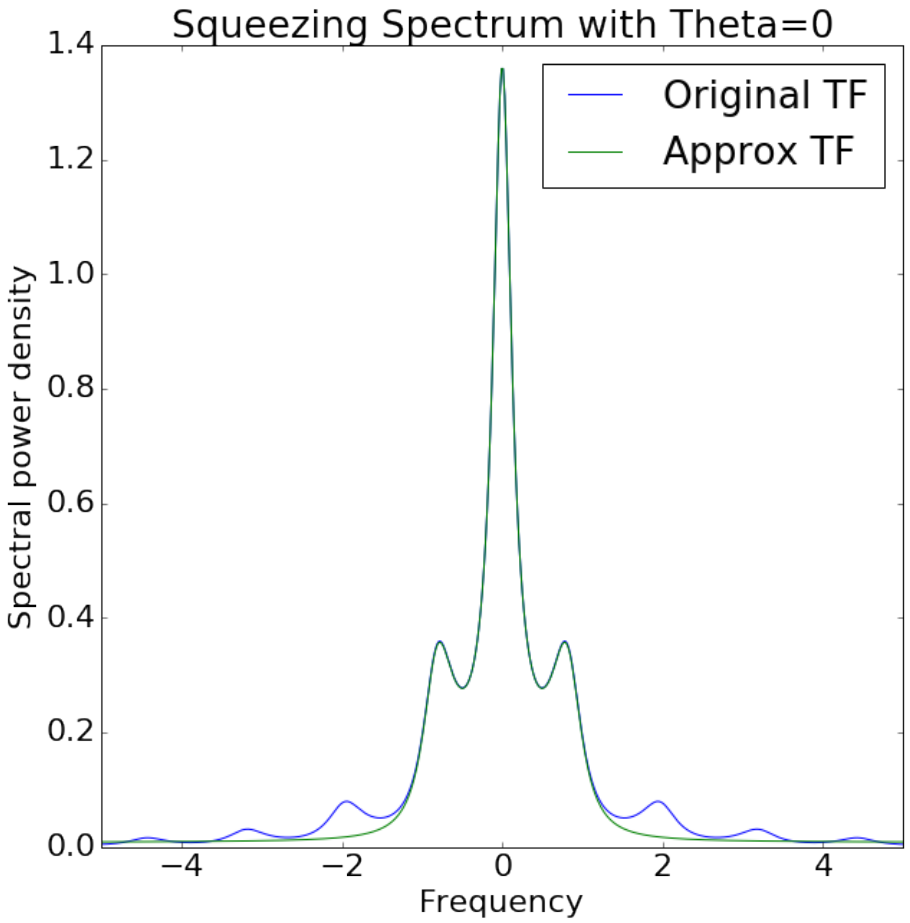

Figure 4.9: The squeezing spectrum of the system in Example 2, along with its reduced counterpart.

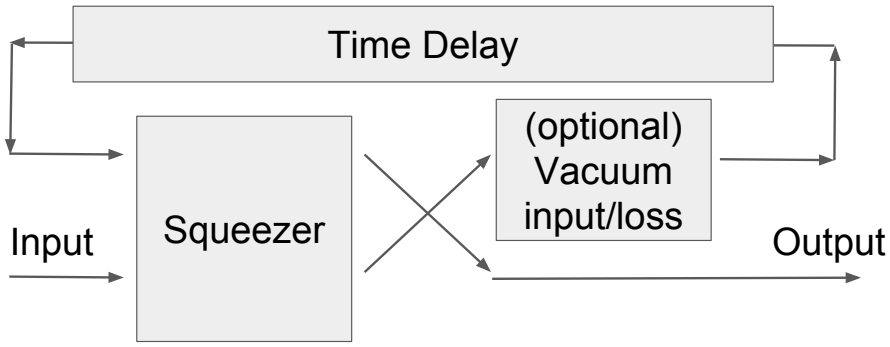

Figure 4.10: The setup of Example 3.

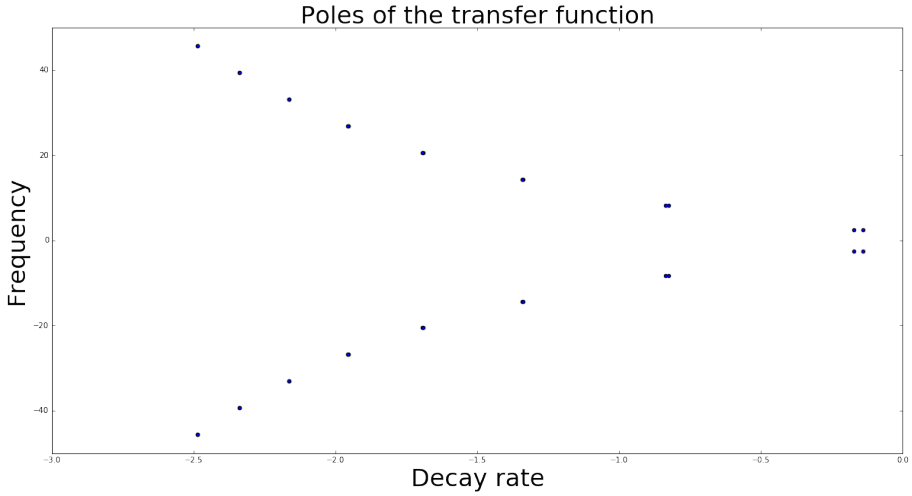

Figure 4.11: The poles of the transfer function of the system in Example 3. The poles for this system all had multiplicity 1.

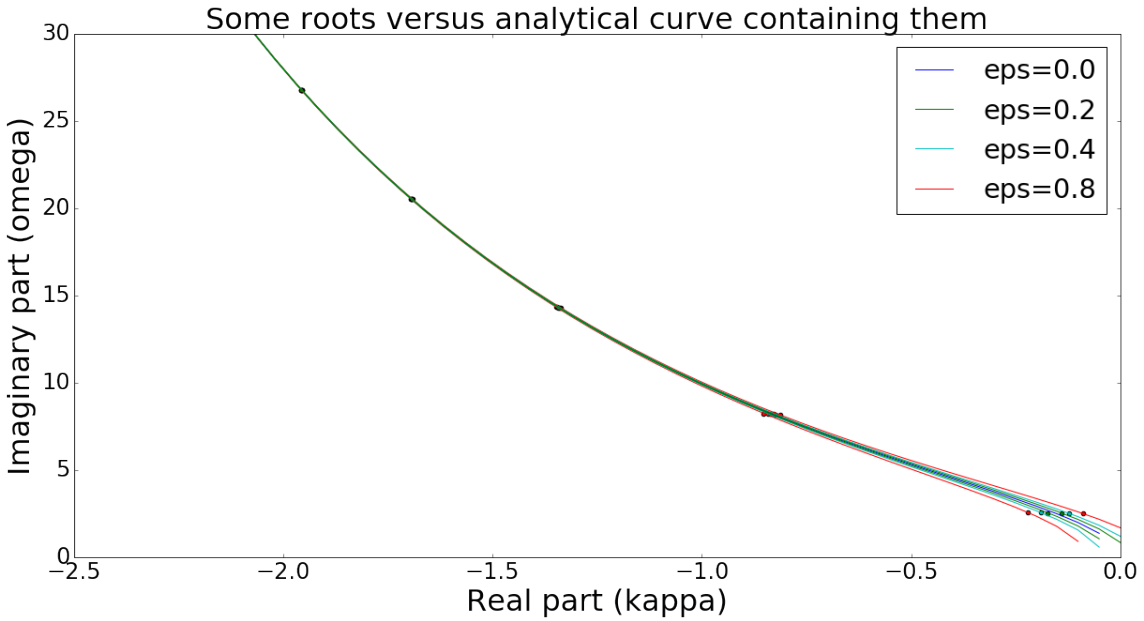

(a)

Figure 4.12

Figure 4.13: The poles of Example 3 with several different squeezing parameters ϵ. When $\epsilon = 0$ there is no squeezing, and the poles become degenerate. As ϵ increases the distance between the split poles increases. The solutions for the poles can be analytically found to be roots of the transcendental equation $k_2 e^{-zT} = \frac{z}{2} \pm \frac{\epsilon}{2} + k$ where $k = \kappa_b + \kappa_c$ and $k_2 = 2\sqrt{\kappa_b \kappa_c}$. The curves along which the poles lie are found by taking the absolute value of the equation.

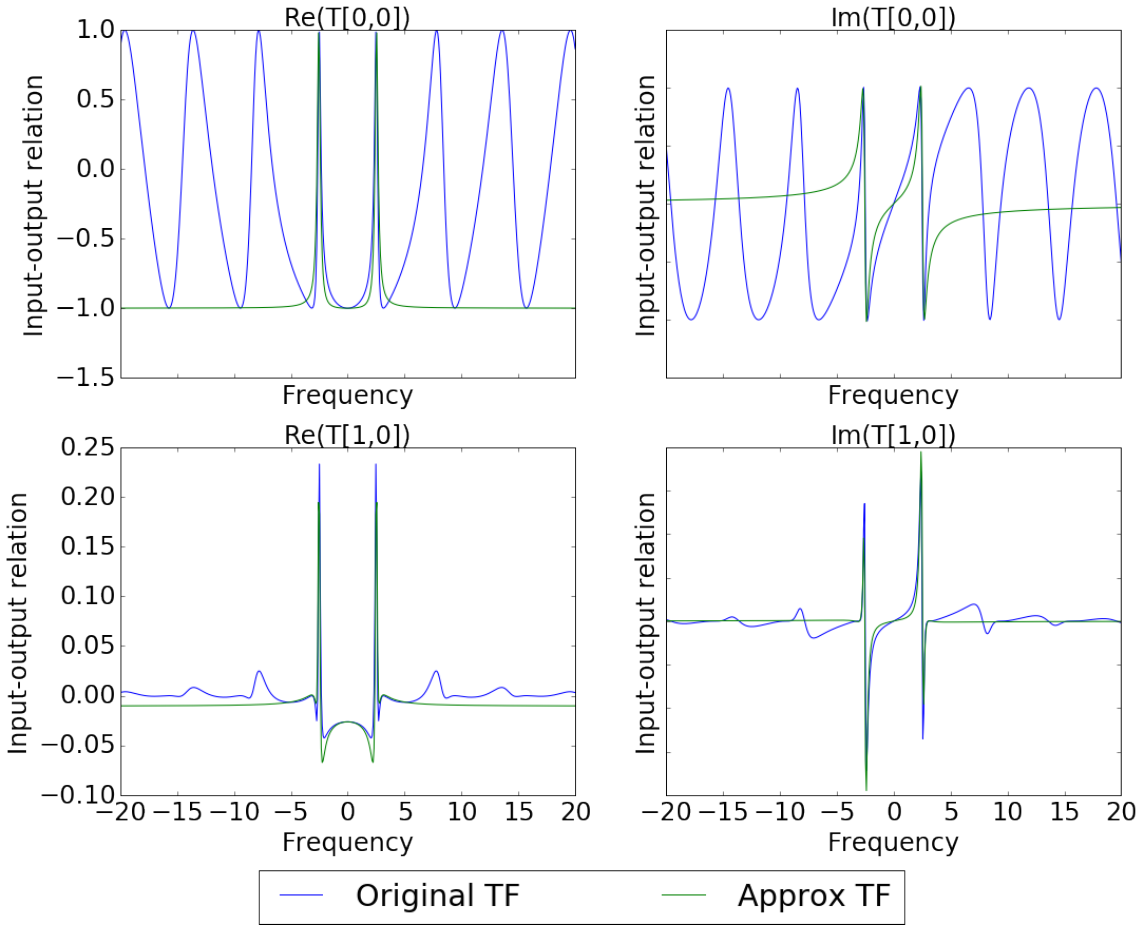

Figure 4.14: The transfer function of Example 3, and the transfer function of an approximation generated using the canonical factors. A constant pre-factor was added so that the two functions match at the origin. The real and imaginary parts of two components are shown along $z = i\omega$ for real values of ω.

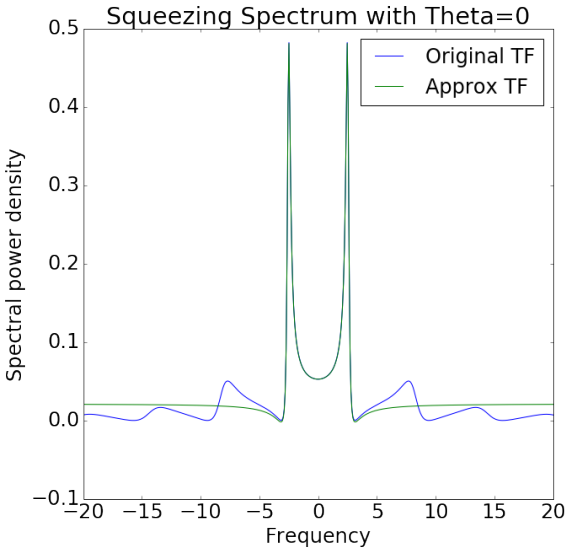

Figure 4.15: The squeezing spectrum of the system in Example 3, along with its reduced counterpart.

Appendix B

Appendix of active systems

B.1 Proof of Lemma 4.6.3

remark B.1.1 *Because of the relationship we found between the zeros and poles for J-unitary functions (along with the eigenvectors at the zeros and poles), the lemma holds for the roots if and only if it holds for the poles. Therefore, it suffices to prove the lemma only for one or the other. We will prove parts (i) and (iii) of the theorem for the poles and part (ii) for the zeros.*

proof for (i):

We begin by showing that for sufficiently large M, for each zero w_0 of $f_S(z)$ such that $|w_0| > M$, there is a radius $\epsilon_M = O(1/M)$ such that exactly one zero z_0 of $f_T(z)$ is within ϵ_M of w_0. To show this, we will use Rouché's Theorem [52]. This theorem states that if $|f_T(z) - f_S(z)| < |f_T(z)|, |f_S(z)|$ for every z on the boundary of some Jordan curve Γ, then $f_T(z)$ and $f_S(z)$ will have the same number of zeros in the interior of Γ.

We can ensure that for sufficiently large M, each ϵ_M is small enough so that it isolates a single zero w_0 of $f_S(z)$. To do this, first note that there is always a positive upper bound $\epsilon_{\max} > 0$ for the radii that isolate the zeros and poles of a not identically zero meromorphic function from other zeros and poles on a bounded set. Using the periodicity of $f_S(z)$ and the boundedness of the real part of the the zeros (Lemma 4.6.1), we can get the desired result. Given a relation $\epsilon_M = O(1/M)$ for sufficiently large M, we can make ϵ_M as small as we like (in particular we can satisfy $\epsilon_M < \epsilon_{\max}$) by requiring M to be sufficiently large.

In order to pick the bounds for Rouché's theorem, we expand $f_S(z)$ at w_0. Explicitly, assuming that leading order terms have order one (see Remark B.1.2), we can expand:

$$f_S(z) = c_1^{(S,w_0)}(z - w_0) + c_2^{(S,w_0)}(z - w_0)^2 + ... \tag{B.1}$$

There is an error bound $k^{(S,w_0)} > 0$ such that if $z \in B_\epsilon(w_0)$, then

$$|f_S(z) - c_1^{(S,w_0)}(z - w_0)| < k^{(S,w_0)}\epsilon^2. \tag{B.2}$$

From this we obtain the bounds for z on $\partial B_\epsilon(w_0)$,

$$|f_S(z)| > |c_1^{(S,w_0)}|\epsilon - k^{(S,w_0)}\epsilon^2, \tag{B.3}$$

$$|f_T(z)| > |c_1^{(S,w_0)}|\epsilon - \delta_M - k^{(S,w_0)}\epsilon^2. \tag{B.4}$$

Above in Eq. (B.4), we introduce $\delta_M = \sup_{\partial B_\epsilon(w_0)} |f_S(z) - f_T(z)|$. Notice sufficient conditions for Rouché's theorem are now $\delta_M < |f_S(z)|, |f_T(z)|$.

From Lemma 4.5.2, the poles of $\tilde{S}(z)$ are contained in a strip of bounded $\Re(z)$. This implies that there is a bound on the real part of all zeros of $f_S(z)$. Using Lemma 4.6.2 (ii), we can bound $\delta_M = O(1/M)$ for large enough M. We can also bound the coefficients $c_1^{(S,w_0)}$ for all zeros w_0 of $f_S(z)$ from below by $C > 0$. This follows from the periodicity of $f_S(z)$ in the imaginary direction, and noting that the bound on the real part of z for the zeros of $f_S(z)$ implies that in each period there are a finite number of zeros. Similarly, we can bound all $k^{(S,w_0)}$ from above by a constant k. If we pick $\epsilon_M = \frac{3\delta_M}{C} = O(1/M)$ for sufficiently large M, the desired conditions for Rouché's theorem follow from the above inequalities.

For the case where $f_S(z)$ and $f_T(z)$ are exchanged, a small modification is needed to obtain the desired ϵ_M, since $f_T(z)$ may not be periodic. First, we need to modify $\epsilon_{\max}$ to ensure the poles z_0 are isolated. This can be done by an application of the triangle inequality. Next, we are interested in bounds for the constants $c_1^{(T,z_0)}$ and $k^{(T,z_0)}$ when expanding $f_T(z)$ at each of its zeros z_0, analogous to the constants used above in Eq. (B.1-B.2). Using Cauchy's integral formula on the ϵ-balls in the above arument, and the error estimate $|f_T(z) - f_S(z)| < \delta_M$, we can obtain the same bounds C and k above for the expansion coefficients $c_i^{(T,w_0)}$ and $k^{(T,z_0)}$, respectively, up to an error of $\delta_M = O(1/M)$. Therefore the desired result holds in this case as well. ■

proof for (ii):

Suppose we are given a pair of roots from part (i), z_0 for $f_T(z)$ and w_0 for $f_S(z)$, along with a

radius ϵ_M such that z_0 is the only root of $f_T(z)$ and w_0 is the only root of $f_S(z)$ inside $B_{\epsilon_M}(w_0)$. From z_0 and w_0 (which are poles of $\tilde{T}(z)$ and $\tilde{S}(z)$) we can find the corresponding roots of $\tilde{T}(z)$ and $\tilde{S}(z)$ (from Claim 4.5.5), which we label $\hat{z}_0$ and $\hat{w}_0$, respectively. Below we will consider all such possible pairs $\hat{z}_0$ and $\hat{w}_0$.

We will show first that

$$\|\tilde{T}(\hat{z}_0) - \tilde{S}(\hat{w}_0)\| = O(\epsilon_M). \tag{B.5}$$

To do this, write

$$\|\tilde{T}(\hat{z}_0) - \tilde{S}(\hat{w}_0)\| \leq \|\tilde{T}(\hat{z}_0) - \tilde{S}(\hat{z}_0)\| + \|\tilde{S}(\hat{z}_0) - \tilde{S}(\hat{w}_0)\|. \tag{B.6}$$

To find a bound for $\|\tilde{T}(\hat{z}_0) - \tilde{S}(\hat{z}_0)\|$ independent of the choice of $\hat{z}_0$ for sufficiently large $|z|$, we can use the bound $\kappa_M = \sup_{|z|>M} \|T_i(z) - S_i\| = O(1/M)$ for $i = 1, 2, 3, 4$.

We can bound

$$\begin{aligned} &\|\tilde{T}(z) - \tilde{S}(z)\| \leq \|T_1(z) - S_1\| \\ &+ \|T_2(z) - S_2\|\|E(z)\|\|(I - T_4(z)E(z))^{-1} - (I - S_4E(z))^{-1}\|\|T_3(z) - S_3\| \end{aligned} \tag{B.7}$$

The $E(z)$ term is bounded for all $\hat{z}_0$, following Lemma 4.6.2 (ii). The term for which obtaining the bound is not obvious is $\|(I - T_4(z)E(z))^{-1} - (I - S_4E(z))^{-1}\|$. We do this below. When $|z|$ is sufficiently large, we can use Lemma 4.6.2 to write $T_4(z) = S_4 + \nu_{\hat{w}_0} D_{\hat{w}_0}(z)$ on each $B_{\epsilon_M}(\hat{w}_0)$ where all the functions $D_{\hat{w}_0}$ are bounded and matrix-valued, and $\nu_{\hat{w}_0} = O(1/|\hat{w}_0|)$. When $z \in B_{\epsilon_M}(\hat{w}_0)$,

$$\begin{aligned} &(I - T_4(z)E(z))^{-1} \\ &= (I - S_4E(z) - \nu_{\hat{w}_0} D_{\hat{w}_0} E(z))^{-1} \\ &= (I - \nu_{\hat{w}_0}(I - S_4E(z))^{-1} D_{\hat{w}_0} E(z))^{-1} (I - S_4E(z))^{-1} \\ &= (I + O(\nu_{\hat{w}_0}))^{-1} (I - S_4E(z))^{-1}. \end{aligned} \tag{B.8}$$

In the final step of Eq. (B.8), we notice that since ϵ_M isolates the zero $\hat{w}_0$ from other zeros and

poles of $\tilde{S}(z)$, the function $(I - S_4E(z))^{-1}$ is bounded on $B_{\epsilon_M}(\hat{w}_0)$. From this we find

$$\begin{aligned}
&(I - T_4(z)E(z))^{-1} - (I - S_4E(z))^{-1} \\
&= [(I + O(\nu_{\hat{w}_0}))^{-1} - I](I - S_4E(z))^{-1} \\
&= (I + O(\nu_{\hat{w}_0}))^{-1}O(\nu_{\hat{w}_0})(I - S_4E(z))^{-1} = O(\nu_{\hat{w}_0}).
\end{aligned} \tag{B.9}$$

Since $\hat{z}_0$ is in $B_{\epsilon_M}(\hat{w}_0)$, This gives the desired bound

$$\|\tilde{T}(\hat{z}_0) - \tilde{S}(\hat{z}_0)\| = O(1/M). \tag{B.10}$$

Further, by a periodicity argument similar to that in part (i), we can make the bound independent of the choice of zeros $\hat{z}_0$ and $\hat{w}_0$.

Next, we obtain a similar bound for $\|\tilde{S}(\hat{z}_0) - \tilde{S}(\hat{w}_0)\|$:

$$\|\tilde{S}(\hat{z}_0) - \tilde{S}(\hat{w}_0)\| \leq \|S_2\|\|E(z)\|\|(I - S_4E(\hat{z}_0))^{-1} - (I - S_4E(\hat{w}_0))^{-1}\|\|S_3\|. \tag{B.11}$$

We notice that $\|E(\hat{z}_0) - E(\hat{w}_0)\| = O(\epsilon_M)$, so using a similar argument as before,

$$(I - S_4E(\hat{z}_0))^{-1} = (I - S_4E(\hat{w}_0))^{-1}(I + O(\epsilon_M)). \tag{B.12}$$

We thus obtain

$$\|\tilde{S}(\hat{z}_0) - \tilde{S}(\hat{w}_0)\| = O(1/M) \tag{B.13}$$

Using Eq. (B.10) and Eq. (B.13), we finally obtain Eq. (B.5).

Next, to relate our analysis to the projectors, we can use the formula [28]

$$P = -\frac{1}{2\pi i}\int_\Gamma R(\zeta, A)d\zeta, \tag{B.14}$$

where $R(\zeta, A) = (A - \zeta)^{-1}$ is the resolvent of a matrix A, and P is the sum of the eigenprojections of all the eigenvalues of A inside the contour Γ.

We will use the second resolvent identity below. It states that for two matrices A and B, and ζ a number not in the spectrum of either,

$$R(\zeta, A) - R(\zeta, B) = R(\zeta, A)(B - A)R(\zeta, B). \tag{B.15}$$

In particular, since $\hat{z}_0$ and $\hat{w}_0$ are roots of $\tilde{T}(z)$ and $\tilde{S}(z)$, respectively, the matrices $\tilde{T}(\hat{z}_0)$ and $\tilde{S}(\hat{w}_0)$ both have the eigenvalue zero. For a sufficiently small contour Γ, the zero eigenvalue becomes isolated for both $\tilde{T}(\hat{z}_0)$ and $\tilde{S}(\hat{w}_0)$. The curve Γ can be made a small, but fixed size for all $\hat{w}_0$ and $\hat{z}_0$. This will allow us to bound the resolvent R below to be bound by a constant. From the second resolvent identity, we can obtain the bound:

$$\|P_T - P_S\| \leq \frac{|\Gamma|}{2\pi} \sup_{\zeta \in \Gamma} R(\tilde{T}(\hat{z}_0), \zeta) \sup_{\zeta \in \Gamma} R(\tilde{S}(\hat{w}_0), \zeta) \|\tilde{T}(\hat{z}_0) - \tilde{S}(\hat{w}_0)\| = O(1/M). \tag{B.16}$$

Above, $|\Gamma|$ indicates the length of the curve Γ. The bound is independent of the choice of $\hat{w}_0$ and $\hat{z}_0$. This completes the proof.

■

proof (iii) The proof follows the first step used to prove (ii), using the poles instead of the zeros. The boundedness of $(I - S_4 E(z))^{-1}$ is obtained by the fixed bound ϵ away from the poles. ■

remark B.1.2 *Note on the rate of convergence: If the zeros have order p instead of* 1*, the scaling of* ϵ_M *follows* $O(M^{-1/p})$*. This can be seen from the order of the terms required in the series expansion used to prove part (i).*

B.2 Proof of Theorem 4.8.1

The roots come in conjugate pairs (Claim 4.5.7), so the set of roots can be partitioned into two conjugate sets: $Z = Z_+ \cup Z_-$ where $Z_- = \{\overline{z} : z \in Z_+\}$. Since we assumed the delays are commensurate, the function $\tilde{S}(z)$ is periodic along the imaginary axis with some period P. Thus the roots in Z_+ (and Z_-) can be ordered as:

$$Z_+ = \Big\{ \underbrace{z_m + iPn}_{z_{m,n}} : m \in \{1, ..., M\}, n \in \mathbb{Z} \Big\} \tag{B.17}$$

where M is the number of roots (in Z_+) per period; because roots come in conjugate pairs, in total there are $2M$ roots per period. To satisfy the condition that all roots are simple (Assumption (6) of Section 4.4.1), we require that the z_n be unique, satisfying $0 < \mathrm{Im}(z_m) < P$ and $\mathrm{Im}(z_m) \neq P/2$. Thus all roots are complex, and a decomposition of the form (4.33) will be possible. We choose the

ordering:

$$\tilde{S}(z) = \Big(\prod_{m=1}^{K} \Big[\prod_{n=-\infty}^{\infty} P_{m,n}(z) \Big] \Big) B(z). \tag{B.18}$$

Here, $P_{m,n}(z)$ is the elementary factor with zeros $(z_{m,n}, \overline{z}_{m,n})$ and poles $(-z_{m,n}, -\overline{z}_{m,n})$ defined in Eq. (4.33).

We first show that each infinite product in Eq. (B.18) converges uniformly on bounded sets. Starting with $m = 1$, consider the terms $P_{1,1}, P_{1,2}, \ldots$ generated by detaching the zeros $z_{1,1}, z_{1,2}, \ldots$ individually from $\tilde{S}(z)$. Since $\tilde{S}(z)$ is periodic with period P, so the projector of $\tilde{S}(z)$ at $z_{m,n}$ is independent of n. Thus the projectors in the terms used to detach the terms $P_{1,1}, P_{1,2}, \ldots$ are the same, and these terms commute. Therefore, these terms can be used to sequentially detach the roots of $\tilde{S}(z)$, giving the expression:

$$\prod_n P_{m,n}(z) = I - V_m V_m^\flat + V_m \prod_n \begin{pmatrix} \frac{z - z_{m,n}}{z + \overline{z}_{m,n}} & 0 \\ 0 & \left(\frac{\overline{z} - z_{m,n}}{\overline{z} + \overline{z}_{m,n}} \right)^* \end{pmatrix} V_m^\flat. \tag{B.19}$$

where we have fixed $m = 1$ for the moment.

The above product converges because one can show [55, Appendix E] that the following series converges uniformly on bounded sets:

$$Q_m(z) \equiv \prod_{n=-\infty}^{\infty} \frac{z - z_{m,n}}{z + \overline{z}_{m,n}} = \frac{\sinh\big(\frac{\pi}{P}(z - z_m)\big)}{\sinh\big(\frac{\pi}{P}(z + \overline{z}_m)\big)} \tag{B.20}$$

After the zeros $z_{1,1}, z_{1,2}, \ldots$ are detached, we obtain a function $\big(\prod_i P_{1,i}(z)\big)^{-1} \tilde{S}(z)$ which is again periodic in the imaginary direction with period P, but has only $2(M-1)$ zeros per period. We can repeat the same procedure for the remaining sequences of zeros $z_{m,1}, z_{m,2}, \ldots$ in Z_+, finding:

$$\tilde{S}(z) = \prod_{m=1}^{K} \left[1 - V_m V_m^\flat + V_m \prod_n \begin{pmatrix} Q_m(z) & 0 \\ 0 & Q_m(\overline{z})^* \end{pmatrix} V_m^\flat \right] B(z). \tag{B.21}$$

$B(z)$ is an entire function that, like $\tilde{S}(z)$ and $Q_m(z)$, is periodic along the imaginary axis with period P. In the limits $\mathrm{Re}(z) \to \pm\infty$, we can show that $B(z)$ tends to a constant by examining the

behavior of $\tilde{S}(z)$ and $Q_m(z)$. For $\tilde{S}(z)$, recall that it is given by (4.28):

$$\begin{aligned}\tilde{S}(z) &= S_1 + S_2 E(z) \left(I - S_4 E(z)\right)^{-1} S_3 \\ &= S_1 + S_2 \left(E(-z) - S_4\right)^{-1} S_3 \end{aligned} \tag{B.22}$$

Using the fact that S_4 is invertible and $E(z) \to 0$ for $\mathrm{Re}(z) \to +\infty$, it is easy to find the limiting behavior of $\tilde{S}(z)$. The limits of $Q_m(z)$ for $\mathrm{Re}(z) \to \pm\infty$ are found using (B.20) and the asymptotic relation $\sinh(x+iy) \to \frac{1}{2}\mathrm{sgn}(x) e^{|x| + iy\,\mathrm{sgn}(x)}$:

$$\tilde{S}(z) \to \begin{cases} S_1 & \mathrm{Re}(z) \to +\infty \\ S_1 - S_2 S_4^{-1} S_3 & \mathrm{Re}(z) \to -\infty \end{cases}, \tag{B.23}$$

$$Q_m(z) \to \begin{cases} e^{-(2\pi/P)\mathrm{Re}(z_m)} & \mathrm{Re}(z) \to +\infty \\ e^{+(2\pi/P)\mathrm{Re}(z_m)} & \mathrm{Re}(z) \to -\infty \end{cases}. \tag{B.24}$$

These limits prove that $B(z)$ tends to a constant for $z \to \pm\infty$, when $\Im(z)$. We also know that $B(z)$ is periodic in the imaginary direction, since it is the product of commensurate periodic functions. Combining these two results, we determine that $B(z)$ has bounded range on the entire plane. By Liouville's theorem, it must be a constant.

■

Rate of convergence

For the purposes of estimating the number of terms needed to maintain a specific maximum level of error using a truncation of the products in Eq. (B.19), we discuss the rate of convergence. The exact number of terms needed will depend on the system, as well as the chosen domain where the approximation is desired. We will show that given specific conditions, the rate of convergence is quadratic. To obtain the rate of convergence of the factorization of $\tilde{S}(z)$, it suffices to consider each of the terms $Q_m(z)$ in Eq. (B.20). Then the rate of convergence for estimating $\tilde{S}(z)$ is determined up to a constant depending on the projectors V_m using Eq. (B.19).

Theorem B.2.1 *For each of the products $Q_m(z)$ in Eq. (B.20), on the domain where $|z| < r$ and z is bound away from the poles by $\delta > 0$, the rate of convergence is quadratic with constant that is determined by δ, the location of the poles, and their periodicity.*

We drop the m index below. The zeros below refer to Z^+ in Eq. (B.17), which correspond to the terms used in the product expansion of $Q(z)$ in Eq. (B.20). Suppose we are interested in the approximation near the origin, and suppose we add terms in the product to the approximation

ordered by the distance of their zeros from the origin. Below we will use the notation $q_n(z) = \frac{z-z_n}{z+\overline{z}_n}$. Let z_0 by the closest zero to the origin from, and let us also suppose we add the terms in pairs with zeros $z_n = z_0 + ipn$ and $\tilde{z}_n = z_0 - ipn$, where p is the periodicity of the zeros. We denote these we the $q_n(z)$ and $q_{-n}(z)$ terms. With this convention we have $Q(z) = \sum_{n=1}^{\infty} q_n(z)q_{-n}(z)$.

Denoting the truncated product $Q^{(N)}(z) = \prod_{n=1}^{N} q_n(z)q_{-n}(z)$ for an integer N, we can write the error $E^{(N)}(z)$ term as

$$E^{(N)}(z) = Q(z) - Q^{(N)}(z) = Q^{(N)}(z)\left(\frac{Q(z)}{Q^{(N)}(z)} - 1\right). \tag{B.25}$$

To find the rate of convergence the following claim will be useful:

Claim B.2.1 *When $|z| < r$ and z is bounded away from poles of $\tilde{S}(z)$ by $\delta > 0$, we have $|Q^{(N)}(z)| < C_1$ for sufficiently large N. Here C_1 may depend on δ.*

Proof: We know $Q(z)$ is a function periodic in the imaginary direction, and therefore we can bound it from above on the domain where z is some fixed constant distance δ away from its poles. In the special case when we interested in real frequency values (z constrained to have purely imaginary values $i\omega$), this is automatically satisfied since the zeros and poles must lie away from the imaginary axis for the system to be stable. On the domain where $|z| < r$ and z is bounded away from the poles by δ, we remark $Q^{(N)}(z) \to Q(z)$ uniformly. Thus we can find a sequence $\epsilon_N \to 0$ such that $|Q^{(N)}(z)| \leq \epsilon_N + Q(z)$, and therefore for sufficiently large N on this domain we can bound $Q^{(N)}(z)$ by a constant C_1. Notice C_1 depends on δ, but also the specific parameters of $Q(z)$ which are determined by the periodicity of the poles P and the location of the poles. ■

Proof of Theorem B.2.1 We can write the product $Q(z)$ as

$$Q(z) = \prod_{n=1}^{\infty} q_n(z)q_{-n}(z) = \prod_{n=1}^{\infty} \frac{z-z_n}{z+\overline{z}_n}\frac{z-\tilde{z}_n}{z+\overline{\tilde{z}}_n} = \prod_{n=1}^{\infty} \frac{(z-z_0)^2 + (pn)^2}{(z+\overline{z}_0)^2 + (pn)^2}. \tag{B.26}$$

Assuming the range of approximation is $|z| < r$, we find as n becomes large each term in the product can be bounded in the form

$$\frac{(z-z_0)^2 + (pn)^2}{(z+\overline{z}_0)^2 + (pn)^2} = 1 + O\left(\left(\frac{z_0}{pn}\right)^2\right) + O\left(\frac{z_0 r}{(pn)^2}\right) + O\left(\left(\frac{r}{pn}\right)^4\right). \tag{B.27}$$

Since we are interested in the limit as n becomes large with r and z_0 fixed, we can write the above bound as $1 + a_n = 1 + O(\frac{1}{(pn)^2})$. When n becomes large we get $\log(1 + a_n) = O(a_n)$. Using this estimate, we will determine the error bound of a truncated product.

Remembering we paired the terms $q_n(z)$ and $q_{-n}(z)$ together, and using the upper bound $1 + a_n$ for each such pair,

$$\frac{Q(z)}{Q^{(N)}(z)} = \prod_{n \geq N} q_n(z) q_{-n}(z) = \exp \sum_{n \geq N} \log(q_n(z) q_{-n}(z)) = \exp \sum_{n \geq N} O(a_n). \tag{B.28}$$

Since $Q^{(N)}(z) \to Q(z)$ uniformly for $|z| < r$, we have $\sum_{n=N}^{\infty} O(a_n) \to 0$ as $N \to \infty$. Therefore we can use the series expansion of the exponential and find

$$E^{(N)} = Q^{(N)}(z) \sum_{n=N}^{\infty} O(a_n). \tag{B.29}$$

We had that $a_n = O(\frac{1}{(pn)^2})$, so the rate of convergence is quadratic. The constant may be found from the limiting upper bound of $Q^{(N)}(z)$ on the domain of interest. This concludes the proof of the theorem. ■

B.3 Proof of Theorem 4.8.2

Sketch of proof

The intuition for the proof of convergence will be to approximate the function $\tilde{T}(z)$ by $\tilde{S}(z)$ for large $|z|$ using Lemma 4.6.3. We will also similarly approximate the detached terms from $\tilde{T}(z)$ with those of $\tilde{S}(z)$ using Eq. (B.41). This approximation and the convergence properties of the factorization of $\tilde{S}(z)$ will then be used to control the convergence of a truncation term $T_\ell(z)$ formed by terms detached from $\tilde{T}(z)$ with zeros far away from the origin (Claim B.3.4). This will result in the convergence result of the detached terms from $\tilde{T}(z)$.

Setup for proof

From Lemma 4.6.3, we intuitively have that the zeros (poles) of $\tilde{T}(z)$ and $\tilde{S}(z)$ become arbitrarily close to one another as $|z| \to \infty$. More specifically, fixing $\epsilon > 0$, we can use the lemma to find a radius R with the following property: There is a one-to-one correspondence between the zeros (poles) of $\tilde{T}(z)$ and $\tilde{S}(z)$ outside $B_R(0)$, such that a zero (pole) z of $\tilde{T}(z)$ and a zero (pole) w of $\tilde{S}(z)$ correspond to each other if and only if $|z - w| < \epsilon = O(1/R)$. We denote the zeros of $\tilde{T}(z)$ and $\tilde{S}(z)$ outside $B_R(0)$ by $Z_R^{\tilde{T}}$ and $Z_R^{\tilde{S}}$ respectively, and the bijection between them by $b_R : Z_R^{\tilde{T}} \to Z_R^{\tilde{S}}$.

To obtain the factorization, we must determine an order for the canonical terms to be detached from $\tilde{T}(z)$. The order we will use for our proof of convergence will be determined as follows. For

terms with zeros inside $B_R(0)$, the order is not important for convergence, since there are a finite number of zeros inside $B_R(0)$. For example, we can pick the zeros according to increasing norm. For terms with zeros outside $B_R(0)$, the order is determined using the order of the corresponding zeros of $\tilde{S}(z)$ in Theorem 4.8.1. That is, we use the one-to-one correspondence b_R between $Z_R^{\tilde{T}}$ and $Z_R^{\tilde{S}}$. The zeros of $\tilde{S}(z)$ come in K sets, where each set contained zeros that were periodic in the imaginary direction. We will denote the zeros of $\tilde{S}(z)$ from each of the K sets and outside of $B_R(0)$ by $Z_R^{\tilde{S},m}$. Each of the $m = 1, ..., K$ sets of zeros correspond to a converging product of terms we will denote by $\prod_{n\in\mathbb{N}} P_{m,n}^S(z)$.

For each $m = 1, ..., K$, denote $Z_R^{\tilde{T},m}$ to be the set of zeros corresponding to $\tilde{S}(z)$ via $Z_R^{\tilde{S},m} = b_R(Z_R^{\tilde{T},m})$. We will detach the zeros one subset $Z_R^{\tilde{T},m}$ at a time. In the static case, the order of zeros within one of the $m = 1, ..., K$ subsets did not matter, since the corresponding projectors used to construct the canonical terms were identical for a given m. However, for the non-static case this is no longer true, and we will require the zeros to be sorted by their norm for each m (i.e. within each subset $Z_R^{\tilde{T},m}$).

Our task is to show the products $\prod_{n\in\mathbb{N}} P_{m,n}(z)$ converge uniformly on compact sets for each m. We will drop the m index and denote each product generated using the zeros $Z_R^{\tilde{T},m}$ as $\prod_n P_n(z)$, (i.e. restrict to a specific index m and drop the finite number of terms with zeros inside $B_R(0)$). Recall the products $\prod_{n\in\mathbb{N}} P_{m,n}^S(z)$ for $\tilde{S}(z)$ converge for each m. If we restrict each such product to $Z_R^{\tilde{S},m}$ (again dropping the finite number of terms with zeros inside $B_R(0)$), we obtain another converging product, which we will denote by $\prod_n P_n^S(z)$ (again dropping the index m). Below, we will say terms $P_n(z)$ and $P_n^S(z)$ correspond to each other if their zeros are related by the bijection b_R.

It will be convenient to use the form of the elementary factors introduced in Section 4.7.3. We can write

$$P_n^S(z) = MF_n^S(z)M^\dagger J, \qquad F_n^S(z) = \text{diag}(a_{w_n}(z), -a_{w_n}(z^*)^*, 1, -1, ..., 1, -1), \tag{B.30}$$

where $a_{z_0}(z) = \frac{z-z_0}{z+z_0^*}$ and M is a fixed J-unitary. Here w_n are the appropriate zeros of $\tilde{S}(z)$. Above in Eq. (B.30), M is fixed due to the periodicity argument used in Section 4.8.1. The terms $P_n(z)$ (with the zeros of $\tilde{T}(z)$) an be written as

$$P_n(z) = \tilde{M}_n F_n(z) \tilde{M}_n^\dagger J, \tag{B.31}$$

$$F_n(z) = \text{diag}(a_{z_n}(z), -a_{z_n}(z^*)^*, 1, -1, ..., 1, -1). \tag{B.32}$$

Here z_n are the appropriate zeros of $\tilde{T}(z)$, and $\tilde{M} = M + \epsilon_{R_n} N_n$ is J-unitary. The N_n are

matrices bounded for all n, and $\epsilon_{R_n} = O(1/R_n)$ for a sequence of R_n with $|z_n|, |w_n| > R_n$. In order to produce the $\tilde{M}_n$ related to M by error ϵ_{R_n}, first apply Lemma 4.6.3(ii) to obtain the error bound between the projectors of $P_n(z)$ and $P_n^S(z)$. Then, using the procedure in Section 4.7.3, we produce the respective M matrices in Eq. (4.41) for $P_n(z)$ and $P_n^S(z)$. Care must be taken to ensure this procedure maintains the error bound for the matrices M and $\tilde{M}$. For example, we can use Gram-Schmidt (with the indefinite basis), appending the same set of initial vectors in both cases.

Since we are interested in the convergence of $\prod_n P_n(z)$ on compact sets, fix $r > 0$. We will show $\prod_n P_n(z)$ converges uniformly on $B_r(0)$. We will approximate $\prod_n P_n(z)$ on $B_r(0)$ using a sequence of functions $T_\ell(z) = \left(\prod_{n=\ell+1}^{\infty} P_n(z)\right)$ for $\ell = 0, 1, ...$ Notice that $\prod_n P_n(z) = \left(\prod_{n=1}^{\ell} P_n(z)\right) T_\ell(z)$. Intuitively, we can think of the $T_\ell(z)$ as the truncation error. If the error can be controlled, then we can obtain a convergence result. We will use the following results for our proof.

Claim B.3.1 *Suppose $z \in B_r(0)$. For sufficiently large R_n, we find the estimate $F_n^S(z) = J + O(1/R_n)$.*

Proof: For large enough R_n, we can use $|a_{w_n}(z) - 1| = O(1/R_n)$ for $|w_n| > R_n$. By direct computation, we find

$$F_n^S(z) = J + O(1/R_n). \tag{B.33}$$

Claim B.3.2 *Suppose $z \in B_r(0)$. For sufficiently large R_n, and corresponding terms $F_n(z)$ and $F_n^S(z)$ having zeros outside $B_{R_n}(0)$, we have $\|F_n(z) - F_n^S(z)\| = O(1/R_n^2)$.*

Proof: First, we show an estimate of the same order for $F_n(z)$ and $F_n^S(z)$:

$$\|F_n(z) - F_n^S(z)\| \leq \|F_n^S(z)\| \|F_n^S(z)^{-1} F_n(z) - I\| \tag{B.34}$$

Here we use the rate of convergence result of Lemma 4.6.3. For estimating the term $\|F_n^S(z)^{-1} F_n(z) -$

$I\|$, one can compute (using $\gamma_n = w_n - z_n = O(1/R_n)$):

$$\begin{aligned} a_{w_n}(z)a_{z_n}(z)^{-1} &= \frac{z-w_n}{z+w_n^*}\frac{z+z_n^*}{z-z_n} = \frac{z-(z_n+\gamma_n)}{z+(z_n+\gamma_n)^*}\frac{z+z_n^*}{z-z_n} = \frac{1-\frac{\gamma_n}{z-z_n}}{1+\frac{\gamma_n^*}{z+z_n^*}} \\ &= \left(1-\frac{\gamma_n}{z-z_n}\right)\left(1-\frac{\gamma_n^*}{z+z_n^*}\right) + O(|\gamma_n|^2) \\ &= 1 - \frac{\gamma_n}{z-z_n} - \frac{\gamma_n^*}{z+z_n^*} + O(|\gamma_n|^2) \\ &= 1 - \frac{\gamma_n}{z-w_n} - \frac{\gamma_n^*}{z+w_n^*} + O(|\gamma_n|^2). \end{aligned} \tag{B.35}$$

For large enough R_n, the terms $(z-z_n)^{-1} = O(1/R_n)$ and $(z+z_n^*)^{-1} = O(1/R_n)$ since $|z_n| > R_n$. Thus we find

$$a_{w_n}(z)a_{z_n}(z)^{-1} = 1 + O(|1/R_n^2|). \tag{B.36}$$

Using Eq. (B.33) and Eq. (B.36) in Eq. (B.34), we find

$$\|F_n(z) - F_n^S(z)\| = (1+O(1/R_n))O(1/R_n^2) = O(1/R_n^2). \tag{B.37}$$

■

Claim B.3.3 *Suppose $z \in B_r(0)$. For sufficiently large R_n, and corresponding product terms $P_n(z)$ and $P_n^S(z)$ having zeros outside $B_{R_n}(0)$, we have $\|P_n(z) - P_n^S(z)\| = O(1/R_n^2)$.*

Proof: We can compute using Eq. B.37,

$$\begin{aligned} \|P_n(z) - P_n^S(z)\| &= \|(M+\epsilon_{R_n}N_n)F_n(z)(M+\epsilon_{R_n}N_n)^\dagger J - MF_n^S(z)M^\dagger J\| \\ &= \|(M+\epsilon_{R_n}N_n)F_n^S(z)(M+\epsilon_{R_n}N_n)^\dagger J - MF_n^S(z)M^\dagger J\| + O(1/R^2) \\ &= \epsilon_{R_n}\|N_nF_n^S(z)M^\dagger J + MF_n^S(z)N_n^\dagger J\| + O(1/R_n^2). \end{aligned} \tag{B.38}$$

Using that M and $\tilde{M} = M + \epsilon_{R_n}N_n$ are J-unitary, we find

$$(M+\epsilon_{R_n}N_n)J(M+\epsilon_{R_n}N_n)^\dagger - MJM^\dagger = 0, \tag{B.39}$$

from which we find

$$N_nJM^\dagger + MJN_n^\dagger = O(1/R_n^2). \tag{B.40}$$

Using Eq. (B.33), Eq. (B.38), and Eq. (B.40), we find

$$\|P_n(z) - P_n^S(z)\| = O(1/R_n^2). \tag{B.41}$$

■

Claim B.3.4 *$T_\ell(z)$ converges uniformly on $B_r(0)$ as $\ell \to \infty$, using the supremum norm.*

Proof of Claim B.3.4

Claim B.3.3 gives us a bound on the estimate error between $P_n(z)$ and $P_n^S(z)$ inside $B_r(0)$ for some sufficiently large R_n, which will be key in showing the convergence of $T_\ell(z)$. Notice that because the zeros w_n of $\tilde{S}(z)$ are periodic, we can replace $O(1/R_n^2)$ by $O(1/n^2)$. Let q be the smallest index of n for which the above estimates Eqs. (B.33, B.41) hold, and also that $R_n > r$.

The next step will be to show that $\| \prod_{n=q}^{p} P_n(z)\|$ is bounded in $B_r(0)$ for all $p = q, q+1, ...$ Our estimate Eq. (B.41) produces

$$\left\| \prod_{n=q}^{p} P_n(z) \right\| \leq \left\| \prod_{n=q}^{p} P_n^S(z) \right\| \prod_{n=q}^{p} \left(1 + \frac{c}{n^2 \|P_n^S(z)\|} \right). \tag{B.42}$$

The product $\prod_{n=q}^{p} P_n^S(z)$ is bounded on $B_r(0)$ over all $p = q, q+1, ...$ since it converges in the limit $p \to \infty$, and it has no poles in $B_r(0)$ (since we ensured $R_n > r$). Also, $\|P_n^S(z)\|$ converges to a constant as $n \to \infty$ because $a_{w_n}(z) \to 1$ as $|w_n| \to \infty$. Finally we can obtain a bound for Eq. (B.42) over all $p = q, q+1, ...$ since $\sum_{n=1}^{\infty} \frac{1}{n^2}$ converges.

Next, we are ready to show the sequence of functions $T_\ell(z)$ is Cauchy with the supremum norm on $B_r(0)$. To see this, we can compute for $z \in B_r(0)$ and $q \leq \ell < k$,

$$\|T_\ell(z) - T_k(z)\| \leq \left\| \prod_{n=q}^{\ell} P_n(z) \right\| \left\| \prod_{n=\ell+1}^{k} (P_n(z) - P_n^S(z)) \right\| \left\| \prod_{k+1}^{\infty} P_n^S(z) \right\|. \tag{B.43}$$

We have shown the first term is bounded over all $\ell = q, q+1, ...,$ and the last term is bounded as discussed above. The middle term can be made arbitrarily small for sufficiently large ℓ and k using the bound in Eq. (B.41). We conclude from this that $T_\ell(z)$ is uniformly Cauchy on $B_r(0)$, and therefore converges uniformly. This completes the proof of Claim B.3.4. ■

Proof of convergence for Theorem 4.8.2. Finally, we can show $\prod_{n=q}^{\infty} P_n(z) = \left(\prod_{n=q}^{\ell} P_n(z) \right) T_\ell(z)$ converges uniformly on $B_r(0)$ using the uniform convergence of $T_\ell(z)$ and the upper bound Eq. (B.42).

Here q is the index used in the proof of Claim B.3.4, the smallest index of n for which the above estimates Eqs. (B.33, B.41) hold, and also that $R_n > r$. Explicitly, supposing $C(z)$ is the function satisfying $T_\ell(z) \to C(z)$ as $\ell \to \infty$ uniformly on $B_r(0)$, we find

$$\left\| \prod_{n=q}^{\infty} P_n(z) - \left(\prod_{n=q}^{\ell} P_n(z) \right) C(z) \right\| \leq \left\| \prod_{n=q}^{\ell} P_n(z) \right\| \|C(z) - T_\ell(z)\|. \tag{B.44}$$

Since q was just a finite integer and hence the finite product of terms P_n with $n < q$ converges, we conclude that $\prod_n P_n(z)$ converges uniformly on $B_r(0)$.

Proof that $B(z)$ is a constant in Theorem 4.8.2. To show $B(z)$ is constant, it suffices to show it is a bounded function, since it is entire (using Liouville's theorem). Since $\tilde{T}(z)$ is not periodic like $\tilde{S}(z)$, we cannot use the same proof as for Theorem 4.8.1. We have $B(z) = \left(\prod_n P_n(z)\right)^{-1} \tilde{T}(z)$, and let $B_S(z) = \left(\prod_n P_n^S(z)\right)^{-1} \tilde{S}(z)$. Since $B_S = B_S(z)$ is constant as found in Theorem 4.8.1, it suffices to show $\|B_S - B_T(z)\|$ is bounded regardless of z.

We apply part (iii) of Lemma 4.6.3, in order to approximate $\tilde{T}(z)$ with $\tilde{S}(z)$ away from their poles z_n and w_n. For a small but fixed ϵ and sufficiently large M, if $|z| > M$ and $z \notin B_\epsilon(w_n)$, $z \notin B_\epsilon(z_n)$

$$\|\tilde{T}(z) - \tilde{S}(z)\| = O(1/M). \tag{B.45}$$

We will next find an estimate for $\|\left(\prod_n P_n(z)\right)^{-1} - \left(\prod_n^S P_n(z)\right)^{-1}\|$ for sufficiently large $|z|$ and $z \notin B_\epsilon(w_n), z \notin B_\epsilon(z_n)$, using the bounds found above. We will show the proof for $\|\prod_n P_n(z) - \prod_n^S P_n(z)\|$ to simplify the notation, since each $P_n(z)$ has the same form as $P_n(z)^{-1}$ (same for $P_n^S(z)$). To do this, we will start with the estimate Eq. (B.35). The terms $(z - w_n)^{-1}$ and $(z + w_n^*)^{-1}$ can be uniformly bounded if we ensure that z is at least ϵ away from each w_n, $-w_n^*$. However, now we cannot bound these terms by $O(1/R_n)$ since z is not confined to $B_r(0)$. Instead we can propagate error terms of the form $O(1/|z-w_n|)$ and $O(1/|z+w_n^*|)$ through the analysis, obtaining an estimate similar to Eq. (B.41),

$$\|P_n(z) - P_n^S(z)\| = O(1/R_n^2) + O(1/(R_n|z - w_n|)) + O(1/(R_n|z + w_n^*|)). \tag{B.46}$$

which holds when $|w_n|, |z_n| > R_n$ for sufficiently large R_n.

We can continue similarly to Eq. (B.42), finding a sufficiently large index q so that

$$\left\|\prod_{n=q}^{\infty} P_n(z)\right\| \leq \left\|\prod_{n=q}^{\infty} P_n^S(z)\right\| \prod_{n=q}^{\infty}\left(1 + c\left(\frac{1}{n^2} + \frac{1}{n^2|z/w_n - 1|} + \frac{1}{n^2|z/w_n^* + 1|}\right)\frac{1}{\|P_n^S(z)\|}\right), \quad \text{(B.47)}$$

for a constant c. Next we examine individual terms above in Eq. (B.47) and check they are all bounded uniformly when $z \notin B_\epsilon(w_n), z \notin B_\epsilon(-w_n^*)$. In this domain we can obtain a bound for $\left\|\prod_{n=q}^{\infty} P_n^S(z)\right\|$ (which depends on our choice of ϵ). This can be done by considering $\prod_{n=1}^{\infty} P_n^S(z)$, which is periodic in the imaginary direction. The product also converges as $\Re(z) \to \pm\infty$, so we conclude $\left\|\prod_{n=q}^{\infty} P_n^S(z)\right\|$ is bounded uniformly for $z \notin B_\epsilon(w_n), z \notin B_\epsilon(z_n)$. We also have $\|P_n^S(z)\|$ are uniformly bounded away from zero when $z \notin B_\epsilon(w_n), z \notin B_\epsilon(-w_n^*)$. As before, $\sum_{n=1}^{\infty} \frac{1}{n^2}$ converges. The terms $\sum_{n=1}^{\infty} \frac{1}{n^2|z/w_n - 1|}$ and $\sum_{n=1}^{\infty} \frac{1}{n^2|z/w_n^* + 1|}$ are bounded uniformly when z is bounded away by the fixed ϵ away from w_n (and $-w_n^*$). We can combine these observations to show that $\left\|\prod_n P_n(z) - \prod_n P_n^S(z)\right\|$ is bounded as long as $z \notin B_\epsilon(w_n), z \notin B_\epsilon(z_n)$ (further, the same holds for $\| \left(\prod_n P_n(z)\right)^{-1} - \left(\prod_n P_n^S(z)\right)^{-1} \|$). With the same conditions on z, since $\prod_n P_n^S(z)$ is also bounded, we find that $\prod_n P_n(z)$ is bounded as well.

Combining the above result with Eq. (B.45), and the boundedness of $\tilde{S}(z)$, we find that for sufficiently large $|z|$ for which $z \notin B_\epsilon(w_n), z \notin B_\epsilon(-w_n^*), z \notin B_\epsilon(z_n)$,

$$\begin{aligned}&\|B(z) - B_S(z)\| \\ &\leq \left\|\left(\prod_n P_n(z)\right)^{-1}\right\| \left\|\tilde{T}(z) - \tilde{S}(z)\right\| + \left\|\tilde{S}(z)\right\| \left\|\left(\prod_n P_n(z)\right)^{-1} - \left(\prod_n P_n^S(z)\right)^{-1}\right\|. \end{aligned} \quad \text{(B.48)}$$

Since we can make ϵ as small as we wish, we can ensure it is small enough so that there is a sequence of discs $B_{r_n}(0)$ with $r_n \to \infty$ as $n \to \infty$ such that none of the boundaries $\partial B_{r_n}(0)$ contain points in any of the ϵ neighborhoods of the balls $B_\epsilon(w_n), B_\epsilon(-w_n^*), B_\epsilon(z_n)$. By the maximum modulus principle, the maximum value of $\|B(z)\|$ on each $B_{r_n}(0)$ is attained on the boundary. Further, this value is bounded independently of z. This implies $B(z)$ is everywhere bounded, and hence a constant (call it B). ■

Rate of convergence:

In practice, it will be useful to truncate an infinite product produced by Theorem 4.8.2 when constructing a reduced model. Thus the rate of convergence of the reduced model as the number of terms used for the approximation increases is useful in practice. In Theorem B.2.1 we discussed the rate of convergence of a particular truncated product produced when the system used in our construction was a static system with time-delayed feedback. In particular, we concluded the rate

of convergence is quadratic under specific conditions. We will show below that when the procedure for constructing the factorization of $\tilde{T}(z)$ is possible, the rate of convergence remains quadratic for the non-static case as well (on the same domain).

In Theorem B.2.1 we required z to belong in a particular domain. Specifically, we require $|z| < r$ for a fixed radius r, and z must be bounded away from the poles by some minimum distance (fixed as $\delta > 0$). Given the same conditions on the domain of z, picking terms according to the construction of Theorem 4.8.2 by detaching factors from $\tilde{T}(z)$ for sufficiently large n (assuming it is possible to construct each individual term) will produce terms corresponding to those detached from $\tilde{S}(z)$ in its analogous procedure. Furthermore, we can apply Claim B.3.3 to obtain the bound in Eq. (B.41). Finally, an application of the triangle inequality produces again a quadratic rate of convergence with the number of terms (albeit with a larger constant).

Chapter 5

Conclusions

I have shown in this dissertation how linear open quantum systems with coherent delayed feedback can be represented as an infinite series product of canonical terms having a single degree of freedom. First we considered passive linear systems, but later we showed how this can be extended to active linear systems as well. The product can be truncated to obtain a finite approximation, which can be used to obtain a simplified model of the given system with few degrees of freedom. The new system is Markovian and has an SLH representation that can be used within the standard SLH framework, making it useful in applications when combined with other components requiring a full quantum simulation. Through several examples this dissertation also shows the intuition behind the factorization, and the interpretation of each factorized term. We hope the methodology will be useful for both simulations and a better understanding of the types of systems it applies to.

Bibliography

[1] Fabrizio Antenucci. Multimode laser theory for open cavities. In *Statistical Physics of Wave Interactions*, pages 9–38. Springer, 2016.

[2] Joseph A. Ball, Israel Gohberg, and Leiba Rodman. Tangential interpolation problems for rational matrix functions. *Proc. Sympos. Pure Math.*, 40, 1990.

[3] Luc Bouten, Ramon Van Handel, and Matthew R James. An introduction to quantum filtering. *SIAM Journal on Control and Optimization*, 46(6):2199–2241, 2007.

[4] Heinz-Peter Breuer, Francesco Petruccione, et al. *The theory of open quantum systems*. Oxford University Press on Demand, 2002.

[5] Howard J Carmichael. *Statistical Methods in Quantum Optics 2: Non-Classical Fields*. Springer Science & Business Media, 2009.

[6] Joshua Combes, Joseph Kerckhoff, and Mohan Sarovar. The slh framework for modeling quantum input-output networks. *Advances in Physics: X*, 2(3):784–888, 2017.

[7] Orion Crisafulli, Nikolas Tezak, Daniel BS Soh, Michael A Armen, and Hideo Mabuchi. Squeezed light in an optical parametric oscillator network with coherent feedback quantum control. *Optics Express*, 21(15):18371–18386, 2013.

[8] L. M. Delves and J. N. Lyness. A numerical method for locating the zeros of an analytic function. *Mathematics of Computation 21, 543-560.*, 1967.

[9] SM Dutra and G Nienhuis. What is a quantized mode of a leaky cavity? In *Modern Challenges in Quantum Optics*, pages 338–354. Springer, 2001.

[10] H. Dym, B. Fritzsche, V. Katsnelson, and B. Kirstein. *Topics in interpolation theory*, volume 95. Springer Science & Business Media, 1997.

[11] CW Gardiner, AS Parkins, and P Zoller. Wave-function quantum stochastic differential equations and quantum-jump simulation methods. *Physical Review A*, 46(7):4363, 1992.

[12] Israel Gohberg, Peter Lancaster, and Leiba Rodman. *Indefinite Linear Algebra and Applications*. Springer Science & Business Media, 2006.

[13] J. Gough and M. R. James. Quantum feedback networks: Hamiltonian formulation. *Communications in Mathematical Physics*, 287.3:1109–1132, 2009.

[14] J. E. Gough, R. Gohm, and M. Yanagisawa. Linear quantum feedback networks. *Phys. Rev. A*, 78(062104), 2008.

[15] JJMR Gough and MR James. Quantum feedback networks: Hamiltonian formulation. *Communications in Mathematical Physics*, 287(3):1109–1132, 2009.

[16] John Gough and Matthew R James. The series product and its application to quantum feedforward and feedback networks. *IEEE Transactions on Automatic Control*, 54(11):2530–2544, 2009.

[17] John E Gough, Symeon Grivopoulos, and Ian R Petersen. Isolated loops in quantum feedback networks. *arXiv preprint arXiv:1705.09916*, 2017.

[18] John E Gough and Guofeng Zhang. On realization theory of quantum linear systems. *Automatica*, 59:139–151, 2015.

[19] John Edward Gough, MR James, and HI Nurdin. Squeezing components in linear quantum feedback networks. *Physical Review A*, 81(2):023804, 2010.

[20] John Edward Gough and Sebastian Wildfeuer. Enhancement of field squeezing using coherent feedback. *Physical Review A*, 80(4):042107, 2009.

[21] Arne L Grimsmo. Time-delayed quantum feedback control. *Physical Review Letters*, 115(6):060402, 2015.

[22] Symeon Grivopoulos, Hendra I Nurdin, and Ian R Petersen. On transfer function realizations for linear quantum stochastic systems. In *Decision and Control (CDC), 2016 IEEE 55th Conference on*, pages 4552–4558. IEEE, 2016.

[23] Ryan Hamerly. Coherent lqg control, free-carrier oscillations, optical ising machines and pulsed opo dynamics. *arXiv preprint arXiv:1608.07551*, 2016.

[24] Robin L Hudson and Kalyanapuram R Parthasarathy. Quantum ito's formula and stochastic evolutions. *Communications in Mathematical Physics*, 93(3):301–323, 1984.

[25] Sanae Iida, Mitsuyoshi Yukawa, Hidehiro Yonezawa, Naoki Yamamoto, and Akira Furusawa. Experimental demonstration of coherent feedback control on optical field squeezing. *IEEE Transactions on Automatic Control*, 57(8):2045–2050, 2012.

[26] Matt James. The SLH formalism and quantum feedback networks. Presentation available at `https://www.newton.ac.uk/files/seminar/20140721150016002-194364.pdf`, 2014.

[27] JR Johansson, PD Nation, and Franco Nori. Qutip: An open-source python framework for the dynamics of open quantum systems. *Computer Physics Communications*, 183(8):1760–1772, 2012.

[28] T Kato. *Perturbation Theory for Linear Operators*, volume 132. W. Springer-Verlag Berlin, 1976.

[29] Joseph Alan Kerckhoff. *Quantum Engineering with Quantum Optics*. Stanford University, 2011.

[30] Manuel Kraft, Sven M Hein, Judith Lehnert, Eckehard Schöll, Stephen Hughes, and Andreas Knorr. Time-delayed quantum coherent pyragas feedback control of photon squeezing in a degenerate parametric oscillator. *Physical Review A*, 94(2):023806, 2016.

[31] Peter Kravanja and Marc Van Barel. *Computing the zeros of analytic functions*. Number 1727. Springer Science & Business Media, 2000.

[32] Sanjay Lall. Lecture notes on state-space realization theory. `http://lall.stanford.edu/svn/engr207c_2010_to_2011_autumn/data/realization_2008_11_15_03.pdf`, November 2008. Accessed: May 24 2017.

[33] James Lam. Model reduction of delay systems using pade approximants. *International Journal of Control*, 57(2):377–391, 1993. DOI: 10.1080/00207179308934394.

[34] Goran Lindblad. On the generators of quantum dynamical semigroups. *Communications in Mathematical Physics*, 48(2):119–130, 1976.

[35] Michael Lubasch, Antonio A Valido, Jelmer J Renema, W Steven Kolthammer, Dieter Jaksch, Myungshik S Kim, Ian Walmsley, and Raúl García-Patrón. Tensor network states in time-bin quantum optics. *Physical Review A*, 97(6):062304, 2018.

[36] Aline I. Maalouf and Ian R. Petersen. Coherent H^∞ control for a class of linear complex quantum systems. *Proceedings of the American Control Conference ACC 2009, St. Louis, Missouri*, 2009.

[37] Aline I. Maalouf and Ian R. Petersen. Coherent H^∞ control for a class of annihilation-operator linear quantum systems. *IEEE Transactions on Automatic Control*, 56(2):309–319, 2011.

[38] Jonas Maziero. Computing partial traces and reduced density matrices. *International Journal of Modern Physics C*, 28(01):1750005, 2017.

[39] Nikolett Német and Scott Parkins. Enhanced optical squeezing from a degenerate parametric amplifier via time-delayed coherent feedback. *Physical Review A*, 94(2):023809, 2016.

[40] Simon E Nigg, Hanhee Paik, Brian Vlastakis, Gerhard Kirchmair, Shyam Shankar, Luigi Frunzio, MH Devoret, RJ Schoelkopf, and SM Girvin. Black-box superconducting circuit quantization. *Physical Review Letters*, 108(24):240502, 2012.

[41] Hendra I Nurdin, Symeon Grivopoulos, and Ian R Petersen. The transfer function of generic linear quantum stochastic systems has a pure cascade realization. *Automatica*, 69:324–333, 2016.

[42] K. R. Parthasarathy. *An introduction to quantum stochastic calculus,*, volume 85 of *Monographs in Mathematics*. Birkhauser Verlag, Basel, 1992.

[43] Ian R. Petersen. Quantum linear systems theory. *Proceedings of the 19th International Symposium on Mathematical Theory of Networks and Systems*, 2010.

[44] Ian R. Petersen. Analysis of linear quantum optical networks. *arXiv preprint arXiv:1403.6214*, 2014.

[45] Hannes Pichler, Soonwon Choi, Peter Zoller, and Mikhail D Lukin. Photonic tensor networks produced by a single quantum emitter. *arXiv preprint arXiv:1702.02119*, 2017.

[46] Hannes Pichler and Peter Zoller. Photonic circuits with time delays and quantum feedback. *Physical review letters*, 116(9):093601, 2016.

[47] MB Plenio and PL Knight. The quantum-jump approach to dissipative dynamics in quantum optics. *Reviews of Modern Physics*, 70(1):101, 1998.

[48] Vladimir Petrovich Potapov. The multiplicative structure of j-contractive matrix functions. *Trudy Moskovskogo Matematicheskogo Obshchestva*, 4:125–236, 1955.

[49] Carl L Prather and André C M Ran. Factorization of a class of meromorphic matrix valued functions. *Journal of Mathematical Analysis and Applications*, 127(2):413–422, 1987.

[50] J. P. Richard. Time-delay systems: an overview of some recent advances and open problems. *Automatica*, 39(10):1667–1694, 2003.

[51] Angel Rivas and Susana F Huelga. *Open quantum systems*. Springer, 2012.

[52] Edward B Saff and Arthur David Snider. *Fundamentals of Complex Analysis for Mathematics, Science, and Engineering*. Prentice-Hall, 1976.

[53] AJ Shaiju and Ian R Petersen. A frequency domain condition for the physical realizability of linear quantum systems. *IEEE Transactions on Automatic Control*, 57(8):2033–2044, 2012.

[54] Gil Tabak. Example for factorizing quantum linear systems with time delays. `https://github.com/tabakg/active_lin_sys_fact/blob/master/sample_active_linear_system_3.ipynb`, February 2018.

[55] Gil Tabak and Hideo Mabuchi. Trapped modes in linear quantum stochastic networks with delays. *EPJ Quantum Technology*, 3(1):3, 2016.

[56] Nikolas Tezak, Armand Niederberger, Dmitri S. Pavlichin, Gopal Sarma, and Hideo Mabuchi. Specification of photonic circuits using quantum hardware description language. *Philosophical Transactions of the Royal Society of London A: Mathematical, Physical and Engineering Sciences*, 370(1979):5270–5290, 2012.

[57] Benoıt Vermersch, P-O Guimond, Hannes Pichler, and Peter Zoller. Quantum state transfer via noisy photonic and phononic waveguides. *Physical review letters*, 118(13):133601, 2017.

[58] SJ Whalen, AL Grimsmo, and HJ Carmichael. Open quantum systems with delayed coherent feedback. *Quantum Science and Technology*, 2(4):044008, 2017.

[59] Robert S Whitney. Staying positive: going beyond lindblad with perturbative master equations. *Journal of Physics A: Mathematical and Theoretical*, 41(17):175304, 2008.

[60] Masahiro Yanagisawa and Hidenori Kimura. Transfer function approach to quantum control-part i: Dynamics of quantum feedback systems. *Automatic Control, IEEE Transactions on*, 48.12:2107–2120, 2003.

[61] G. Zhang and M. R. James. Quantum feedback networks and control: A brief survey. *Chinese Science Bulletin*, 57(18):2200–2214, 2012.